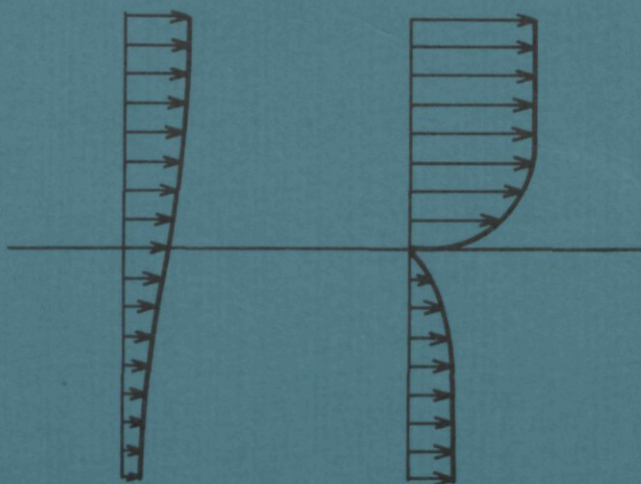# COPOLYMERS AT A LIQUID-LIQUID INTERFACE AND THEIR RETARDING EFFECT ON MASS TRANSFER BETWEEN BOTH PHASES

B. J. R. SCHOLTENS

COPOLYMERS AT A LIQUID-LIQUID INTERFACE AND THEIR RETARDING EFFECT ON MASS TRANSFER BETWEEN BOTH PHASES

Dit proefschrift met stellingen van

BOUDEWIJN JAN ROBERT SCHOLTENS

doctorandus in de chemie, geboren te 's-Gravenhage op 7 juli 1950, is goedgekeurd door de promotoren Dr. B. H. Bijsterbosch, lector in de Fysische en Kolloidchemie, en Dr. Ir. S. Bruin, hoogleraar in de Proceskunde.

De Rector Magnificus van de Landbouwhogeschool,

J. P. H. VAN DER WANT

Wageningen, 24 januari 1977

B. J. R. SCHOLTENS

COPOLYMERS AT A LIQUID-LIQUID INTERFACE AND THEIR RETARDING EFFECT ON MASS TRANSFER BETWEEN BOTH PHASES

PROEFSCHRIFT

TER VERKRIJGING VAN DE GRAAD
VAN DOCTOR IN DE LANDBOUWWETENSCHAPPEN
OP GEZAG VAN DE RECTOR MAGNIFICUS,
DR. IR. J. P H. VAN DER WANT,
HOOGLERAAR IN DE VIROLOGIE,
IN HET OPENBAAR TE VERDEDIGEN
OP VRIJDAG 13 MEI 1977
DES NAMIDDAGS TE VIER UUR IN DE AULA
VAN DE LANDBOUWHOGESCHOOL TE WAGENINGEN

STELLINGEN

I

De grensvlakactiviteit van polyvinylalcohol-acetaat copolymeren aan het water-butanol grensvlak wordt in zeer belangrijke mate door de intra-moleculaire vinylacetaatverdeling bepaald.

Dit proefschrift, hoofdstuk 3 en 6.

II

Voor het vaststellen van de gemiddelde polymerisatiegraad van polyvinylalcohol is het gebruik van de Japanse Industriële Standaard K 6726-1965 sterk af te raden.

III

Ten onrechte veronderstelt Toyoshima dat de oplosbaarheid van polyvinylalcohol in water door kinetische factoren wordt bepaald.

Toyoshima, K. (1973) in 'Polyvinyl alcohol properties and applications', ed. Finch, C. A., J. Wiley and Sons Inc., London, p. 22.

IV

Het is een illusie dat onderzoek naar electrolyttransport door een water–olie grensvlak kan leiden tot een beter begrip van diffusie door een celmembraan.

Dit proefschrift, hoofdstuk 4, 5 en 6.

V

De 'ongeroerde laag' aan een grensvlak in een geroerd systeem is een, hydrodynamisch gezien, onrealistische veronderstelling om mathematisch een eenvoudige, benaderde oplossing te vinden voor een overdrachtsproces. Het is daarom irrelevant om, ter verklaring van deze laag, bijzondere eigenschappen te postuleren voor de vloeistof dichtbij dat grensvlak.

Drost-Hansen, W. (1971) in 'Chemistry of the cell interface', part B. ed. Brown, H. D., Academic Press, New York, p. 92–93.

VI

De dempende werking van geadsorbeerde lagen op turbulente vloeistofstroming aan een vrij grensvlak is door Davies principieel fout uitgewerkt; één extra aanname leidt echter tot hetzelfde, aannemelijke, eindresultaat.

Davies, J. T. (1972) 'Turbulence phenomena', Academic Press, New York, p. 252.

VII

Ideale warmte-isolatie is met de formulering die BEEK en MUTTZALL voor de warmteflux geven een koud kunstje.

BEEK, W. J. en MUTTZALL, K. M. K. (1975) 'Transport phenomena', J. Wiley and Sons Inc., London, p. 12.

VIII

De molecuulgewichten van de componenten van het menselijk factor VIII complex zijn veeleer gelijk dan verschillend.

NEWMAN, J., HARRIS, R. B. and JOHNSON, A. J. (1976), Nature **263**, 612–3.

IX

De methode die GROVES en SEARS voorstellen om ζ-potentialen te meten is niet aan te bevelen: de argumenten die zij aandragen om de bruikbaarheid aan te tonen zijn onjuist en bovendien zijn er principiële, door hen niet onderkende nadelen aan deze methode verbonden.

GROVES, J. N. en SEARS, A. R. (1975) J. Colloid Interface Sci. **53**, 83–9.

X

De tegenstrijdigheden die het artikel van DEŽELIĆ et al. bevat, zijn terug te brengen op een onjuiste aanname over de reversibiliteit van eiwitadsorptie.

DEŽELIĆ, G., DEŽELIĆ, N. en TELIŠMAN, Ž. (1971) Eur. J. Biochem. **23**, 575–81.

XI

De oppervlaktegeleiding door WRIGHT en JAMES bij hogere zoutconcentraties bepaald, moet wel met de nodige korrels zout worden genomen.

WRIGHT, M. H. en JAMES, A. M. (1973) Kolloid-Z.u.Z. Polym. **251**, 745–51.

XII

Het gebruik van zakrekenmachines bij examens zou verboden of in ieder geval genormaliseerd moeten worden.

XIII

In iedere telefooncel dient, naast het bij storingen te draaien nummer, ook te worden aangegeven, wáár men dit kan draaien.

B. J. R. SCHOLTENS
Wageningen, 13 mei 1977

aan mijn Ouders
voor Rees

VOORWOORD

Aan het begin van dit proefschrift wil ik graag allen bedanken, die op enigerlei wijze aan de totstandkoming ervan hebben bijgedragen. Dat dit altijd tot een nuttige of noodzakelijke maar meestal ook heel plezierige samenwerking heeft geleid, wil ik hier nog eens met nadruk stellen.

In de eerste plaats dank ik natuurlijk mijn ouders, die in mijn opvoeding een solide fundament hebben gelegd voor mijn wetenschappelijke nieuwsgierigheid en vorming. De manier waarop jullie mijn opleiding en onbezorgde studententijd hebben mogelijk gemaakt, zal ik altijd zeer blijven waarderen.

Dat de tijd, waarin het hierin beschreven onderzoek is uitgevoerd, voor mij is omgevlogen, ligt voor een niet onaanzienlijk gedeelte aan de ontspannen sfeer op ons lab, die nooit een remmend effect op mij scheen te hebben.

Beste Bert, zeergeleerde promotor, ondanks al jouw drukke commissie-werk vond je toch steeds tijd voor mijn onderzoek. Ik ben je dankbaar voor je suggesties, de grote mate van vrijheid die je me liet, en de critische precisie waarmee je dit manuscript hebt bestudeerd en verbeterd.

Beste Solke, hooggeleerde promotor, hoewel jij pas later in dit onderzoek betrokken werd, ben jij met jouw scherp analytisch inzicht een belangrijke stimulans voor mij geweest om het proces stofoverdracht in detail te doorgronden. Ik dank je voor de vele vruchtbare discussies en waardevolle ideeën.

Hooggeleerde Lyklema, beste Hans, dat jij nu eens geen promotor bent is voor ons lab een unicum, maar voor jouw spaarzame 'eigen' tijd vast een zegen. Ik zal me jouw creatieve kijk op de kolloidchemie altijd blijven herinneren. Hopelijk heeft deze ook mij geïnspireerd.

Geleerde de Keizer, beste Arie, ik ben je erg dankbaar voor je enorme hulp bij de automatisering van de transportmetingen.

Geleerde van der Put, beste Arnold, of we het PO-effect vaak genoeg hebben toegepast weet ik niet, maar ik dank je voor de vele discussies en de plezierige sfeer.

Truus Swinkels, door jouw vele, nauwgezette metingen zijn we op het goede spoor geraakt. Na jouw vertrek is dit door Anton Korteweg niet alleen vakkundig gevolgd maar ook verder uitgezet. Jullie assistentie bij de zeer tijdrovende experimenten is voor mij onmisbaar geweest.

Simon Maasland dank ik voor zijn technische medewerking bij het ontwikkelen van de opstellingen.

I am also indebted to John Stageman for correcting the English text, and that in such a short time.

Voor het accuraat uittikken en het onvermoeibaar verbeteren van mijn fouten dank ik Clara van Dijk en Sjan van Dijk heel hartelijk, evenals Gert Buurman voor het tekenen van de figuren.

Rees, door jouw liefdevolle verzorging en hulp heb ik de moed er ook op de soms moeilijke momenten in kunnen houden.

CONTENTS

GLOSSARY OF ABBREVIATIONS AND SYMBOLS

B1–B5	blocky PVA-Ac copolymers (ch. 3.3)
buOH	1-butanol
buwa	buOH saturated with water
DSC	differential scanning calorimetry
GPC	gel permeation chromatography
IAM	interface-active molecule
IR	infrared
isobuOH	isobutanol
MHS	Mark-Houwink-Sakurada
ppm	parts per million
PVA	polyvinyl alcohol
PVA-Ac	polyvinyl alcohol-acetate
PVAc	polyvinyl acetate
R1, R2	random PVA-Ac copolymers (ch. 3.3)
TGA	thermal gravimetric analysis
UV	ultraviolet
VA	vinyl alcohol
VAc	vinyl acetate
wabu	water saturated with buOH

SYMBOLS

Symbols that appear infrequently or in one section only are not listed. The numbers in parentheses after the description refer to the equation in which the symbol is first used or properly defined. Boldface symbols are vectors or tensors.

A	interfacial area (m^2); (4.2–1)
a	ratio of V_b and V_w; (4.2–1)
c	molar concentration ($kmol.m^{-3}$); for (co)polymers: weight concentration ($kg.m^{-3}$)
D	diffusion coefficient ($m^2.s^{-1}$)
$f_\pm$	mean activity coefficient; (2.3–1)
g	gravitational acceleration (9.81 $m.s^{-2}$)
$J^*, \mathbf{J}^*$	molar flux relative to $\mathbf{v}^*$ ($kmol.m^{-2}.s^{-1}$); (5.2–2)
K	average overall mass transfer coefficient ($m.s^{-1}$); (5.2–18)
K^*, K_v^*	viscosimetric constants ($dl.mol^{1/2}.g^{-3/2}$); (3.3–15), (3.3–18)
k	(average) partial mass transfer coefficient ($m.s^{-1}$); (5.2–14)
k_i	viscosimetric constant; (3.3–7)
L	a characteristic length of the system (m)

$\bar{M}_w, \bar{M}_v, \bar{M}_n$	weight, viscosity and number averaged molecular weight (g.mol^{-1})
m_{12}	distribution coefficient ($= c_1/c_2$)
N	rotation speed (s^{-1}), usually expressed in min^{-1}
$\bar{P}$	mean degree of polymerization
p	sequence probability; (3.3–1)
p	fraction of train segments of one macromolecule
R	overall mass transfer resistance (s.m^{-1}); (5.2–24)
R	gas constant (8.315 J.K^{-1}.mol^{-1})
R_N	retardation (K_b/K_β) at rotation speed N
r	partial mass transfer resistance (s.m^{-1}); (5.2–21)
r	radial distance in cylindrical coordinates (m)
S	amount of (co)polymer spread (mg.m^{-2})
T	(absolute) temperature (K, °C)
t	time (s)
V	volume (m^3)
$v, \mathbf{v}$	velocity (m.s^{-1})
W^n	molecular weight fraction of a given sequence length n; (3.3–4)
x	mole fraction
x, y, z	rectangular coordinates (m)
z	excluded volume parameter; (3.3–20)
α	linear expansion factor; (3.3–9)
Γ	interfacial excess amount (mol.m^{-2}); for (co)polymers often expressed in mg.m^{-2}
γ	interfacial tension (N.m^{-1})
Δ	adsorbed layer thickness (m)
δ	boundary layer thickness (m)
η	viscosity (kg.m^{-1}.s^{-1})
$[\eta]$	intrinsic viscosity (dl.g^{-1}); (3.3–7)
θ	fraction of the interface covered with train segments
κ	specific conductance (Ω^{-1}.m^{-1})
ν	kinematic viscosity (m^2.s^{-1})
Π	interfacial pressure $= \gamma_o - \gamma$ (N.m^{-1})
ρ	density (kg.m^{-3})
$\tau, \boldsymbol{\tau}$	momentum flux (kg.m^{-1}.s^{-2}); (5.2–12); shear stress; (6.5–1)
Φ, Φ_o	viscosimetric constants (mol^{-1}); (3.3–15), (3.3–18)
$\phi'', \boldsymbol{\phi}''$	molar flux relative to stationary coordinates (kmol.m^{-2}.s^{-1}); (5.2–3)
χ	polymer-solvent interaction parameter; (3.3–23)

OVERLINES

$-$	average value

In general, the superscripts refer to the quantity or substance mentioned.

e	equilibrium value
p	in the presence of (co)polymers
t	at time t; theoretical
$*$	molar average; (5.2–1)

SUBSCRIPTS

In general, the subscripts refer to the quantity or substance mentioned.

b	refers to the buwa phase
bw	refers to the buwa-wabu equilibrium system
exp	means an experimental value
ib	refers to isobuOH saturated with water
ibw	refers to mutually saturated isobuOH and water
N	refers to the rotation speed in the buwa phase
o	unperturbed; at infinite dilution
r	relative; (3.3–7)
r	radial (6.3–1); at distance r (6.3–9)
re	ratio excess; (3.3–7)
w	refers to the wabu phase
η	determined by viscosimetry
σ	interfacial property

DIMENSIONLESS GROUPS

Re	Reynolds number $= v\rho L/\eta$
Sc	Schmidt number $= \mu/(\rho D)$

1. INTRODUCTION

1.1. POLYMER ADSORPTION

In the last two decades, many theoretical and experimental studies have been performed on the mechanism of polymer adsorption and on the conformation which polymers attain at interfaces.

These studies are important not only from a purely scientific point of view, but also in relation to the variety of different applications of polymers at interfaces: as stabilizers of emulsions, foams and suspensions, as flocculation agents, adhesives, wetting agents and also as soil improvers. To comprehend this wide variety of effects brought about by polymer adsorption, a basic knowledge of the adsorption mechanism and of the detailed structure of the adsorbed macromolecules is indispensable.

Several different theoretical models, all based on a statistical thermodynamic approach, have been proposed to describe the final adsorption state. These are mainly applicable to homopolymers. The general acceptance of any of these models has been hampered by either the severe difficulty in experimental verification or the limited applicability of the theory itself. These different approaches and their results have been reviewed and discussed by STROMBERG (1967), VINCENT (1974) and LIPATOV and SERGEEVA (1974 & 1976). For a more complete theoretical introduction we refer, therefore, to these reviews.

Fortunately, general agreement exists on some of the theoretical aspects of homopolymer adsorption from not too poor solvents:

I. In spite of large differences in adsorption energy, polymers are able to adsorb at many dissimilar interfaces. This is attributed to the large number of segments per molecule that may gain free energy upon adsorption. However, as adsorption is, under the given circumstances, usually attended by a loss of entropy, it is generally assumed that there exists a critical minimum adsorption energy per segment below which no adsorption takes place. It must be remembered that there is not always an overall loss of entropy for the whole system, due to solvent or reconformation effects.

II. Usually, only portions of the segments are in direct contact with the interface in what are called trains, whereas the remainder sticks out into the solution as loops and tails. This explains why much more polymer material can be accomodated at the interface than necessary to form a flat monolayer.

III. The structure of the adsorbed layer depends mainly on the polymer-solvent, polymer-interface and polymer-polymer interactions, and, in addition, on the chain flexibility, the mean molecular weight and the concentration of the polymer.

The parameters that have mainly been used to characterize the conformation of adsorbed polymers are:

a) the total interfacial excess of adsorbed polymer, Γ, usually expressed in mg.m^{-2};
b) the average fraction of train segments of one macromolecule, p;
c) the fraction of the interface covered with train segments, θ;
d) the segment density distribution as a function of the distance to the interface, $\rho(z)$;
e) the adsorbed layer thickness, Δ.

These parameters are not all independent: e.g. the polymer conformation is fully characterized by the interfacial area A and $\rho(z)$.

Many experimental studies have been performed to verify the different theoretical approaches and to relate the experimentally accessible parameters Γ, p, θ and Δ with the factors that determine the structure of the adsorbed polymer layer (as mentioned under III). The following methods and techniques have been applied to obtain the various characteristics:

1. interfacial tension (γ) measurements, or determination of the difference in polymer concentration before and after adsorption (or spreading), as well as direct measurements of the interfacial concentration (e.g. ADAMS et al., 1971), to obtain Γ;

2. microcalorimetry (e.g. KILLMANN and WINTER, 1975; NORDE, 1976) and electrical double layer measurements (e.g. KOOPAL and LYKLEMA, 1975) as well as infrared (IR; e.g. FONTANA and THOMAS, 1961), electron spin resonance (ESR; FOX et al., 1974; ROBB and SMITH, 1974) and nuclear magnetic resonance spectroscopy (NMR; MIYAMOTO and CANTOW, 1972; COSGROVE and VINCENT, 1977), to determine p or θ;

3. ellipsometry (e.g. STROMBERG et al., 1970), measurements of the thickness of free polymer films (SONNTAG, 1976; VAN VLIET, 1977) and hydrodynamic measurements (e.g. FLEER, 1971; GARVEY et al., 1974 & 1976), to obtain Δ;

4. Monte Carlo simulation calculations (e.g. CLAYFIELD and LUMB, 1974; CLARK et al., 1975) that may, in principle, yield all these parameters.

Consequently, there seems to be a luxury of methods to test the theories; however, most of them are of rather limited applicability or provide only indirect information. We shall first consider the more general restrictions that inherently limit the application of these theories to the true adsorption process.
– One of the thwarting problems in polymer adsorption is the frequently established irreversibility of the adsorption process on the time scale of an experiment. However, the consequences of this phenomenon have repeatedly been neglected. Irreversibility implies, in any case, that the application of thermodynamic approaches, so also the use of statistical thermodynamics, is not allowed for a description of the actual adsorption state. It must also be realized that a steady state does not necessarily imply thermodynamic equilibrium.
– A closely related inconvenience inherent in polymer adsorption are the long relaxation times that may arise during the process. Although it is

generally assumed that reconformations of adsorbed polymers are the main cause of these frequently observed time effects, diffusion to the interface may also contribute to this phenomenon, but only at very low polymer concentrations. It is obvious that, mostly, the relaxation times for Γ, p and Δ are different. Thus, Γ or Δ may have a steady value, whereas p is still changing due to intramolecular reconformations.

Besides these rather universal limitations encountered in investigating polymer adsorption, all of the methods mentioned before have their specific restrictions as well:

ad 1. The measurement of γ is restricted to liquid-liquid or liquid-gas interfaces. In addition, application of Gibbs' adsorption law leads to improbably low values for the interfacial area per molecule, and is not allowed when the adsorption is irreversible. This point has been stressed by LANKVELD and LYKLEMA (1972); they proposed a local reversibility between segments in loops and trains. Therefore, $\partial\gamma$ must be primarily related with the sub-interface concentration. This new unknown parameter is only related to the bulk concentration provided the conditions of bulk and interface remain unchanged.

The measurement of changes in bulk concentrations is almost completely limited to systems with large interfacial areas (foam, sol, suspension or emulsion), but radiolabelled polymers can increase the applicability of this method. The determination of the available interfacial area is a separate problem, as it may depend on the cross-sectional area or on the adsorption free energy of the adsorbing molecules.

ad 2. Microcalorimetry and double layer measurements may both yield information concerning p or θ. However, these methods are indirect, as several assumptions must be made in the interpretation of the measured quantities.

All spectroscopic techniques are very direct. They seem promising for large solid-liquid interfaces. With IR spectroscopy, it is assumed that all adsorbed segments, and only these, give rise to a shift in IR absorption. Therefore, p and θ will be underestimated with this method. In addition, the method is limited to solvents that do not absorb IR radiation appreciably and to systems with low scattering.

In ESR spectroscopy, the incorporation of a spin label in the polymer and the analysis of the signal are the limiting factors, whereas the main problem with NMR spectroscopy is the sophisticated equipment required. Both methods detect a decrease in segmental motion. Since small loops also display restricted motion, they will partly be counted as trains. Consequently, both methods will overestimate p and θ.

ad 3. Ellipsometric measurements are mainly confined to systems with a large difference in refractive index between the adsorbed layer and the substrate. In addition, the latter must have a macroscopic and very homogeneous surface. A root mean square thickness can be calculated for the actual polymer film from the measured value of an equivalent homogeneous film thickness by assuming a function for $\rho(z)$.

Measurements of the thickness of free polymer films constitute a new interesting tool for the study of polymer adsorption at gas-liquid interfaces. In general this method will give too high values for Δ due to the polymers that may have been stuck to adsorbed ones during the draining process.

Viscosity, ultracentrifugation or electrophoresis measurements of bare and covered particles yield a hydrodynamic layer thickness that can be transformed into a value for Δ after some assumptions have been made.

ad 4. The Monte Carlo method allows the theoretical simulation of all configurations of a reversible system assuming a certain model. This can also lead to the determination of all thermodynamic properties of the system. The method seems promising, but has, as a result of the enormous computer requirements, up to now only been applied to one isolated polymer near an interface. As it is well known that the configuration of a single macromolecule is not typical for – and may be very different from – its configuration in an assembly of macromolecules in an adsorption layer, where inter-molecular interactions play an important role, the method has, up to now, only been of limited use. In addition, this method will always suffer from the approximations used to simplify the model (e.g. lattice model, perfect flexibility, no self exclusion).

1.2. OBJECTIVES OF THIS STUDY

From the preceding section it can be inferred that only measurements of γ and Γ are available to characterize macromolecular adsorption at liquid-liquid interfaces. However, these methods are not so very informative and have only limited applicability. Obviously, there is an urgent need for new experimental methods to characterize and elucidate polymer adsorption at liquid-liquid interfaces. Of course, this field of polymer and interface science is also of special interest to biochemists and technologists.

Recently, DE JONGE-VLEUGEL and BIJSTERBOSCH (1973) have proposed a quite unconventional technique to determine the degree of coverage, θ, of a liquid-liquid interface. They measured the rate of transport of electrolytes through the interface between mutually saturated water and 1-butanol in a stirred transport vessel. The presence of polyvinyl alcohol in the water phase appeared to decrease this rate drastically. This retarding effect was attributed to polymer adsorption at the liquid-liquid interface, and the decrease was even related directly to θ.

The aim of the present study is to further elaborate this approach and to attempt to prove the hypotheses that de Jonge-Vleugel and Bijsterbosch had to make in the interpretation of their measurements. In addition, we intend to use this method, together with the conventional techniques, to characterize the conformation of macromolecules at a liquid-liquid interface.

To obtain a better insight in the factors that may retard the transport rate, we first have made an analysis of the rate-determining step without adsorbed

polymers. With some preliminary experiments, we were able to demonstrate that the complex hydrodynamic conditions near the interface play a crucial role in the transfer process (SCHOLTENS and BIJSTERBOSCH, 1976; this study, chapter 4).

A lot of very relevant information on these phenomena could be obtained from the basic principles of chemical engineering. Therefore, we have made a thorough literature study on the fundamentals of diffusion, forced and spontaneous convection and on the influence of interface-active molecules thereupon. These aspects and the relevant experimental results taken from this discipline will be discussed in chapter 5.

LANKVELD and LYKLEMA (1972) found that, for polyvinyl alcohol, the adsorption at the water-paraffin interface is rather insensitive to the molecular weight of the polymer. They did measure, however, large differences in interfacial activity due to variations in the ever-present vinyl acetate groups in polyvinyl alcohol. We have found that different preparations with an almost identical acetate content and molecular weight still may display very different interfacial activities (chapter 4.3). An objective of the present study is, therefore, to investigate systematically the influence of not only the acetate content on the adsorption process, but also of the intra-molecular acetate distribution. For that purpose, we have prepared and characterized seven polyvinyl alcohol-acetate copolymers, differing only in acetate content and distribution (chapter 3). It will be shown that it is especially this intra-molecular acetate distribution that plays an important part in the solution and interface properties of the copolymers.

Finally, we shall describe the KCl transport measurements in a transport vessel with an improved flow pattern near the liquid-liquid interface (chapter 6). The effect of the different copolymers on the transport rate will be investigated. These measurements and the applicability of the proposed method will be discussed and related to the results obtained in the preceding chapters.

2. MATERIALS

2.1. GENERAL

In this chapter we have collected the relevant data on the materials used, with exception of the macromolecular preparations, which are treated in ch. 3. In particular, the physical properties of mutually saturated water and 1-butanol (wabu and buwa) and their KCl solutions are discussed. Consequently, our attention is not diverted by these considerations in subsequent chapters.

Unless otherwise stated, the quality of the chemicals was A.R. and the water was distilled once. KCl, K_2CO_3 (laboratory grade), 1-propanol, 1-butanol (buOH), 1-decanol, pyridine and stearic acid were obtained from E. Merck AG; isobutanol and acetic acid anhydride from J.T. Baker Chemicals BV; sodium dodecylsulphate and saponin (laboratory grade) from BDH Chemicals Ltd.; 1-octanol and polyethylene glycol (PEG 4000, practical) from Fluka AG; sodium oleate (pure) from Brocades-Stheeman & Pharmacia; Span 80 from Atlas Powder Co., and ω-aminocaproic acid from Aldrich Chemical Co. Inc.. Chromatography materials like Sephadex G-75, G-200 and Blue Dextran as well as K 25/100 and K 50/100 columns were obtained from Pharmacia Fine Chemicals. Poval PVA (Kuraray) was kindly supplied by Mitsubishi International GmbH, and Polyviol PVA by Wacker Chemie GmbH.

All glassware used was cleaned successively with chromic acid, dilute nitric acid, tap water and, finally, with distilled water. If necessary, the volumetric glassware was calibrated by weighing.

2.2. 1-BUTANOL

BuOH was always distilled before use. After completion of an experiment, the buwa solution was dehydrated with K_2CO_3 and the buOH was recovered by distillation; in general, the middle fraction (b.p. = 116–118 °C) was used again.

The relevant physical properties of water, buOH and their mutually saturated solutions as determined in this study are collected in table 2.2–1. The buOH fractions used for these measurements were distilled between 117 and 117.5 °C. Buwa and wabu solutions were made up by shaking required amounts of the components in a thermostatted water bath controlling to ±0.02 °C. To ensure saturation, there was always a small excess of the relevant component. After equilibration, they were kept in the bath for at least one day, in order to get clear solutions. The absolute densities (ρ) were measured with a pycnometer

TABLE 2.2–1. Physical properties of water, wabu, buwa and buOH at two temperatures.

	mole fraction		absolute density ρ $kg . m^{-3}$	viscosity η $kg . m^{-1} . s^{-1}$	kinematic viscosity v $m^2 . s^{-1}$
	x_{water}	x_{buOH}			
$T = 20.00 \pm 0.02\,°C$					
water	1.000	0.000	998.2	1.002×10^{-3}	1.004×10^{-6}
wabu	0.981	0.019	987.3	1.435×10^{-3}	1.454×10^{-6}
buwa	0.503	0.497	847.6	3.394×10^{-3}	4.004×10^{-6}
buOH	0.000	1.000	809.8	2.948×10^{-3}	3.640×10^{-6}
$T = 25.00 \pm 0.02\,°C$					
water	1.000	0.000	997.1	0.890×10^{-3}	0.893×10^{-6}
wabu	0.982	0.018	986.7	1.215×10^{-3}	1.231×10^{-6}
buwa	0.505	0.495	844.1	2.893×10^{-3}	3.427×10^{-6}
buOH	0.000	1.000	806.2	2.590×10^{-3}	3.213×10^{-6}

that was calibrated with boiled distilled water. The viscosity of the solutions was determined as described in ch. 3.3.4. All data are the mean value of at least three independent measurements leading to estimated inaccuracies of less than 0.2 $kg.m^{-3}$ for the density and less than 2×10^{-6} $kg.m^{-1}.s^{-1}$ for the viscosity data.

The solubility of buOH in water decreases with increasing temperature, while the reverse holds for the solubility of water in buOH. It is notable that buwa is more viscous than buOH, which may be due to hydrogen bonding between water and the alcohol molecules. It is highly uncertain, however, whether these observations allow any conclusions to be drawn as to the structure of the wabu and buwa solutions (FRANKS and IVES, 1964).

2.3. KCl SOLUTIONS

Unknown concentrations of KCl solutions were determined by conducto-metric titration with a standard $AgNO_3$ solution. To that end, a 10 ml sample of the KCl solution was pipetted. In order to decrease the solubility of AgCl, 10 ml ethanol was added and the solution was made up to 100 ml with distilled water. The titration of this solution was performed with a Metrohm Herisau Potentiograph (E 436), that was connected to an automatic buret (Metrohm Herisau E 436-D) and that recorded the conductivity with a conductivity meter (Philips PR 9510 cell with PW 9501 meter).

The distribution coefficient of KCl between buwa and wabu ($m_{bw} = c_b^s/c_w^s$) at $25.00 \pm 0.02\,°C$ was determined for the concentration range 0.02–0.15 $mol.l^{-1}$ in the water phase (fig. 2.3–1); m_{bw} can be considered to be constant within the range 0.04–0.15 $mol.l^{-1}$ and to amount to 1.72×10^{-2}. The KCl solutions were equilibrated in the same way as described in ch. 2.2.
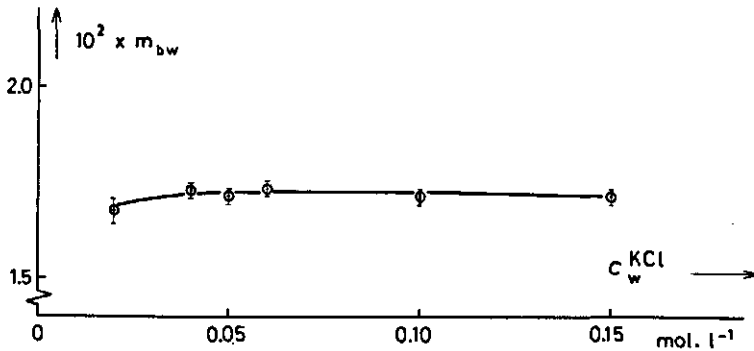
FIG. 2.3-1. The distribution coefficient of KCl between buwa and wabu as a function of the equilibrium KCl concentration in wabu ($25.00 \pm 0.02\,°C$).

Some useful physical properties of the equilibrated KCl solutions in wabu (0.100 M) and in buwa (1.72 mM) – the limiting values for a normal transport experiment – are summarized in table 2.3–1. Evidently, the solubility of water in buOH at 25°C decreases slightly with increasing KCl concentration (compare to table 2.2–1). The low value of m_{bw} means that the composition of wabu with respect to water and buOH may be considered to be constant during a normal transport experiment, while c_w^{KCl} decreases with less than 2%. The variation of the absolute density of KCl solutions of wabu and of their equilibrium buwa solutions with the KCl concentration in the wabu phase can be seen in fig. 2.3–2. Linear regression analysis of the data yielded $\partial\rho_w/\partial c_w^{KCl} = 0.0499$ kg.mol^{-1} and $\partial\rho_b/\partial c_b^{KCl} = -0.477$ kg.mol^{-1}.

In general, the diffusion coefficient of an electrolyte, D, is dependent on its concentration, c, and mean activity coefficient, $f_\pm$ (e.g. MONK, 1961). At low concentration, this can be expressed by:

$$D = D_o\,(1 + \partial\ln f_\pm/\partial\ln c) \tag{2.3–1}$$

where D_o is the diffusion coefficient at infinite dilution of the electrolyte ($f_\pm = 1$). During a transport experiment, D_w^{KCl} can safely be taken constant due to the

TABLE 2.3–1. Physical properties of 0.1 M KCl in wabu and its equilibrium buwa solution at $25.00 \pm 0.02\,°C$.

| | mole fraction | | absolute density ρ kg . m^{-3} | viscosity η kg . m^{-1} . s^{-1} | kinematic viscosity ν m^2 . s^{-1} |
	x_{water}	x_{buOH}			
0.100 M KCl in wabu	0.980	0.018	991.7	1.201×10^{-3}	1.211×10^{-6}
1.72 mM KCl in buwa	0.502	0.498	843.3	2.868×10^{-3}	3.401×10^{-6}
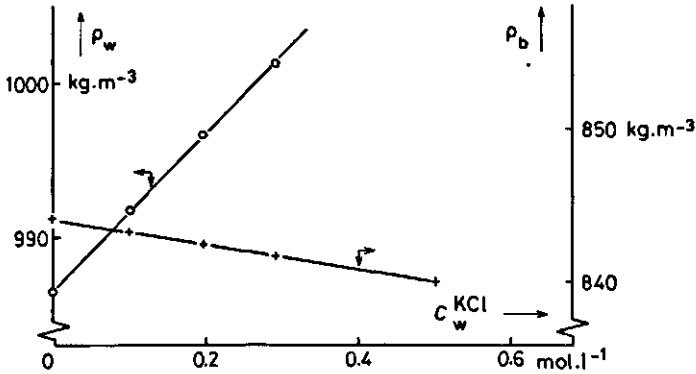
FIG. 2.3–2. The absolute densities of KCl solutions in wabu and of their equilibrium buwa solutions as a function of the equilibrium KCl concentration in wabu (25.00 ± 0.02 °C).

small variation of c_w^{KCl}. On the contrary, a considerable change in $f_\pm^{KCl}$ may be expected over the concentration range $c_b^{KCl} = 0$ to 1.72 mM because of the much lower relative dielectric constant (ε_b) of this medium. In order to determine $f_\pm^{KCl}$ and $\partial \ln f_\pm^{KCl}/\partial \ln c_b^{KCl}$, we applied the Debye-Hückel theory, which accurately predicts $f_\pm^{KCl}$ in water for concentrations up to 0.1 mol.l^{-1} (MAC-INNES, 1961 p. 164):

$$-\log f_\pm = \frac{A\sqrt{c}}{1 + \beta a \sqrt{c}} \tag{2.3–2}$$

where A and β are constants for a given solvent, and a is the distance of closest approach of the oppositely charged ions. A and β depend on the relative dielectric constant of the solvent and on the absolute temperature. The Kirkwood theory (HASTED, 1973) was applied to estimate ε_b and ε_w, using known values for water and buOH at 25°C (HANDBOOK, 1972). This resulted in $\varepsilon_w = 73$ and $\varepsilon_b = 27.4$, which is in good agreement with experimental values for mixtures of water with 1-propanol or isobuOH of the same molarity (FRANKS and IVES, 1964). With these estimated values of ε, A and β were calculated for both phases from their values for water at 25°C (MACINNES, 1961 p. 144). In table 2.3–2, $f_\pm^{KCl}$ and $\partial \ln f_\pm^{KCl}/\partial \ln c_b^{KCl}$ are summarized for different KCl concentrations. It can be inferred that, during a normal transport measurement, D_b^{KCl} will decrease by 6% at most.

The considerable decrease of $f_\pm^{KCl}$ in buwa in the concentration range is due to the low value of ε_b: this makes the interactions between the ions relatively strong, and suggests that incomplete dissociation of KCl in buwa should also be considered. Very accurate conductance measurements are essential for calculating the dissociation constant (MACINNES, 1961; MONK, 1961; DAVIES, 1962; NASH and MONK, 1958). The conductivity measurements in the present study do not have the required high absolute accuracy. Possible stray capacitance and polarisation effects were avoided by the usual methods, but

TABLE 2.3–2. Activity coefficients of KCl in wabu and buwa at 25 °C.

Phase	c^{KCl} (mol . l^{-1})	$f_\pm^{KCl}$ *)	$\partial \ln f_\pm^{KCl}/\partial \ln c_b^{KCl}$ *)
wabu	0.100	0.752	
buwa	0.0002	0.926	−0.027
	0.0005	0.887	−0.057
	0.0010	0.847	−0.078
	0.0014	0.823	−0.090

*) Calculated with the Debye-Hückel theory (2.3–2), using:
$A_w = 0.564\ l^{1/2} . mol^{-1/2}, \beta_w a = 1.386\ l^{1/2} . mol^{-1/2}$
$A_b = 2.45\ l^{1/2} . mol^{-1/2}, \beta_b a = 2.265\ l^{1/2} . mol^{-1/2}$.

the measurements are considered mainly valuable as a way of determining the concentration of KCl in buwa. Despite possible objections, the extended form of the limiting Onsager-Fuoss equation (e.g. MONK, 1961) was applied to the data. For KCl concentrations up to 6×10^{-3} mol.l^{-1} in buwa, no association could be inferred. At 10^{-2} mol.l^{-1}, the method failed in determining an association constant, probably due to the erroneous effects mentioned above. Results from NASH and MONK (1958) and MacINNES (1961 p. 215) for KCl and HCl in solutions of comparable ε also suggest that KCl is completely dissociated even at this low ε and relatively high concentration.

A continuous registration of the KCl concentration in buwa (c_b^{KCl}) is possible by measuring the specific conductance (κ_b^{KCl}) in this phase. This requires a standard graph of the relation between κ_b^{KCl} and c_b^{KCl}. The procedure to obtain the data for such a graph was as follows. The experimental set-up was the same as with a normal transport measurement (ch. 4). The stirrer was stopped intermittently and κ_b^{KCl} was determined when the phases were stationary. A sample was pipetted near the conductance cell, and κ_b^{KCl} was determined again. The KCl concentration of the sample was found by conductometric titration as described before. A rather unconventional plot was made of the KCl concentration against the mean value of the two determined specific conductances (fig. 2.3–3). With a curve fitted by regression analysis, the following relationship was established for the concentration range between 0.1 and 1.6 mmol.l^{-1}:

$$c_b^{KCl} = 0.03614\ (\kappa_b^{KCl})^{1.1304}\ mmol\ .\ l^{-1} \qquad (2.3–3)$$

where κ_b^{KCl} is expressed in $\mu\Omega^{-1}$. cm^{-1}.

For higher KCl concentrations (between 2 and 10 mmol . l^{-1}), the following formula holds:

$$c_b^{KCl} = 0.0204\ (\kappa_b^{KCl})^{1.300}\ mmol\ .\ l^{-1} \qquad (2.3–4)$$

A few transport experiments will be described with isobuOH instead of buOH (see ch. 6). For the distribution coefficient of KCl between the mutually

$$c_b^{KCl} = 0.03614 \, (K_b)^{1.1304} \quad mmol.l^{-1}$$
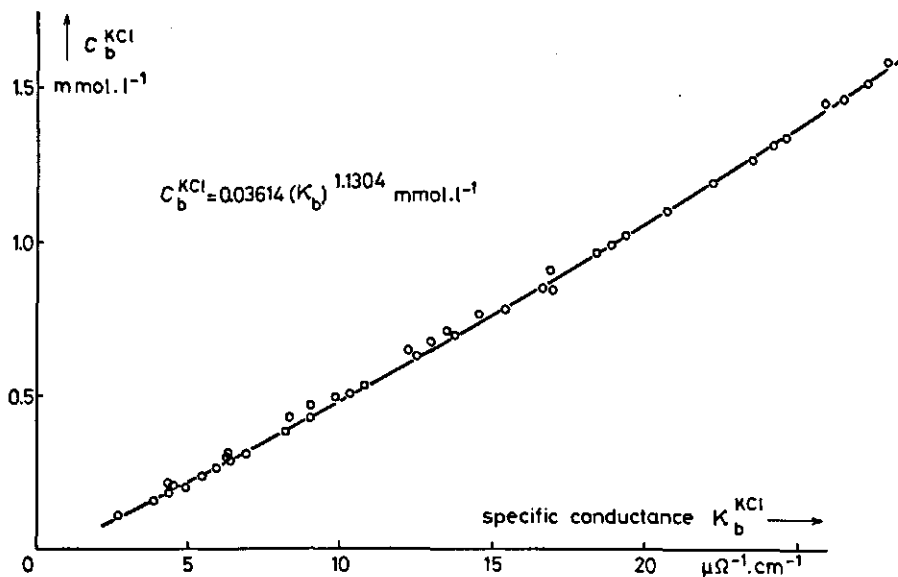
FIG. 2.3–3. The KCl concentration in buwa as a function of the specific conductance of that solution (25.00 ± 0.02 °C).

saturated phases ($m_{ibw} = c_{ib}^e/c_w^e$), the value of 9.47×10^{-3} applies when the aqueous equilibrium concentration is 0.1 mol.l^{-1}.

In the concentration range of 0.05 to 0.90 mmol.l^{-1} KCl in the isobuOH-water phase, the following relation was obtained:

$$c_{ib}^{KCl} = 0.0356 \, (\kappa_{ib}^{KCl})^{1.1921} \; mmol \, . \, l^{-1} \tag{2.3–5}$$

3. POLYVINYL ALCOHOL AND POLYVINYL ALCOHOL-ACETATE COPOLYMERS

3.1. GENERAL PROPERTIES

Polyvinyl alcohol (PVA) is a water-soluble non-ionic polymer with a wide variety of industrial applications. A relatively simple chemical structure $(-(CH_2CHOH)_n-)$ has led to its use as a model compound for hydrophilic polymers in physico-chemical studies (GLASS, 1968; LANKVELD, 1970; FLEER, 1971; BELTMAN, 1975; GARVEY et al., 1974 & 1976; KOOPAL, 1977; VAN VLIET, 1977). The commercial samples generally used for these studies may be considered to be copolymers (PVA-Ac), since they contained up to 15% vinyl acetate groups.

The following reviews deal with the properties and applications of PVA and PVA-Ac: PRITCHARD (1970) and FINCH (1968 & 1973a).

The preparation of PVA is usually started with the polymerization of vinyl acetate (VAc). This can be carried out as bulk, solution, emulsion or suspension polymerization, usually free radical initiated. Many important properties and irregularities of the resulting polymer originate from this first step, e.g.: molecular weight distribution, stereoregularity and the presence of branching, carbonyl groups ($>C = O$), 1,2-glycol groups ($-CH_2CHOH-CHOHCH_2-$), (conjugated) double bonds and terminal carboxyl groups (ZWICK and BOCHOVE, 1964; FRIEDLANDER et al., 1966; HACKEL, 1968; FUJII, 1971; NORO, 1973a; ADELMAN and FERGUSON, 1975).

During polymerization, branching may take place by chain transfer directly from the C–C backbone or via an acetate side chain (NORO, 1973a). It has often been established experimentally that the original PVAc has a higher average degree of polymerization $\bar{P}$ than the fully saponified product derived from it. Reacetylation of PVA results in PVAc with the same $\bar{P}$ as the saponified product. This is strong evidence for the occurrence of side chains attached to ester groups of PVAc that split off during saponification. However, there is no unanimity in the estimation of the velocity constants of the transfer reactions, and thus in establishing the relative frequency of occurrence of the two types of side chains (NORO, 1973a). FUJII (1971) and FINCH (1973b) assumed that the amount of side chains in PVA is small. FRIEDLANDER et al. (1966) and NOZAKURA et al. (1972a & b), however, showed that branching in PVA may amount to a considerable weight fraction of the total.

Head-to-head polymerization results in 1,2-glycol groups in PVA. The proportion depends on the polymerization temperature and on the degree of conversion (NORO, 1973a). Commonly, PVA and PVA-Ac contain about 0.5–1.5 mole % of these irregularities (PRITCHARD, 1970; TOYOSHIMA, 1973) which decrease the crystallinity and the melting point of PVA and PVA-Ac.

16

Termination of the polymerization usually takes place by disproportionation. The nature and number of end groups can vary considerably, depending a.o. on the type and amount of catalyst employed and on the number of hydrolysable branches. However, since the total amount of end groups is usually very small, they will not markedly affect the overall properties of the (co)polymers.

Various saponification methods can be applied to convert PVAc into PVA-Ac and PVA. Of these, alcoholysis (in methanol) and hydrolysis (in acetone-water mixtures) are the most important (HACKEL, 1968; SAKURADA, 1968; NORO, 1970 & 1973b). In both cases, acid or alkaline catalysis can be employed. PVA-Ac can also be obtained by reacetylation of PVA (BERESNIEWICZ, 1959a; HAYASHI et al., 1964a & 1965a; TUBBS, 1966; SAKURADA, 1968). Since all hydrolysable side chains have been split off in PVA, incompletely saponified PVA-Ac may be more branched than PVA or reacetylated PVA-Ac. Therefore, these copolymers may differ in branching and molecular weight distribution. The different methods of hydrolysing PVAc have a pronounced influence on the formation of structural irregularities and (for PVA-Ac) on the sequence length distribution of residual acetate groups.

Acid-catalysed hydrolysis and alcoholysis sometimes lead to unstable end groups, conjugated double bonds or carbonyl groups. This is due to the elevated reaction temperature, the presence of H^+ and O_2, and the low rate of hydrolysis. The residual acetate distribution is random (HACKEL, 1968; SAKURADA, 1968; NORO, 1970).

Alkaline catalysis is much faster and produces less structural defects. The reaction is autocatalytic, due to accumulation of catalyst near hydroxyl groups of PVA-Ac. This results in a blocky*) distribution of the residual acetate groups (BERESNIEWICZ, 1959b; SAKURADA, 1968; SHIRAISHI and TOYOSHIMA, 1973). NORO (1970) found that the more heterogeneous the reaction medium the more blocky is the intra-molecular acetate distribution and the broader is the inter-molecular degree of acetylation (see also BERESNIEWICZ, 1959b): during hydrolysis, the copolymer precipitates (the molecules with the highest molecular weight first), and the reaction continues on the solid phase by alkaline catalyst adsorbed near hydroxyl groups. The more apolar the solvent, the quicker this adsorbed phase reaction starts, which, in turn, increases the effect on the intra- and inter-molecular acetate distribution. This mechanism explains the common experimental observation that the high molecular weight fractions have a lower acetate content than the low molecular weight fractions of the same sample (BERESNIEWICZ, 1959b; BRAVAR et al., 1974).

*) In this study, the following types of copolymers are distinguished:
– random copolymers: the different monomer units are spread randomly (= statistically) over the chain;
– blocky copolymers : the average length of a series of the same monomer units is longer than for a random copolymer;
– block copolymers : contain only one series of the same monomer units and thus at most two of the other.

Reacetylation in a homogeneous medium (an aqueous PVA solution containing acetic acid) has a very low reaction rate and results in a random acetate distribution (SAKURADA and SAKAGUCHI, 1956; HAYASHI et al., 1964a & 1965a, see NORO, 1973b). PVA can also be esterified with acetic acid anhydride in hot pyridine, that serves as a catalyst and swelling agent (BERESNIEWICZ, 1959a; PRITCHARD, 1970). The acetate distribution resulting from this reaction has never been investigated as far as we know, but because of the inhomogeneity of the system this may well be blocky.

The intra-molecular acetate distribution governs important physical properties of the copolymer, e.g.: crystallinity, melting point (TUBBS et al., 1968), rate of dissolution and solubility in water (MOORE, 1968) and interfacial activity (HAYASHI et al., 1964 & 1965; TOYOSHIMA, 1968; NORO, 1970; SHIRAISHI, 1970). Qualitative and semi-quantitative information on this distribution can be obtained from IR spectroscopy (NAGAI and SAGANE, 1955; TUBBS, 1966; TSUNEMITSU and SHOHOTA, 1968), thermal analysis (TUBBS, 1966), colour intensity of the complex with iodine (HAYASHI et al., 1963; ZWICK, 1965) and emulsion stability and adsorption studies (HAYASHI et al., 1964 & 1965; TOYOSHIMA, 1968; SHIRAISHI, 1970; NORO, 1970).

The solubility and rate of dissolution of PVA and PVA-Ac in water are rather complex matters. Although the heat of dissolution of PVA becomes less negative with increasing temperature, PVA has to be dissolved in water at elevated temperatures to achieve a reasonable rate of dissolution. The many –OH groups of the polymer have a high affinity for water, but strong inter- and intra-molecular hydrogen bonding in the solid (the crystalline regions) extensively slow down the rate of dissolution. A temperature near the boiling point of water is needed, or at any rate above the glass temperature of PVA ($\pm 75\,^\circ$C) to break the internal hydrogen bonds in the solid and to dissolve the polymer. According to MATSUMOTO and IMAI (1959) stirring is needed for a few hours at 95–98 °C to dissolve PVA uniformly, otherwise the solution is not stable and shows a striking increase of viscosity with time.

Factors that oppose these internal hydrogen bonds also influence the solubility characteristics. The most important of these are stereoregularity and the presence of acetate groups, branching and other structural irregularities. It is most probable that the crystallinity of PVA proceeds in the order highly syndiotactic > atactic > isotactic (FINCH, 1973a p. 216). All commercial samples are derived from vinyl acetate and are essentially atactic (TINCHER, 1965; SAKURADA, 1968; FUJII, 1971; FINCH, 1973a p. 209). For this reason, differences in solubility behaviour between these samples cannot be attributed to differences in tacticity. Branching and structural irregularities decrease the crystallinity in the solid and facilitate dissolution, but usually the amount of these defects is low in PVA, and so they do not play an important role. The only remaining and probably the most important factor that can influence internal hydrogen bonds is the acetate content of the copolymer. PVA-Ac may have an acetate content up to about 30 mole % without losing its solubility in

water completely, but the VAc groups have a pronounced influence on the detailed solubility characteristics. The decrease in crystallinity of the solid due to bulky acetate groups facilitates the dissolution of the copolymer at lower temperature, but the hydrophobic character of the VAc groups leads to the critical temperature of phase separation of the copolymers decreasing with increasing acetate content (SHAKHOVA and MEERSON, 1972).

The final PVA and PVA-Ac solutions also behave differently at room temperature. In spite of the radical dissolution procedure, it is most probable that even dilute PVA solutions form aggregates at room temperature due to inter-molecular hydrogen bonds (PRITCHARD, 1970; GRUBER et al., 1974; KLENIN et al., 1974; KOLNIBOLOTCHUK et al., 1974). Probably, water is not a very good solvent for PVA, substantiated by the high value of the solvent-polymer interaction parameter χ in very dilute solutions (0.50 found by KAWAI, 1958, and 0.49 by FLEER, 1971), a relatively high Huggins coefficient (MATSUMOTO and IMAI, 1959; this study ch. 3.3.4) and a low exponential factor in the Mark-Houwink-Sakurada relation (PRITCHARD, 1970). The same factors that decrease the crystallinity of solid PVA and PVA-Ac (and increase the rate of dissolution) prevent aggregation in solution; thus, by introducing acetate groups in PVA, the stability of its solution is increased but the temperature of phase separation is lowered. The intra-molecular acetate distribution is of importance in improving the solubility characteristics of PVA-Ac. A single block of vinyl acetate groups has no effect on the rate of dissolution, and block copolymers precipitate in water when the insoluble vinyl acetate block is too long (TUBBS et al., 1968; SHIRAISHI, 1970). Thus, a random distribution seems to be most effective in decreasing the crystallinity of the solid and in stabilizing aqueous PVA-Ac solutions. The behaviour of blocky copolymers lies in between these extremes, and depends on the average sequence length and on the inter-molecular acetate distribution. The broader this distribution, the lower is the average acetate content needed to achieve phase separation at a given temperature.

Addition of 1-propanol or 1-butanol to an aqueous PVA solution increases its stability, although the polarity of the solvent decreases (WOLFRAM and NAGY, 1969). This has been explained by assuming, in addition to hydrogen bonds between mutual –OH groups, hydrophobic interaction between the alkyl chain of the alcohols and the non-polar basic chain of PVA. The temperature of phase separation of PVA-Ac is lowered by these additives (SHAKHOVA and MEERSON, 1972).

In conclusion, it can be stated that an elevated temperature is required to dissolve PVA in water and that aggregates are formed in PVA solutions at room temperature. Probably, water is a poor solvent for PVA. By introducing acetate groups in PVA, the rate of dissolution is increased, the aggregation in solution prevented, and the temperature of phase separation lowered. The more random the acetate distribution, the greater is this influence of the acetate groups on the solubility characteristics.

The interfacial properties of PVA and PVA-Ac have been investigated in many different ways: γ-measurements (e.g. HAYASHI et al., 1964; GLASS, 1968; LANKVELD and LYKLEMA, 1972), measurements of the thickness of free polymer films (VAN VLIET, 1977) as well as hydrodynamic measurements (e.g. FLEER, 1971; GARVEY et al., 1974 & 1976) have been performed and, in addition, measurements on emulsions stabilized by these macromolecules (TOYOSHIMA et al., 1968; SHIRAISHI, 1970; LANKVELD, 1970), and double layer capacity measurements (KOOPAL and LYKLEMA, 1975).

From these investigations it can be inferred, that the interfacial activity of PVA-Ac increases with acetate content, while the molecular weight of the copolymer is hardly of any influence. Often experiments have been performed with PVA-Ac containing approximately 12 mole % VAc, which in most cases exhibited high affinity isotherms. A very serious drawback of these copolymers is, that they are unfit for confirming theoretical adsorption models that have been developed for homopolymers, especially when the acetate distribution is not random. It is evident that the more hydrophobic VAc parts may increase the adsorption on a hydrophobic interface by enthalpic or entropic effects. The former refer to preferential interactions of the VAc groups with the interface (e.g. van der Waals forces). The latter may arise either by the release of solvent molecules with a relatively low entropy upon adsorption of VAc, or by a more disorganized conformation of the adsorbed copolymers.

Although it is very probable that not only the VAc content but also its intra-molecular distribution plays an important part in the adsorption process, very few investigations have been performed on this subject. HAYASHI et al. (1964 & 1965) were the first who did some experiments with blocky and random PVA-Ac. They found that at high concentrations the blocky copolymers were stronger interface-active, whereas at very low concentrations the opposite held. The inaccessibility of the Japanese literature and the difficulty of establishing this distribution for the commercial samples mostly in use are probably the reasons that no attention has been paid to this point in the many studies dealing with the interfacial properties of PVA-Ac. In ch. 3.3 and ch. 6 we shall further investigate the influence of the acetate distribution on the solution and interface properties of PVA-Ac.

3.2. DESCRIPTION OF THE COMMERCIAL PVA-AC TYPES USED

Because of the extensive experience with Polyviol PVA-Ac samples in our laboratory (LANKVELD, 1970; FLEER, 1971; KOOPAL, 1977), some of these were also selected for this study. They are listed in table 3.2–1, together with their degree of polymerization and acetate content. A more comprehensive description of them is given by KOOPAL (1977).

Poval PVA-Ac samples (table 3.2–1) were used to investigate whether or not the effects measured with Polyviol (and ascribed to copolymer adsorption, see ch. 4.3) were attributable to an accidental property of those preparations.

TABLE 3.2–1. Properties of Polyviol and Poval PVA-Ac samples.

sample code	degree of polymerization[*]) (unknown average)	acetate content[*]) %	acetate content[0]) (mol %, number average)
Polyviol:			
V 03/20	300	1.5	1.5
V 48/20	2000	1.5	1.3
V 03/140	300	12	12.1
V 40/140	2200	12	11.6
Poval:			
105	500	1–2	1.9
124	2400	1–2	1.4
205	500	11–13	10.0
224	2400	11–13	12.2

[*]) according to the supplier.
[0]) measured according to Japan Industrial Standard K 6726–1965 (FINCH, 1973 p. 565).

It appeared that Poval samples with approx. 2 mole % acetate groups (105 and 124) have quite different interfacial properties from the comparable Polyviol PVA-Ac types (ch. 4.3). This discrepancy in interfacial activity may be brought about by irregularities in chemical structure or by a different acetate distribution, as there is no clue to this effect in their overall acetate content. Spectroscopic and thermal-analytic methods can supply a greater insight in these presumed structural differences.

UV spectra were recorded with a Beckman Acta C III spectrophotometer. All aqueous PVA-Ac solutions were 0.1 % by weight.

The spectra of pure PVA-Ac should only exhibit a small absorption peak at about 213 nm, due to the acetate groups present. All Polyviol samples, however, displayed very strong absorption bands at 225, 280 and 330 nm. According to MATSUMOTO et al. (1958) and HAAS et al. (1963) these should be assigned to conjugated carbonyl groups of the following form:

$$- (C = C)_n - \overset{\displaystyle O}{\overset{\displaystyle \|}{C}} -$$
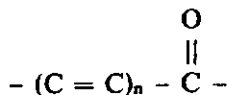
with $n = 1$, 2 and 3, referring, respectively, to the wavelengths mentioned. Haas et al. showed convincingly that the presence of acetaldehyde or oxygen during the polymerization of vinyl acetate brings about polyunsaturated aldehyde groups. TSUNEMITSU and SHOHOTA (1968) showed that these hydrophobic groups increase the interfacial activity of the polymer. Molar optical densities determined by NISHINO (1961) enabled the estimation of the carbonyl content

of the samples. On the basis of the degree of polymerization this resulted, in our case, in approximately one conjugated group per Polyviol molecule. This also suggests, that these conjugated carbonyl structures may be present as end groups.

Poval PVA-Ac samples did not exhibit any of these peaks. As expected, the height of the peak at 213 nm appeared to be roughly proportional to the acetate content of the copolymers. The UV spectra of two comparable PVA-Ac samples, viz. V 03/20 and 105, can be seen in fig. 3.2–1.
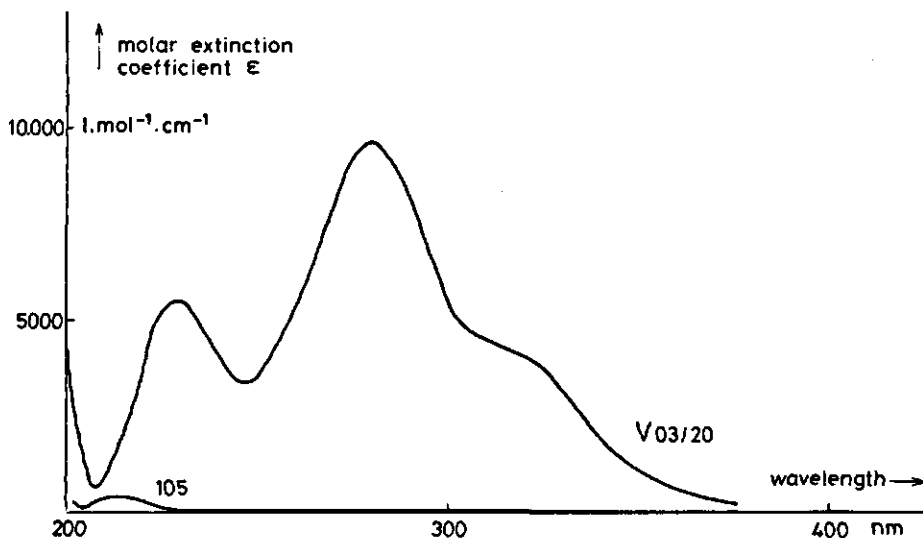
FIG. 3.2–1. The molar extinction coefficient of Polyviol V 03/20 and Poval 105 as a function of the UV wavelength.

In order to study the microstructure of the PVA-Ac copolymers, IR spectra were taken. They were run on a Hitachi EPI G–3 spectrophotometer. The samples were ground, sieved (mesh 0.05 mm), mixed with KBr and compressed into wafers with a hydraulic press.

Fig. 3.2–2 shows the IR spectra of PVA-Ac 105 and 205 as examples. We shall only discuss the relevant characteristics, as a more comprehensive summary of the main features of the IR spectrum of PVA can be found in FINCH (1973a p. 214).

The absorption peaks are all quite broad. According to PRITCHARD (1970), this is probably caused by differences in symmetry between molecules in crystalline and in glassy regions. There may even exist regions of intermediate crystallinity. All these regions themselves have a mixed symmetry due to different placement of hydroxyl (and acetate) groups along the (co)polymer chain. This gives a set of slightly shifted equivalent frequencies that result in a broad absorption peak.

Meded. Landbouwhogeschool Wageningen 77-7 (1977)

FIG. 3.2–2. IR absorption spectra of Poval 105 and 205.

The peaks at 916 and 850 cm^{-1} (skeletal vibrations) enable a semiquantitative estimation of the stereoregularity of the (co)polymers (MURAHASHI et al., 1966; KENNEY and WILLCOCKSON, 1966). As the 916 cm^{-1} peak is strongly influenced by the crystallinity, and thus also by the presence of acetate groups, this estimation is only applicable to samples with low acetate content. The samples under investigation all yielded values of A_{916}/A_{850}*) between 0.25 and 0.30. This implies roughly equal percentages of isotactic and syndiotactic diads and triads, irrespective whether the relation of Murahashi et al. or that of Kenney et al. was used. Thus, these samples can be qualified as essentially atactic.

The intensity of the 1144 cm^{-1} peak has been correlated with the degree of crystallinity of the PVA sample (TADOKORO et al., 1957; HAAS, 1957). It is also influenced, however, by the moisture content and the thermal history of the sample (HAAS, 1957; KENNEY and WILLCOCKSON, 1966).

Polyviol samples exhibited stronger absorption at 1144 cm^{-1} than comparable Poval PVA-Ac's. However, the spectrum of a cast film of the Poval sample (prepared as described in ch. 3.3.2) showed an absorption peak that was similar to the equivalent Polyviol copolymer. Thus, the observed differences in absorption of comparable Poval and Polyviol samples in KBr are probably due to a different thermal history and/or moisture content and not to pronounced differences in crystallinity. This was further affirmed by the fact that the volatile content of the Povals (4 weight %) was higher than that of the Polyviol samples (2 weight %). As expected, the absorption of the peak of 1144 cm^{-1} decreases with increasing acetate content. This is ascribed to the lower crystallinity of the copolymer due to the presence of bulky acetate groups.

A simple qualitative estimation of the intra-molecular acetate distribution has been suggested by NAGAI and SAGANE (1955). They attributed the shift of the ester carbonyl peak from 1735 to 1715 cm^{-1} to hydrogen bonding of the $>C = O$ group with an adjacent hydroxyl group (see also TUBBS, 1966; GULBE-

*) The absorbance A ($= {}^{10}\log (I_o/I)$) was calculated from the interpolated background intensity, I_o and the measured intensity, I.

KIAN and REYNOLDS, 1973). PVA-Ac samples that are partly hydrolysed with an alkaline catalyst (creating blocky copolymers) have a peak at 1735 cm^{-1}, which corresponds to PVAc. Randomly reacetylated samples have a peak at 1715 cm^{-1} with a shoulder at 1735 cm^{-1}. The 1735 cm^{-1} peak shifts to 1715 cm^{-1} when the blocky copolymer is dissolved in D$_2$O (COHEN STUART, 1976), also supporting the hypothesis that this shift is due to hydrogen bonding. We have analysed our spectra bearing all this information in mind, together with the fact that the spectrum of a blocky copolymer will display more clearly the aspects of the spectrum of a mixture of the two homopolymers than that due to a random copolymer.

In our case, the samples with low acetate content exhibited a peak at 1715 cm^{-1} and a shoulder at 1735 cm^{-1}, whereas the others had a peak at 1735 cm^{-1} cm^{-1} and a shoulder at 1715 cm^{-1}. The shoulder at 1735 cm^{-1} of the low acetate Polyviol samples was slightly stronger than for comparable Poval samples. The shoulder at 1715 cm^{-1} for the samples with the higher acetate content was slightly stronger for the Poval samples. Thus, it can be concluded that the acetate distribution is blocky for the PVA-Ac samples containing 11–13% acetate (slightly more blocky for Polyviol than for Poval). Although all samples were saponified by alkaline alcoholysis (WACKER, 1975; KURARAY, 1976), the almost completely saponified samples seem to have a more random acetate distribution (Poval slightly more than Polyviol). At very low acetate content, the differences in absorption frequencies of the blocky and random PVA-Ac's decrease. In the limiting case of one or two acetate groups per molecule, all carbonyl groups have an adjacent hydroxyl group and, therefore, it seems likely that the method does not discriminate between two separate acetate groups and one block of two acetate groups. The fact that, in general, Polyviol PVA-Ac samples seem to be slightly more blocky than comparable Povals may be due to small differences in the conditions of hydrolysis.

The melting point of a semicrystalline copolymer depends on the mean sequence length of the crystallizable units. FLORY (1955) treated this problem theoretically, and experimental evidence has been obtained in reasonable agreement with this theory (JACKSON, 1963; TUBBS, 1965 & 1966). In principle, the acetate distribution in PVA-Ac can be estimated from the difference in melting point between the copolymer and its (PVA) homopolymer, and its acetate content (TUBBS, 1966; this study ch. 3.3.3). In this section, only qualitative conclusions are possible, since the corresponding homopolymers were neither commercially available nor prepared.

Melting points were determined with the Du Pont 990 Thermal Analyser (Differential Scanning Calorimeter). Each determination required a sample of approximately 20 mg which was heated at a rate of 5 or 10 K.min^{-1} under a nitrogen atmosphere. Melting points were identified with the minimum of the melting endotherm (see also ch. 3.3.3). This point appeared to be reproducible and is probably very close to the point at which the melting process ends, which is, by definition, the melting point of a (co)polymer. The rate of

TABLE 3.2–2. Dependence of the melting points of the commercial PVA-Ac samples on their acetate content.

sample code	acetate content mole %	melting point (DSC) K
Polyviol:		
V 03/20	1.5	492
V 48/20	1.3	497
V 03/140	12.1	460
V 40/140	11.6	458
Poval:		
105	1.9	500
124	1.4	502
205	10.0	471
224	12.2	460

heating had no influence on the melting point in this trajectory. Table 3.2–2 summarizes the sample codes, their acetate content and their melting point. The melting points of Poval PVA-Ac's are systematically higher than those of comparable Polyviol samples, except for the 224. This may be due to some branches in 224 that may occur at higher conversion and that have been split off in PVA-Ac 124. The lower melting points of Polyviol PVA-Ac's may be due to a higher 1,2-glycol content, more branching, or the presence of conjugated carbonyl structures (especially important for V 03/20 and V 03/140), as the tacticity is almost the same for all samples.

An attempt was made to fractionate the various samples and to determine their molecular weight distribution by means of gel permeation chromatography (GPC). GARVEY et al. (1974) successfully used Sephadex G-75 to fractionate PVA-Ac with a polymerization degree between the low and high molecular weight products of this study.

Therefore, a K 25/100 column was packed with this gel, as described by FISCHER (1971). The column was thermostatted with a jacket at 25.0°C. To prevent bubble formation in the column, all solutions and the eluant were deaerated before use. The samples were applied with a syringe in the tubing of the lower adaptor. The flow was upward in order to decrease the tendency of the bed to pack. The fractions were collected with an LKB 3400 B Radirac fraction collector with a 9.8 ml syphon.

Before use, the column packing was checked with a Blue Dextran solution. We also checked that the samples did not adsorb at the gel. The optimal sample concentration was determined by applying different sample volumes and concentrations, keeping the total amount of (co)polymer constant. The elution patterns at high sample concentrations changed with the sample concentration. This effect was ascribed to zone broadening due to a too high relative viscosity of the solutions. Since no broadening was detectable at sample concentrations below approx. 0.5 weight % (depending on the molecular weight),

a concentration of 0.3 weight % was chosen for all experiments at a flow rate that was never higher than 60 ml per hour. However, the elution curves of Blue Dextran and the PVA-Ac solutions appeared to be almost identical, although their average molecular weights differ by at least a factor 100. The samples with the lowest polymerization degree were the only ones exhibiting different elution diagrams, their low molecular weight tail being much longer. Therefore, it was concluded that the fractionation range of Sephadex G-75 for PVA-Ac lies at molecular weights below 20 000.

Further investigation of the GPC applicability was carried out by packing a K 50/100 column with G-200. The fractionation range of this gel lies at molecular weights that are about five times higher than for G-75. As the elution diagrams of Blue Dextran and also of high and low molecular weight PVA-Ac samples were different now (see fig. 3.2–3), the usefulness of this gel was investigated further.

To achieve the highest possible concentration in the collected fractions, we determined the maximum sample volume that did not give rise to peak broadening. After having assessed that the elution curves were reproducible, we fractioned Poval 124 by applying 50 ml samples (0.3 weight %). As the maximum yield in one fraction amounted to only 10 mg PVA-Ac (after 10–15 hours elution), the corresponding fractions of 20 different runs were combined and a few of these solutions were freeze-dried (Leybold Heraeus GT2).

These fractions and all unfractionated commercial samples were analysed with an analytical gel permeation chromatograph (Waters Associates). The columns were calibrated with highly monodisperse polystyrene (PS) samples from Pressure Chemical Company, Pittsburg, since well-defined narrow molecular weight fractions of PVA were not available. Details of the columns, eluant and calibration procedure are described by KOOPAL (1977).

The molecular weight of PVA-Ac was estimated by assuming an identical stretched chain length for PVA-Ac and PS at every elution volume. Although this simple approach is perhaps not the most realistic one, we felt it was suitable for the comparison of the resulting molecular weight distributions of the
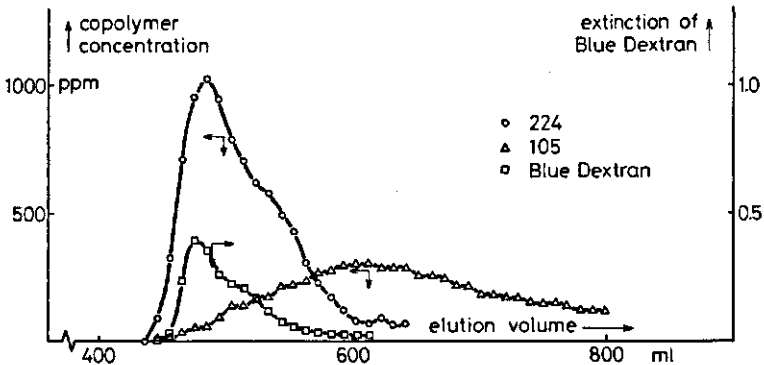

FIG. 3.2–3. Elution curves of Blue Dextran, Poval 224 and 105 in a K 50/100 column packed with Sephadex G-200.

TABLE 3.2–3. GPC results of the commercial PVA-Ac samples.

sample code	$\overline{M}_n$	$\overline{M}_v$*)	$\overline{M}_w$	$\overline{M}_w/\overline{M}_n$
Polyviol:				
V 03/20	10000	22000	25000	2.4
V 48/20	29500	151000	189000	6.4
V 03/140	9000	26500	32000	3.6
V 40/140	34000	444000	645000	19
Poval:				
105	21000	41500	46500	2.2
124	91000	194000	220000	2.4
205	19500	39000	43500	2.2
224	68000	165000	191000	2.8
Poval 124**):				
124/51	167000	276000	301000	1.8
124/56	122000	216000	241000	2.0
124/64	84000	163000	186000	2.2

*) calculated using a $= 0.7$.
**) fractionated with Sephadex G-200 in a K 50/100 column.

different PVA-Ac samples and for a rough determination of the efficiency of the preparative fractionation method. Table 3.2–3 summarizes the average molecular weights thus obtained. No correction was made for the Gaussian peak broadening that was due to the imperfection of the instrument (the elution diagrams of PS with $\overline{M}_w/\overline{M}_n < 1.1$ yielded $\overline{M}_w/\overline{M}_n = 1.4$ with this analytical GPC). The values for V 40/140 may be not correct due to a slightly shifted base line.

Generally speaking, it can be stated that Polyviol PVA-Ac has a considerable broader molecular weight distribution than comparable Poval PVA-Ac's. Moreover, the variations in molecular weight distribution are much larger for Polyviol than for Poval samples. These are probably caused by the different polymerization methods employed for Polyviol samples: those with a low $\overline{P}$ being produced by bulk polymerization, and those with a high $\overline{P}$ by emulsion polymerization (WACKER, 1975). This means that it is impossible to determine the Mark-Houwink-Sakurada relation for the Polyviol preparations based on their $\overline{M}_w$ or $\overline{M}_n$ values, which conclusion is supported by the unsuccessful efforts of FLEER (1971) and KOOPAL (1977) to establish this relation for Polyviol samples. In addition, the high molecular weight preparations may contain interface-active admixtures that were necessary to emulsify the monomers. In contrast, the Poval samples are all prepared by continuous solution polymerization (KURARAY, 1976), and thus the width of their molecular weight distribution is affected only by the different degrees of conversion (FLORY, 1953 p. 334), resulting in slight differences between these, without any admixtures present.

Obviously, PVA-Ac can be fractionated with GPC, but the improvement is limited and the yield is poor. The sharpness of the fractions may be en-

larged by using longer or multiple columns and smaller sample volumes.

In general, copolymer fractionation may be attended by special difficulties due to the uneven distribution of the monomers over the molecules. Although one of the monomers may be present in the copolymer in a large excess, the amount and distribution of the other monomers may also play an important part during fractionation. For this reason, differences in adsorption behaviour (mainly of importance in foam fractionation and GPC), in solubility in a given solvent (primarily in precipitation fractionation), and in molecular dimensions in solution (in GPC) will result in additional fractionation on chemical composition. These difficulties may be avoided for PVA-Ac by fractionating the homopolymers (PVA or PVAc). The fractions can be converted to copolymers afterwards. If PVAc is used as homopolymer, it should have been hydrolysed completely and reacetylated to avoid a later influence of hydrolysable side-chains on the molecular weight.

Summarizing, the following conclusions can be drawn. From UV spectra it was gathered that all Polyviol samples contain approximately one conjugated carbonyl group per molecule. The acetate distribution in Poval PVA-Ac is in all probability slightly more random than in Polyviol, as was inferred from the IR spectra. Nevertheless, the melting points of Polyviol PVA-Ac's are lower than those for comparable Poval samples. As the tacticity was identical, this was attributed to a higher content of chain irregularities in Polyviol samples. We inferred from GPC that the molecular weight distribution of Poval PVA-Ac's approaches the most probable distribution. The Polyviol PVA-Ac's, however, have a much broader distribution, while the emulsion polymerized samples may contain interface-active admixtures. Therefore, taking all these observations into account, Poval samples seem more suitable as model compounds than Polyviol samples.

3.3. Preparation and characterization of PVA-Ac copolymers with identical degree of polymerization but with different monomer composition

3.3.1. *Introduction*

The acetate content and distribution in PVA-Ac have a pronounced influence on the interfacial activity of the copolymers, much more so than differences in molecular weight. We made a systematic study on the influence of these two factors by changing them independently.

For that purpose, copolymers were prepared in two different ways by reacetylation of a completely hydrolysed PVA. This ensured that the starting material did not contain further hydrolysable side chains which could change the molecular weight distribution during the reaction. A Kuraray sample (PVA-H, Lot no. 340345) was chosen for reasons explained in ch. 3.2. PVA-H has a mean degree of polymerization of 1700–1800 and a degree of hydrolysis higher than 99.9 mole % (KURARAY). The polymer is hygroscopic (it con-

tained 9.2 weight % moisture before use) and containes about 3 weight % ashes. These ashes consisted of absorbed salt and salt formed between PVA and sodium ions. The absorbed salt is mainly sodium acetate (inferred from its IR absorption band at 1570 cm^{-1}) that could be removed by extracting the polymer thoroughly with acetone.

Blocky copolymers were prepared by partial reacetylation of PVA-H, swollen in pyridine, with acetic acid anhydride. A detailed description of the experimental conditions can be found in appendix A. The five samples are numbered B1–B5.

Two random copolymers (R1 and R2) were prepared by a homogeneous reaction of acetic acid with PVA in water, as described in appendix B.

These preparative methods ensured that all samples had an identical degree of polymerization and tacticity. In table 3.3–1 we have collected some of their properties. The absorbance refers to the colouring intensity of the complex between the ester oxygens of PVA-Ac and I_2 (PRITCHARD et al., 1972). It is well known to increase with acetate content, especially when the acetate distribution is blocky (NORO, 1970). These results are a first indication that the B samples are more blocky than the R preparations.

Oxidation or dehydration might have taken place during acetylation at the elevated reaction temperatures, in spite of the almost oxygen-free atmosphere. The UV spectra of the acetylated samples showed them to be free of any conjugated carbonyl structures.

To further characterize the (co)polymers, IR spectroscopy and thermal analysis were applied. The experimental details were identical to those described in ch. 3.2. In addition we studied the solution properties of these (co)polymers in water and wabu, and their interfacial properties at the wabu-buwa interface.

3.3.2. IR spectroscopy

Unfortunately, the R samples could not be ground into fine particles (a necessity for IR measurements with KBr wafers), probably because of the

TABLE 3.3–1. Some specifications of PVA-H and of the reacetylated samples.

sample code	volatile content (weight %)	degree of hydrolysis mole fraction VA	absorbance A^*) (at 480 nm)
PVA-H	0.8	>0.999	0.0
B1	<0.1	0.976	0.0
B2	<0.1	0.932	0.1
B3	<0.1	0.880	0.5
B4	<0.1	0.787	1.6
B5	<0.1	0.733	1.8
R1	0.8	0.937	0.1
R2	0.8	0.834	0.2

*) The solutions measured consisted of 2 ml aqueous solution of $0.006 \, mol \, . \, l^{-1} \, I_2$ and 0.018 $mol \, . \, l^{-1} \, KI$, added to 8 ml of an aqueous (co)polymer solution of 0.5% by weight.

low level of crystallinity. Therefore, films were cast on a metal plate out of 0.5% aqueous solutions. The films were dried in an oven at 80°C (B4 and B5 were dried at lower temperatures with a ventilator, as they precipitate in water at 80°C) and they were removed carefully from the plate before they were cooled down, to prevent tearing.

An increasing intensity of absorption at 606, 950, 1250 and 1380 cm^{-1} with acetate content was similar for the B and R series. These wave numbers are ascribed to the out-of-plane bending of CH_3COO-, the CH_3- rocking, the C-O- stretching and the CH_3- wagging vibration respectively, in analogy with the IR spectrum of PVAc (STOKR and SCHNEIDER, 1963).

Differences between B and R samples were observed at 916, 1144, 1715 and 1735 cm^{-1}. In fig. 3.3–1, we have plotted the absorbance of all samples at these wavenumbers. The skeletal vibration of PVA at 916 cm^{-1} has been decreased more strongly in R than in B samples. The B samples are thus showing more of the spectrum characteristic of PVA, indicative of a blocky acetate distribution. This effect is still more pronounced with the crystalline-sensitive 1144 cm^{-1} band: B5 shows an absorption peak, whereas R2 does not.

Further evidence for the assumed distributions was obtained from the $C = O$ stretching vibrations at 1715 and 1735 cm^{-1}. The R samples have a high absorbance at 1715 cm^{-1} with a shoulder at 1735 cm^{-1}, whereas all B samples (except B1 which has a very low acetate content) display a strong peak at 1735 cm^{-1} with a shoulder at 1715 cm^{-1}. The B samples are thus showing more of the spectrum of PVAc, again indicative of a blocky acetate distribution. At very low acetate content, it is difficult to discriminate between blocky and random copolymers, as both are almost homopolymers.

These measurements and the observed differences in crystallinity indicate also that the B samples were indeed more blocky than the R preparations.

3.3.3. *Thermal analysis*

The melting process of a crystalline homopolymer occurs over a range of a few degrees when the rate of heating is slow enough. The temperature at which this process ends abruptly is called the melting point (T_M). In copolymers, the range of melting is much broader and the melting point (T_M) is ill-defined. This is due to differences in sequence size of crystallizable units by the presence of non-crystalline comonomer units.

It is known that the crystallinity and melting point of PVA-Ac vary with the tacticity, 1,2-glycol content and with the content and distribution of residual acetate groups (TUBBS, 1966; TUBBS et al., 1968). The greater the portion of these bulky acetate groups and the more random their distribution in a given copolymer, the less crystalline it is and the more its melting point has been decreased. Data on the melting point depression caused by non-crystalline copolymer units can be analysed according to two different theories (FLORY, 1955; BAUR, 1966a & b).

Flory assumed that the crystallization process proceeded according to an ordered selection: as the melt is cooled, the longest sequences will crystallize
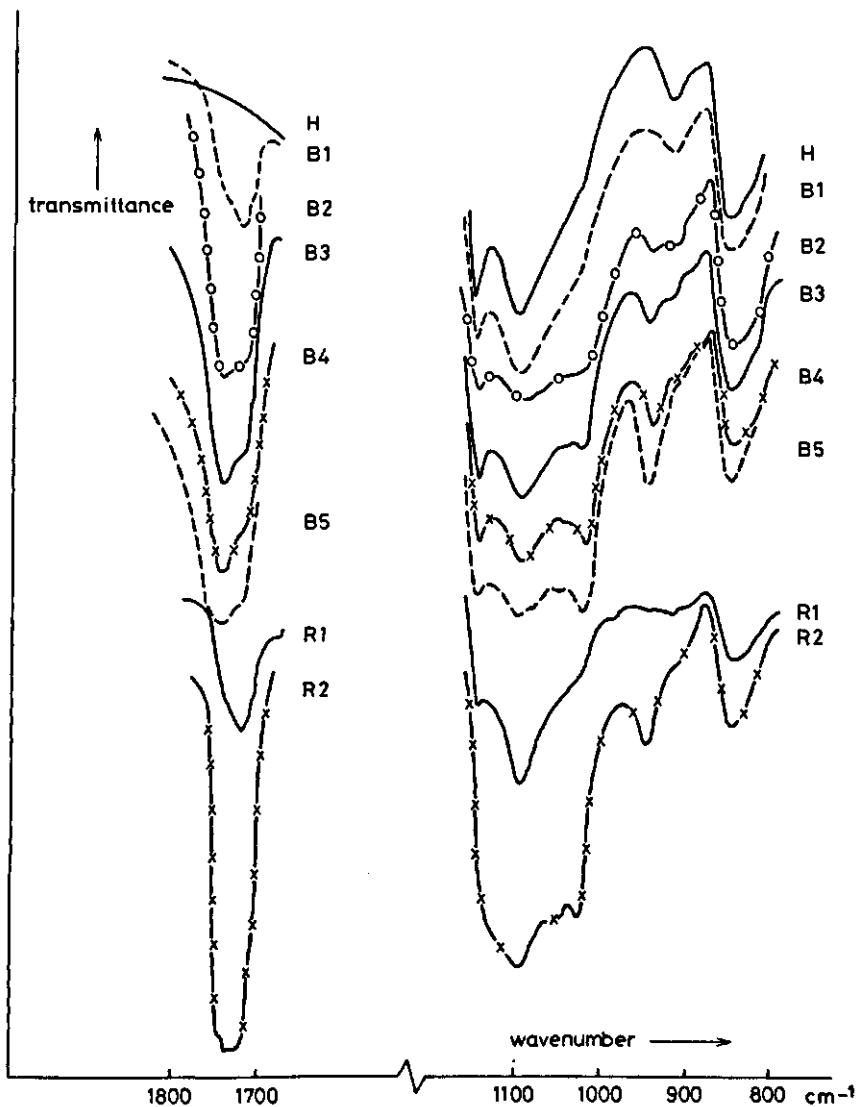
FIG. 3.3–1. IR absorption peaks of PVA-H and its reacetylated copolymers. The transmittance axis is shifted for the different spectra in order to comprime them into one graph.

first, followed by successively shorter ones. The melting process was considered to proceed in a reverse way. Flory derived the following expression for the melting point of a copolymer:

$$(T_M)^{-1} - (T_M^o)^{-1} = - (R/\Delta H) \ln p_A \qquad (3.3-1)$$

where T is expressed in K;

R = the gas constant $(8.315 \text{ J.K}^{-1}.\text{mol}^{-1})$;

ΔH = the heat of fusion per mole of crystalline segments (J.mol^{-1});

p_A = the sequence probability of the crystallizable monomer (vinyl alcohol); it is supposed to be independent of the number of preceding A groups in the sequence.

Baur treated this problem by a different approach. He assumed that all sequence lengths were present in the melt and in crystalline parts during any part of the melting process. His expression for the melting point depression was:

$$(T_M)^{-1} - (T_M^0)^{-1} = -(R/\Delta H) (\ln p_A - 2(1-p_A) x_A) \qquad (3.3-2)$$

where x_A is the mole fraction of crystallizable monomers.

BAUR (1966) and TUBBS et al. (1968) showed that the latter theory predicted a value of ΔH that compared better with results obtained with other techniques. We shall demonstrate that the differences in monomer distribution, as predicted by both theories, are less pronounced.

For random copolymers, p_A equals the mole fraction x_A of the crystallizable groups, and for blocky copolymers p_A is greater than x_A (FLORY, 1955). Melting points of random copolymers (with known p_A) enable the calculation of ΔH, using (3.3-1) or (3.3-2). When the melting point of the blocky copolymer is known, the same formulas enable the calculation of p_A for that copolymer.

TUBBS (1966) suggested a method to calculate the sequence length distribution of a blocky copolymer from this value of p_A. He assumed an identical, normalized sequence length distribution of crystallizable units for copolymers that melt at the same temperature. This assumption means that the number of vinyl alcohol – vinyl acetate pairs, normalized to the amount of vinyl alcohol units present, is the same for all copolymers with the same T_M. This leads to the sequence probability of the vinyl acetate units (p_B), as the number of A–B pairs is equal to the number of B–A pairs:

$$x_A (1 - p_A) = x_B (1 - p_B) \qquad (3.3-3)$$

When maximum randomness is also assumed for the determination of the sequence distribution of the B units, the molecular weight fractions W_A^n and W_B^n of a given sequence length n of A and B monomers may, according to FLORY (1953 p. 320), be calculated with:

$$W_A^n = n x_A (1 - p_A)^2 p_A^{n-1} \qquad (3.3-4)$$

$$W_B^n = n x_B (1 - p_B)^2 p_B^{n-1} \qquad (3.3-5)$$

These considerations lead to the conclusion that the melting point of a PVA-Ac copolymer may yield direct information on the acetate sequence length distribution if two reasonable assumptions are made. There must, of course, be no admixtures present in the samples that might influence the melting point, and the copolymers must have identical tacticity. This was guaranteed for all acetylated PVA-Ac copolymers by their method of preparation.

32
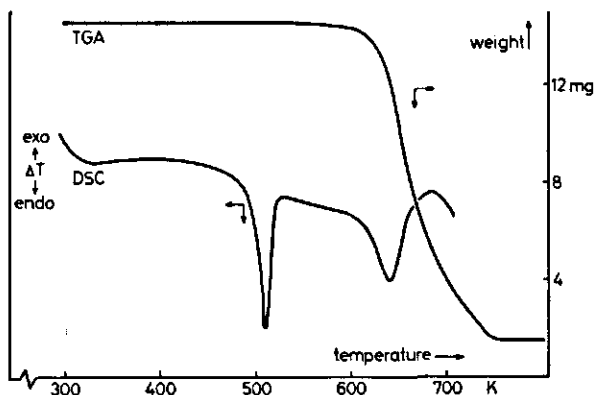
FIG. 3.3-2. Thermal analysis of PVA-H (explanation is given in the text).

The DSC measurements were combined with a thermogravimetric analysis (TGA, with a DuPont 950), in order to make sure that the endotherm was due to the melting process and not to decomposition. In all cases, decomposition started at temperatures above 580 K; thus, it can be concluded that the melting point was not affected by decomposition. A typical example of a DSC and a TGA plot (for PVA-H) is shown in fig. 3.3-2.

The melting points of all samples were determined, except for R2. This sample did not show an endotherm. The statistically divided acetate groups were probably so effective in decreasing the crystallinity, that no crystalline regions were present any more. The results of the measurements are collected in fig. 3.3-3, where the observed melting points of the samples are plotted against their acetate content. The ΔH for vinyl alcohol segments was calculated

FIG. 3.3-3. Melting points of PVA-H and of the reacetylated copolymers as a function of their acetate content.

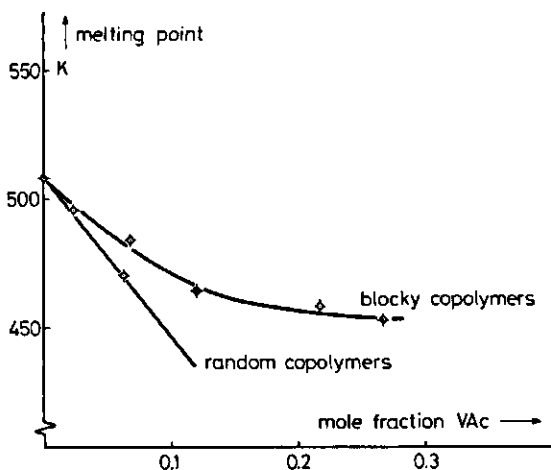| sample code	mole fraction vinyl alcohol	$T_M(K)$	L_{VA}*)	L_{VAc}*)		
PVA-H	1.00	508				
R1	0.937	470	16	1.1		
R2	0.834	–	6	1.2		
			$L_{VA}^0)$	$L_{VAc}^0)$	$L_{VA}^+)$	$L_{VAc}^+)$
B1	0.976	496	52	1.3	¹ 54	1.3
B2	0.932	484	26	1.7	26	1.9
B3	0.880	464	14	1.9	13	1.8
B4	0.783	458	12	3.3	11	2.9
B5	0.733	453	11	3.9	9	3.3

L_{VA} = number averaged vinyl alcohol sequence length.
L_{VAc} = number averaged vinyl acetate sequence length.
*) The distribution of the random copolymers was calculated directly with (3.3–4) and (3.3–5) using $p_A = x_A$ and $p_B = x_B$.
⁰) Calculated with (3.3–1).
⁺) Calculated with (3.3–2).

from the melting points of PVA-H and R1 using both methods. Next, p_A could be calculated for all copolymers with (3.3–1) or (3.3–2), using known values for T_M, T_M^0, ΔH and x_A. The vinyl acetate sequence length distribution was calculated with (3.3–5), using (3.3–3) to determine p_B. Table 3.3–2 summarizes the results of these measurements and calculations. It can be inferred, that the values of the mean vinyl alcohol and vinyl acetate sequence lengths (L_{VA} and L_{VAc} respectively) of the copolymers are not very sensitive to the method of calculating p_A. This is in contrast with the values of ΔH, for which we found 3.4 kJ.mol⁻¹ with Flory's theory, and 9.6 kJ.mol⁻¹ with Baur's theory. Fig. 3.3–4 contains the vinyl acetate sequence length distribution using Baur's method.

The melting point of the fully hydrolysed PVA-H corresponds well to values found for atactic PVA (500–513 K; TUBBS and WU, 1973). Our value for ΔH, calculated with Baur's method, agrees well with the values of 8.4 and 10.5 kJ.mol⁻¹ found by HAMADA and NAKAJIMA (1966), using the diluant method with ethylene glycol and water respectively, and is about 30% higher than that found by TUBBS (1966). This discrepancy may be due to a different tacticity or 1,2-glycol content of the samples or to a difference in the detection of the melting points.

The absolute values of the mean sequence lengths calculated with this method may be open to some doubt because of several assumptions that had to be made to interpret the measurements quantitatively. At any rate, the results are very useful for a mutual comparison. Once again, it can be inferred that the B samples have a more blocky distribution than the R samples.
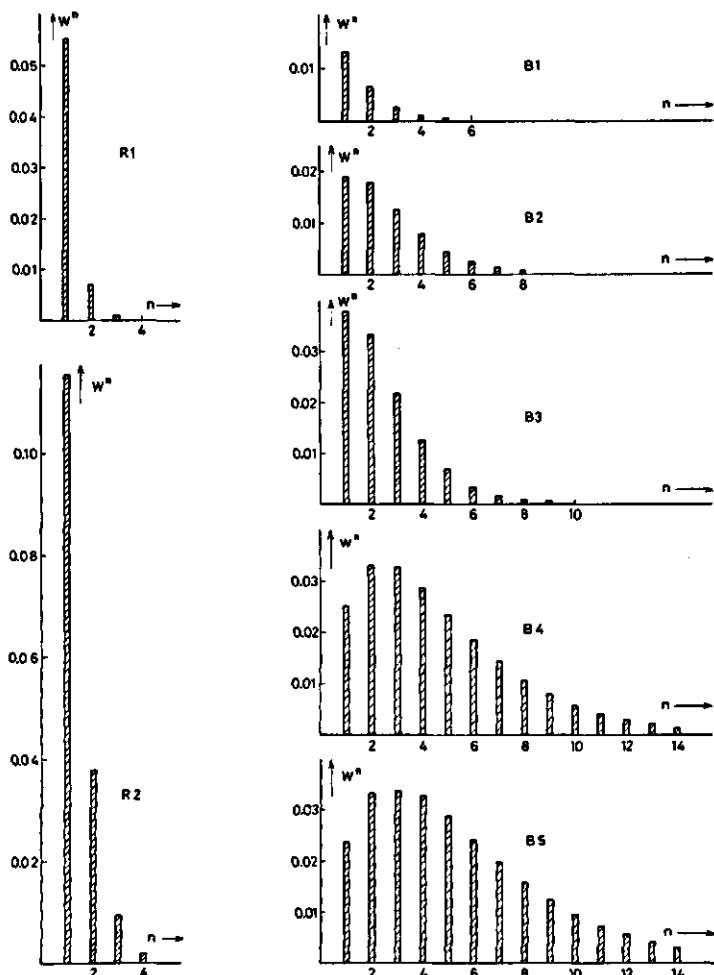
FIG. 3.3–4. Sequence length distribution of VAc monomers in the copolymers. The mole-fraction vinyl acetate that forms sequences of length n, W^n, is plotted against n.

3.3.4. Viscosimetry

3.3.4.1. Theory

Viscosity measurements constitute experimentally one of the easiest methods for determining mean molecular weights of high polymers, but they suffer the disadvantage of yielding only relative results. However, the results may also be interpreted in terms of solvent quality and mean molecular dimensions of the polymers in solution. All these facts together make the method very attractive and widely used.

The concentration dependence of the viscosity of dilute polymer solutions can be expressed in an empirical power series in the concentration:

$$\eta = \eta_o + h_1\eta_o c + h_2\eta_o c^2 + h_3\eta_o c^3 + \ldots \qquad (3.3\text{--}6)$$

where η denotes the viscosity of the solution (at concentration c, usually in g.dl^{-1}), η_o the viscosity of the solvent, and $h_1, h_2, h_3 \ldots$ are constants for a given polymer-solvent-temperature combination. Rearrangement leads to the more familiar equation

$$\frac{\eta - \eta_o}{\eta_o c} = \frac{\eta_r - 1}{c} = \frac{\eta_{re}}{c} = [\eta] + \sum_{i=1}^{\infty} k_i [\eta]^{i+1} c^i \qquad (3.3\text{--}7)$$

where η_r is the relative viscosity, η_{re} the viscosity ratio excess, $[\eta]$ the intrinsic viscosity (dl.g^{-1}), k_i is a dimensionless parameter that takes into account the influence of $i+1$ polymer-polymer interactions and k_1 is usually called the Huggins coefficient.

The intrinsic viscosity of a polymer solution is related to the viscosity averaged molecular weight ($\bar{M}_v$) by the empirical Mark-Houwink-Sakurada (MHS) equation:

$$[\eta] = k\,\bar{M}_v^a \qquad (3.3\text{--}8)$$

where k and a are constants depending on the polymer and on the quality of the solvent. They can be established by determining $[\eta]$ of monodisperse fractions. The $\bar{M}_v$ of any sample can thus be calculated with (3.3–8), provided that k and a are known for a polymer-solvent-temperature combination. Qualitatively, the solvent power can be inferred from a, the value of which is in between 0.5 (Θ solvent) and 1.0 (good solvent).

Many theories have been proposed to relate the solvent power with the values of $[\eta]$, k and a. The treatments we follow have been described by FLORY (1953), TANFORD (1961), KURATA and STOCKMAYER (1963) and YAMAKAWA (1971).

The dimensions of a flexible, linear polymer coil of random configuration in solution can be described by the root mean square (r.m.s.) radius of gyration, $(\bar{s^2})^{1/2}$, that can be obtained from light scattering measurements, or by the r.m.s. end-to-end distance $(\bar{h^2})^{1/2}$. These parameters can be correlated with the unperturbed chain dimensions (in a Θ solvent) by:

$$\bar{s^2} = \alpha_s^2\,\bar{s_o^2} \qquad (3.3\text{--}9)$$

$$\bar{h^2} = \alpha_h^2\,\bar{h_o^2} \qquad (3.3\text{--}10)$$

The parameters α_s and α_h are the linear expansion factors. They express the extent to which the molecular dimensions are perturbed by the excluded volume effect. In a solvent that is better than a Θ solvent, α_s and α_h increase slowly with molecular weight. The subscript o refers to the unperturbed chain. Provided that we know the fixed bond lengths, the valence angles between the backbone atoms and the restriction in rotation, $\bar{h_o^2}$ can be calculated with random flight statistics:

$$(\overline{h_o^2})^{1/2} = P^{1/2}L \tag{3.3-11}$$

P represents the number of monomers in the molecule, and L the effective monomer length. Under the given conditions, the following relation holds:

$$\overline{s_o^2} = \overline{h_o^2}/6 \tag{3.3-12}$$

All theoretical approaches try to relate $[\eta]$ to $(\overline{h_o^2})^{1/2}$ and to the excluded volume that is implied in α_h.

In Flory's model, the polymer is regarded as a continuous cloud of segments distributed around the molecular centre of mass according to a Gaussian function. In this model, α_s and α_h cannot be distinguished from each other:

$$\alpha_s = \alpha_h = \alpha \tag{3.3-13}$$

Flory and Fox derived the following equation, representing a polymer as an equivalent hydrodynamic sphere, impenetrable to the solvent:

$$[\eta] = \alpha^3 \, K^* \, \overline{M}_v^{1/2} \tag{3.3-14}$$

with

$$K^* = \Phi \left(\frac{\overline{h_o^2}}{\overline{M}_v} \right)^{3/2} \tag{3.3-15}$$

Φ is the so-called universal Flory constant. It depends, however, on the solvent quality (and therefore on α) and on the molecular weight distribution of the polymer, so it is not a constant. This limits the applicability of (3.3–15) seriously.

This drawback can be partly removed by introducing the viscosity expansion factor α_η defined by

$$[\eta] = \alpha_\eta^3 \, [\eta]_o \tag{3.3-16}$$

where $[\eta]_o$ denotes the intrinsic viscosity in a Θ solvent, so that

$$[\eta] = \alpha_\eta^3 \, K_o^* \, \overline{M}_v^{1/2} \tag{3.3-17}$$

with

$$K_o^* = \Phi_o \left(\frac{\overline{h_o^2}}{\overline{M}_v} \right)^{3/2} \tag{3.3-18}$$

Now Φ_o is independent of the solvent quality but still dependent on the mole-molecular weight distribution, and K_o^* is a constant that relates $\overline{M}_v$ to the unperturbed coil dimensions. However, a new unknown parameter has been introduced: α_η. It can easily be shown that $\alpha_\eta < \alpha$ by introducing the concept of an equivalent hydrodynamic sphere with radius R. A better solvent causes a lower segment density but also a greater freedom of motion for the solvent in

the coil and thus a smaller increase in R than in $(\overline{h_o^2})^{1/2}$. Kurata and Yamakawa were the first to emphasize the difference between α_η and α. They developed an approximate first-order perturbation theory for the intrinsic viscosity on basis of the Kirkwood-Riseman theory, describing the polymer as a string of monomers. They arrived at only a very slight difference between α_s and α_h. We shall ignore this and assume that (3.3–13) is applicable. The excluded volume effect on the frictional properties was approximated by:

$$\alpha_\eta^3 = 1 + 1.55\,z \tag{3.3-19}$$

that holds for $|z| < 0.15$; z is the excluded volume parameter defined by:

$$z = \left(\frac{3}{2\pi \overline{h_o^2}}\right)^{3/2} \beta\, \overline{P}^2 \tag{3.3-20}$$

where β is the binary cluster integral and $\beta \overline{P}^2$ is just twice the total excluded volume between the segments. β has large positive values in good solvent systems and is zero in a Θ solvent. It can be seen that, at positive values of β, α_η increases with P (and therefore with $\overline{M}_v$), a fact commonly observed for $[\eta]/[\eta]_o$. From the dependence of α_η on $\overline{M}_v$ it can be seen that (3.3–17) is equivalent to the MHS equation (3.3–8). Kurata and Yamakawa proposed the following semi-empirical closed expression for α_η as a function of α:

$$\alpha_\eta^3 = \alpha^{2.43} \tag{3.3-21}$$

The approach of Kurata and Yamakawa provides us with the tool to calculate, unequivocally, the molecular dimensions of a polymer in solution when $[\eta]_o$, or K_o^* and $\overline{M}_v$ are known. With (3.3–16) or (3.3–17), α_η^3 can be calculated and, under the proper conditions, α with (3.3–21). Since a Θ solvent is not always known for a polymer, some graphical methods have been proposed to estimate K_o^*. These methods are only applicable when the constants of the MHS equation are known for the polymer-solvent combination. The simplest method (that of Stockmayer and Fixman) consists of the elimination of α_η from (3.3–17) with the use of (3.3–19). This results in

$$[\eta]/\overline{M}_v^{1/2} = K_o^* + 1.55\,K_o^*\,z \tag{3.3-22}$$

As z is proportional to $\overline{M}_v^{1/2}$, extrapolation of $[\eta]/\overline{M}_v^{1/2}$ against $\overline{M}_v^{1/2}$ to zero molecular weight yields K_o^* as the intercept.

At higher values of z, this approach may still yield the correct value of K_o^*, but z (and thus α, that is a function of z; YAMAKAWA, 1971 p. 91) will be underestimated. The correct relation between α_η and z for these cases has not yet been derived theoretically. However, empirical relations suggest that the factor 1.55 in (3.3–19) must be replaced by a factor in between 1.05 and 1.55. Therefore, equation (3.3–19) will only lose its absolute significance, and it can still be used to give useful relative information.

The last link in the chain relating viscosimetric properties with the solvent quality is the relationship between z, or α, and the polymer-solvent interaction

38   *Meded. Landbouwhogeschool Wageningen 77-7 (1977)*

parameter χ. The value of χ is 0.5 for Θ solvents and lower for better solvents. Flory derived the following approximate relation:

$$\alpha^5 - \alpha^3 = 2\,C_M\,(1/2 - \chi)\,\overline{M}_v^{1/2} \tag{3.3-23}$$

or

$$z = (4/3^{3/2})\,C_M(1/2 - \chi)\,\overline{M}_v^{1/2} \tag{3.3-24}$$

for a given polymer-solvent-temperature system, C_M is a constant factor that can be calculated from simple physical properties (FLORY, 1953 p. 599). However, since the definition of C_M is still open to doubt (STOCKMAYER, 1955; YAMAKAWA, 1971) the χ parameter derived from viscosimetry has only significance at very small values of z or else as a relative measure.

The next section reviews methods of obtaining values for the intrinsic viscosity $[\eta]$ and the Huggins coefficient k_1. Evaluation of $[\eta]$ and k_1 from experimental η, c and η_o data is based on various empirical equations of closed form that all assume a different fixed relationship between k_i and k_1. By a series expansion to an equation similar to (3.3–7), this relationship can be obtained. The main empirical equations are summarized in table 3.3–3, together with the relation of their k_1 with the Huggins coefficient of (3.3–7) and the intrinsic connection between k_1 and k_2 of each equation.

Application of these equations yields mutually different results for the values of $[\eta]$ and the Huggins coefficient. Differences among the intercepts $[\eta]$ are not very serious, but the tangents may differ significantly. Dividing this slope by the intercept $[\eta]$ enlarges the differences in Huggins coefficients that may amount up to a few hundred per cent.

SAKAI (1968a) showed with a simulation method, that the extrapolation must be limited to a definite concentration range $(0.1 \leqslant [\eta]\,c \leqslant 0.5)$, and that all equations have systematic errors. The inherent relation between k_1 and k_2 of each equation imposes a definite curvature on η_{re}/c as a function of c. Of course, an appropriate extrapolation is only possible when the curvature of the equation to which the experimental points belong (that is unknown a priori) coincides with the curvature of the used equation. That different curvatures lead to different values of $[\eta]$ and especially of k_1 can be seen from fig.

TABLE 3.3–3. Empirical viscosity-concentration relationships.

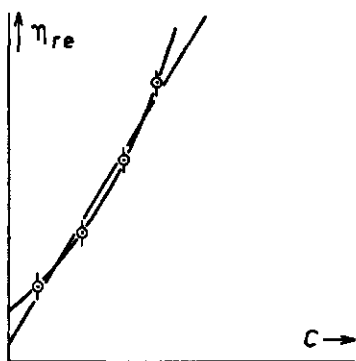| Method		Equation	$k_1^*)$	$k_2^*)$
Huggins	(H)	$\eta_{re}/c = [\eta]_H + k_H[\eta]_H^2\,c$	k_H	0
Schulz & Blaschke	(S)	$\eta_{re}/c = [\eta]_S + k_S[\eta]_S\,\eta_r$	k_S	k_1^2
Martin	(M)	$\ln(\eta_{re}/c) = \ln[\eta]_M + k_M[\eta]_M\,c$	k_M	$k_1^2/2$
Kraemer	(K)	$\ln \eta_r/c = [\eta]_K - k_K[\eta]_K^2\,c$	$1/2 - k_K$	$k_1 - 1/3$
Arrhenius	(A)	$\ln \eta_r/c = [\eta]_A + k_A[\eta]_A \ln \eta_r$	$1/2 - k_A$	$k_1^2 - 1/12$

*) Defined in equation (3.3–7).

FIG. 3.3–5. The influence of the curvature of two empirical equations on the values obtained for $[\eta]$ and k_1.

3.3–5. Sakai showed that the Huggins plot always underestimates $[\eta]$ and overestimates the Huggins coefficient. The opposite is true for the Schulz and Blaschke plot. The other plots are all useful in some cases (for certain values of k_1). Sakai recommends a simple and convenient method. Reliable results for poor solvent systems can be obtained by using the Martin plot or by averaging the values of $[\eta]$ resp. k_1 derived from the Huggins and the Schulz and Blaschke plot.

A fundamentally different approach is that of MARON and REZNIK (1969). They assumed that the differences inherent in the Huggins and the Kraemer extrapolation methods are only due to the fact that the general relationship (3.3–7) is approximated by series that have been terminated too soon. They suggested that the Huggins resp. Kraemer equation should read:

$$\eta_{re}/c = [\eta]_H + k_{H_1}[\eta]_H^2\, c + k_{H_2}[\eta]_H^3\, c^2 \qquad (3.3\text{–}25)$$

and

$$\ln \eta_r/c = [\eta]_K - k_{K_1}[\eta]_K^2\, c - k_{K_2}[\eta]_K^3\, c^2 \qquad (3.3\text{–}26)$$

They argued that $[\eta]_H$ should be equal to $[\eta]_K$. By series expansion of the logarithmic term in (3.3–26) and by equating comparable terms of (3.3–25) and (3.3–26), they found ultimately:

$$\Delta/c^2 = (\eta_{re} - \ln \eta_r)/c^2 = [\eta]^2/2 + (k_{H_1} - 1/3)\,[\eta]^3\, c \qquad (3.3\text{–}27)$$

A plot of Δ/c^2 versus c yields a straight line, and from the intercept $[\eta]$ can be derived. Insertion of this $[\eta]$ in (3.3–25) and (3.3–26), rearrangement of both equations and division by c yields two equations linear in c, from which the values of the four k_i's can be obtained.

This method provides the key to determine the curvature of the equation to which the experimental points belong without any presupposition on a rela-

40   *Meded. Landbouwhogeschool Wageningen 77-7 (1977)*

tionship between k_1 and k_2. The only assumption that was made is, that both (3.3–25) and (3.3–26) are able to describe the experimental observations satisfactorily.

3.3.4.2. Experimental

Solutions were made up as described in ch. 3.3.6 and were always used within 24 hours. Solutions and pure solvent were filtered through a membrane filter (pore size 0.8×10^{-6} m) under N_2 pressure. To avoid any dust, all work with these solutions and the cleaned capillaries was done in an anti-dust cabinet (Slee). After the usual cleaning procedure, all glassware was rinsed with filtered distilled water.

The measurements were performed with an automatic viscometer (Viscomatic MS type 53000, Fica) with electronic measurement of the efflux time ($\pm$ 0.01 s). The capillaries with dilution vessel were thermostatted within $0.005\,°C$ with a Haake FE thermostat. Three capillaries were used with efflux times for water at $25\,°C$ of 270, 180 and 97 s respectively. The capillary constants were obtained by repeated measurement of the efflux time of distilled water at 15.00, 20.00 and $25.00\,°C$. The density and viscosity of water at those temperatures were obtained from the HANDBOOK (1972). An automatic dilution module was used when water was the solvent. Its reproducibility was thoroughly tested and was within 0.05%. The dilution with wabu of $25.00\,°C$ was performed with a calibrated pipette.

Two different solutions were made up for each sample, while the (co)polymer concentration always was in the range $0.1 \leqslant [\eta]c \leqslant 0.5$. Each solution was measured with two different capillaries at $25.00\,°C$. The weight averaged mean of these results was used for extrapolation. In the worst case, the difference in the values of η_{re}/c was 1.5%, but often it was less than 0.3%. Shear corrections were not applied at these relatively low molecular weights (BERESNIEWICZ, 1959b; PRITCHARD, 1970).

A PTS-BASIC program was written to fit the empirical extrapolation methods to the experimental data, using a linear regression analysis. Weight factors were attributed to the experimental points in each plot, in order to give all data identical absolute errors, a requisite for proper analysis.

3.3.4.3. Results and discussion

A viscometric study was undertaken to determine both the $\overline{M}_v$ of the samples used and the influence of the VAc groups on the conformation of the copolymers. In addition, we studied the influence of buOH on the molecular dimensions and on the solvent quality.

The values of $[\eta]$ and k_1 as obtained from measurements at $25.00\,°C$ by application of the different empirical equations (see table 3.3–3) are collected in table 3.3–4 and 3.3–5*). For the sake of comparison, the coefficients k_1

---

*) Sample B5 was not used in these experiments because its solutions were not stable at $25\,°C$ (see ch. 3.3.6). The viscometric parameters for B1 were only determined in water.

TABLE 3.3–4. Intrinsic viscosity and Huggins coefficient values in water at 25.00 °C.

Extrapolation method:	Huggins	Schulz & Blaschke	Martin	Maron & Reznik		Kraemer	Arrhenius
$[\eta]$ (dl.g^{-1}):							
PVA-H	0.803	0.836	0.822	0.821		0.826	0.826
B1	0.863	0.900	0.888	0.883		0.887	0.888
B2	0.878	0.906	0.895	0.892		0.894	0.895
B3	0.831	0.861	0.848	0.847		0.849	0.850
B4	0.654	0.669	0.664	0.662		0.666	0.666
R1	0.799	0.830	0.816	0.815		0.819	0.819
R2	0.757	0.779	0.772	0.768		0.770	0.770
k_1:					*)		
PVA-H	0.683	0.426	0.524	0.536	0.14	0.493	0.493
B1	0.629	0.388	0.470	0.498	0.11	0.462	0.460
B2	0.567	0.376	0.448	0.464	0.10	0.445	0.442
B3	0.586	0.379	0.462	0.467	0.11	0.450	0.448
B4	0.72	0.51	0.59	0.61	0.16	0.56	0.56
R1	0.609	0.384	0.475	0.480	0.12	0.457	0.456
R2	0.551	0.373	0.436	0.459	0.09	0.440	0.437

*) This second column contains the values of k_2 determined with (3.3–25).

TABLE 3.3–5. Intrinsic viscosity and Huggins coefficient values in wabu at 25.00 °C.

Extrapolation method:	Huggins	Schulz & Blaschke	Martin	Maron & Reznik		Kraemer	Arrhenius
$[\eta]$ (dl.g^{-1}):							
PVA-H	0.902	0.940	0.925	0.922		0.924	0.925
B2	0.942	0.986	0.967	0.964		0.964	0.966
B3	0.878	0.915	0.899	0.897		0.898	0.899
B4	0.48	0.54	0.51	0.50		0.53	0.54
R1	0.880	0.913	0.900	0.896		0.896	0.898
R2	0.751	0.773	0.760	0.762		0.762	0.763
k_1:					*)		
PVA-H	0.564	0.348	0.427	0.445	0.09	0.431	0.426
B2	0.537	0.326	0.407	0.420	0.08	0.418	0.410
B3	0.551	0.340	0.421	0.433	0.09	0.426	0.420
B4	1.9	0.8	1.2	1.4	0.6	1.0	0.9
R1	0.513	0.327	0.397	0.416	0.07	0.413	0.405
R2	0.518	0.350	0.431	0.417	0.11	0.425	0.421

*) This second column contains the values of k_2 determined with (3.3–25).

obtained with the different equations are expressed in the Huggins coefficient of equation (3.3–7). The values of k_2 obtained with the method of Maron and Reznik are also collected. In most cases, the standard deviation in $[\eta]$ is less than 0.002 dl.g^{-1} in water and less than 0.003 dl.g^{-1} in wabu (except in the case of B4 where it amounts to 0.009 dl.g^{-1}). The standard deviation of k_1 amounts to 0.005 or less in water and wabu (except for B4 in water and wabu,

and for R2 in wabu, in which cases it amounts to 0.015, 0.07 and 0.010 respectively).

The differences in our results, inherent to the empirical equations, are analogous to those described by SAKAI (1968a). From the values of k_1 it can be concluded that water and wabu are rather poor solvents for PVA and PVA-Ac. Therefore, the Martin extrapolation seems most reliable. As expected, its results compare very well with those obtained with the more generally applicable method of Maron and Reznik. The values obtained with the Kraemer and Arrhenius extrapolation also agree satisfactorily with the results of both preceding methods. This close agreement is caused by the almost identical values of k_2 in the different equations (these can be calculated from the relations between k_1 and k_2 as given in table 3.3–3). No unambiguous relation between k_1 and k_2 can be inferred from our results. Even changes in $[\eta]$ and k_1 are not always related in the same way (an increase in $[\eta]$ should correspond with a decrease in k_1). The values of $[\eta]$ and k_1 that will be used from now on are the averages obtained according to Martin, and Maron and Reznik. They are collected in columns 2–5 of table 3.3–6 and in fig. 3.3–6.

Provided that the constants of the MHS equation are known, we can calculate $\overline{M}_v$ of PVA-H from its $[\eta]$ value. Actually, many different sets of constants for PVA in water have been published (PRITCHARD, 1970; KURATA et al., 1975), but most of them were determined with poorly defined polymers of unknown molecular weight distribution. In previous work in our laboratory (LANKVELD, 1970; FLEER, 1971; BELTMAN, 1975; VAN VLIET, 1977), the specifications of Kuraray were used, however, without knowing whether the given
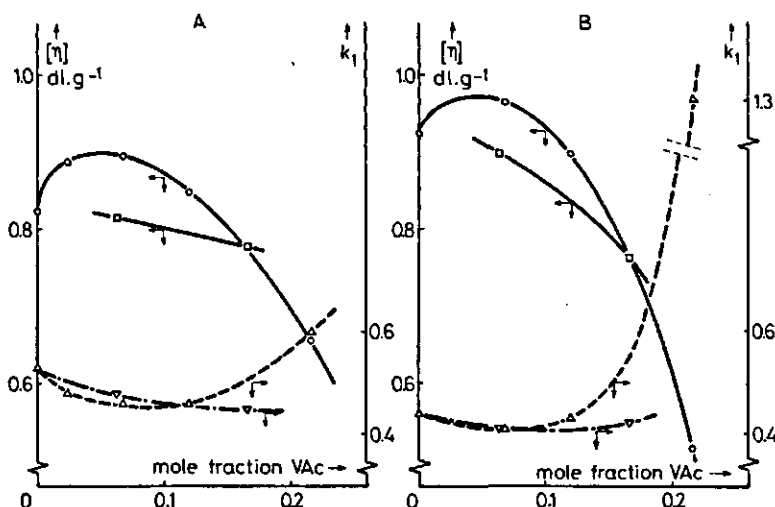
FIG. 3.3-6. Viscometric properties as a function of the acetate content of the (co)polymers; A is in water, B in wabu (25.00 ± 0.02 °C).
O, □: intrinsic viscosity of the blocky respectively random copolymers
△, ▽: Huggins coefficient of the blocky respectively random copolymers.

TABLE 3.3–6. Viscosimetric properties of PVA and PVA-Ac copolymers (for explanation see text).

	$[\eta]_{water}$	$k_{1\ water}$	$[\eta]_{wabu}$	$k_{1\ wabu}$	$\overline{M}_v$	$[\eta]_o^c$	α_{water}	α_{wabu}
PVA-H	0.822	0.53	0.924	0.44	118×10^3	0.546	1.20	1.33
B1	0.886	0.48	–	–	121×10^3	0.552	1.26	–
B2	0.894	0.46	0.965	0.41	126×10^3	0.564	1.25	1.34
B3	0.848	0.46	0.898	0.43	132×10^3	0.577	1.18	1.23
B4	0.663	0.60	0.51	1.3	142×10^3	0.600	1.04	0.92
R1	0.816	0.48	0.898	0.41	125×10^3	0.562	1.17	1.26
R2	0.770	0.45	0.761	0.42	137×10^3	0.588	1.11	1.11

molecular weights were $\overline{M}_n$, $\overline{M}_v$ or $\overline{M}_w$ ($\overline{M}_v$ was assumed, but this is incorrect).

Perhaps the only determination of these constants that is really satisfactory stems from MATSUMOTO and OHYANAGI (1960). The $\overline{M}_w$ and $\overline{M}_n$ of their samples were determined with different methods (light scattering, osmotic pressure and end group analysis). Their MHS equation, recalculated to 25°C (PRITCHARD, 1970) reads:

$$[\eta] = 4.67 \times 10^{-4}\ \overline{M}_v^{0.64}\ (dl\ .\ g^{-1}) \tag{3.3–28}$$

Application of this equation to PVA-H yields $\overline{M}_v = 118 \times 10^3$ (g.mol^{-1})*). Of course, this relation can also be used to determine K_o^* and $[\eta]_o$ with the Stockmayer-Fixman plot (eq. (3.3–22)). This leads to $K_o^* = 15.9 \times 10^{-4}$ (dl.mol$^{1/2}$. g$^{-3/2}$) and $[\eta]_o = 0.546$ (dl.g^{-1}). Using $\Phi_o = 2.1 \times 10^{23}$ (mol^{-1}) (KURATA et al., 1975), we calculated $(\overline{h_o^2})^{1/2} = 31$ nm. Our value of K_o^* is in good agreement with that of WOLFRAM et al. (1968) and GARVEY et al. (1974).

We can now calculate $\overline{M}_v$ of all copolymers, assuming again (as in the analysis of the melting points) that the blocks of VAc monomers are distributed randomly over the molecules. Under this condition, the calculation is straightforward from the $\overline{M}_v$ of PVA-H and the degree of acetylation (column 6 of table 3.3–6).

In order to examine the influence of the acetate content and distribution on the molecular dimensions, we would like to compare values of α or χ of all (co)polymers. Therefore, we needed the value of $[\eta]_o$ for all preparations. However, as no Θ solvent was available, and as no value of K_o^* could be determined experimentally, the best procedure seemed to assess a value for K_o^*. To that end, we could assume that either $\overline{h_o^2}$ or K_o^* are constant for all samples. The correct values of K_o^* will very probably be in between these approximations. By assuming K_o^* to be constant, we obtained the maximum value for the calculated intrinsic viscosity in a Θ solvent, $[\eta]_o^c$, and thus minimum values for α_η, z and α. Actually, we thus calculated $[\eta]_o$ for PVA homopolymers with an $\overline{M}_v$ equal

*) The values of $\overline{M}_v$ calculated with this equation are in reasonable agreement with those obtained with GPC (ch. 3.2). From the MHS constants which Kuraray use (KURARAY, 1976), we infer that their molecular weights are $\overline{M}_n$ values.

to that of the copolymers (column 7 in table 3.3–6). Now, $\alpha_{\eta\,water}$ and $\alpha_{\eta\,wabu}$ could be estimated for all copolymers from columns 2 and 7, respectively 4 and 7, using $\alpha_{\eta}^3 = [\eta]/[\eta]_\delta^c$.

In most cases, the application of equations (3.3–19) and (3.3–21) was unfit to obtain z, respectively α, from α_{η} since z appeared to be larger than 0.15. But, as we were interested in determining the minimum effect of the acetate groups on the solvent quality, we still applied (3.3–19) to calculate z, and this value was used in the original expression of α as a function of z (YAMAKAWA, 1971 p. 91). The results are collected in columns 8 and 9 of table 3.3–6.

It must be borne in mind that, by application of equation (3.3–19), all values obtained for z and α are probably too low. Moreover, the assumption of constant K_η^* for all copolymers means that the values are the more too low, the higher the acetate content is. Although α_{η} is also a smooth function of the molecular weight (for PVA-H, $\alpha_{\eta} \sim \overline{M}_v^{0.05}$, compare (3.3–14) and (3.3–28)), we can neglect this effect as it would decrease the influence of the acetate groups on α_{η} with at most 1 % (for B4). Therefore, the differences in the calculated α's can be attributed to the influence of specific interactions due to the VAc groups.

The influence of acetate groups on the molecular dimensions in water can be deduced directly from α_{water}. Only B1 and B2 are more expanded than PVA-H, while all other copolymers display a greater contraction at higher acetate content. The low value of α for R1 as compared to B1 and B2, that has an almost identical acetate content, is striking. This may possibly be explained as follows. It is well known that two kinds of polymers may show incompatibility. This is caused by the relatively small gain in entropy of mixing for polymers as compared to low molecular weight materials. The same reasoning applies to copolymers (STOCKMAYER et al., 1955; DONDOS et al., 1974). This means that block copolymers with a few long blocks exhibit segregated conformations to avoid any contribution of energetically unfavourable interactions between two chemically unlike blocks of the chain. The presence of a large number of smaller blocks makes this segregation impossible in space, and expansion of the coil will result to avoid these unfavourable interactions. In random copolymers, the differences in chemical structure within a chain between two unlike segments become less distinct due to the many near-neighbour interactions. Therefore, it can be stated that whether a copolymer is more expanded than its homopolymers depends on the balance of three contributions: the solvation free energies of the different monomers, the near-neighbour interactions, and the interactions between two chemically unlike blocks of the chain.

Of course, the second effect is less important in blocky than in random PVA-Ac copolymers, as the former have less VA-VAc neighbour contacts. The net effect, therefore, is an expansion for the blocky copolymers (due to the repulsion of unlike VA and VAc sequences), until at higher acetate content the greater number of unfavourable interactions prevails (the VAc-VA near-neighbour and the VAc-H$_2$O interactions). In the random copolymers,

almost all VAc monomers have two VA near-neighbours, and these un-favourable interactions dominate the balance, resulting in a net shrinkage. Of course, the observed facts cannot be explained by the destructive influence of the bulky VAc groups on inter- or intra-molecular H-bonding in the solution. This would lead to an opposite dependence of α_{water} on the acetate distribution. Probably, this effect, although present, plays only a minor part in samples with 1-2% acetate as can be deduced from extrapolation of α_{water} of the random copolymers to 0% VAc content. From these results we must also infer that the mechanism that causes an increase in the rate of dissolution is totally different from the mechanism that improves the stability of the solution, a fact never reported previously for PVA-Ac.

In relation to the above discussion, it is worth mentioning that AMAYA and FUJISHIRO (1956) found a minimum in the dilution enthalpy of aqueous solutions of PVA-Ac containing 6-8% acetate groups and a sharp increase with higher acetate content. Very probably they used blocky copolymers. These results also suggest a maximum expansion of the PVA-Ac copolymer at that acetate content.

In literature, only two studies were found in which the influence of acetate content on $[\eta]$ and k_1 was determined systematically. TOYOSHIMA (1968) reported a behaviour similar to that of our blocky copolymers. He used commercial samples that were blocky too. BERESNIEWICZ (1959b) described a dependence very similar to that of our random copolymers, although the distribution in his samples also was probably blocky. The reason for this difference is not clear.

The influence of buOH on the conformation of PVA and the copolymers can be inferred from the last two columns of table 3.3–6 and also from fig. 3.3–7, where the fractional increase in α due to buOH ($= \alpha_{wabu}/\alpha_{water}$) is plotted as a function of the acetate content.
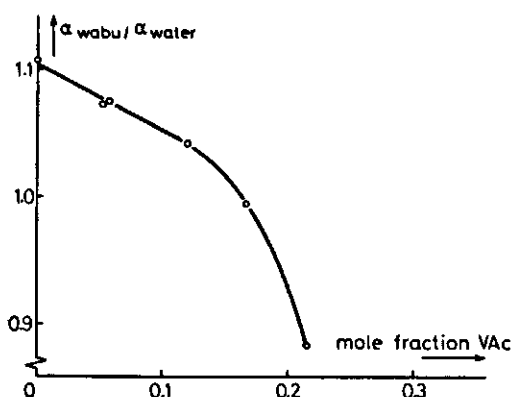

FIG. 3.3–7. The ratio of the calculated expansion factors in wabu and water as a function of the acetate content of the copolymers.

Addition of buOH to an aqueous PVA solution increases α_η and thus α and, in addition, the stability of the solution (see ch. 3.3.6). This can be caused by the fact that the homogeneous wabu phase is simply a better solvent for PVA, or by preferential orientation of buOH at the PVA molecules. The very fact that PVA is insoluble in pure buOH provides some support for the latter mechanism. Thus, by hydrophobic interactions between apolar parts of buOH and the backbone of the (co)polymers, unfavourable interactions of these parts with water are prevented. Another effect that also supports this view must be mentioned. During all viscometric experiments, a few drops of buwa were present on the wabu solution in order to guarantee saturation with buOH. During the first few hours of a new measurement, we observed a steady slight increase in η of the PVA(-Ac) solutions (up to 1 %), but this was never seen when only pure wabu was measured. Probably, the adsorption of buOH onto the $-CH_2-CH-$ backbone resulted in a slight undersaturation of the wabu solution. Of course, the solution was not diluted until the efflux time became constant. After dilution these effects were no longer found. These observations and their interpretation very much resemble the results of WOLFRAM and NAGY (1969), who studied the influence of low molecular weight alcohols on the conformation of PVA.

The introduction of acetate groups in the PVA chain makes the system very complicated and the effects to be expected from this, obscure. A copolymer chain that is more expanded or stiffer in wabu will be less influenced by the incompatibility of unlike segment blocks. This is indeed found (compare PVA-H and B2 in table 3.3–6, columns 8 and 9). Still, the decrease in $\alpha_{wabu}/\alpha_{water}$ (and thus the relative increase in α caused by buOH) seems independent of the acetate distribution. This can be explained by assuming that VAc groups prevent the adsorption of buOH at that place of the chain. As the mean VOH block length is much longer in blocky than in random copolymers (see ch. 3.3.3), we may expect a higher stabilization of the blocky copolymers. Apparently, this last effect, accidentally, just compensates the decrease in expansion due to incompatibility. This mechanism also explains that α_{wabu} decreases more steeply with acetate content than α_{water}.

Although many attempts have been made to derive a theoretical correlation between the Huggins coefficient (k_1 in equation (3.3–7)) and the solvent quality, none is yet satisfactory. The problem is very complex, particularly as k_1 is independent of molecular weight, whilst α (and therefore χ) is not. In Θ solvents, k_1 can be estimated to be in between 0.5 and 0.7 (SAKAI, 1968b), whereas its value decreases with increasing solvent quality.

Most relations between k_1 and α_η are empirical (e.g. SAKAI, 1968b; DREVAL et al., 1973) and are, therefore, of restricted applicability to other polymer-solvent systems. Thus, the use of these relations cannot compete in accuracy with the determination of α_η from $[\eta]$.

However, it must be borne in mind that k_1 yields information on the solvent

quality from peripheral coil-coil interactions. In homopolymers, the chemical composition of the molecule is homogeneous. However, the peripheral composition of a copolymer coil is not necessarily the same as the mean overall composition, that determines α_η. Therefore, it is obvious that, for copolymers, a decrease in α_η will not have to coincide with an increase in k_1. In buwa, this at first sight conflicting behaviour was observed for B3, R1 and R2.

Provided this reasoning is correct, we may conclude that the solvent quality of wabu at the periphery of the coils is about equal for all samples, except for B4 and B5. This also implies that, for the former copolymers, the mean peripheral acetate content is less than the mean overall acetate content.

It must be stressed again that the preceding discussion will give analogous results for comparison of the copolymers when other values are used for $[\eta]_0^c$ or for the numerical factor in (3.3–19).

We think that the values of α provide a good means to mutually compare the perturbed dimensions of the blocky and random copolymers. Calculation of the χ parameters provides no new information, as their values will also have only a relative significance. This is caused by the uncertainty in the values of z, α and C_M. However, for PVA-H we can apply (3.3–24), as its value for K_0^c is rather certain. The originally proposed definition for C_M (by Flory) yields $\chi = 0.484$, whereas the relation proposed by Stockmayer yields $\chi = 0.469$. Thus, there values also support the conclusion that water is a poor solvent for PVA.

3.3.5. *Interfacial tension measurements*

3.3.5.1. Introduction

Because of the relatively low interfacial tension between wabu and buwa (at 25°C: 1.8 mN.m^{-1}; DAVIES and RIDEAL, 1961), not all measuring techniques are equally suitable for the determination of the effect of adsorbed copolymers on this interfacial tension. To that end, the drop-volume and the drop-shape method were selected in this study. The first method is very simple and accurate, but its use for polymer solutions has been disputed recently (LANKVELD, 1970). The latter one is a static method. In the range of 0–2 mN.m^{-1}, both methods may be reproducible within 0.02 mN.m^{-1}.

With the drop-volume method, a drop of the heavier liquid (density ρ_1) is formed (extremely) slowly in the less dense phase (density ρ_2). At the moment of detachment from the tip of the tube (of radius r), by gravity only, the drop volume V is given by:

$$V = \frac{2\pi r \gamma f}{(\rho_1 - \rho_2)g} \qquad (3.3–29)$$

where γ is the interfacial tension between the two phases, g the gravitational

acceleration, and f an empirically determined correction factor depending on $r/V^{1/3}$ (STRENGE, 1969; WILKINSON and KIDWELL, 1971). HARTLAND and SRINIVASAN (1974) introduced the theoretical basis for this correction factor: both the interfacial tension and the negative excess pressure force due to the curved interface may support the drop at the point of detachment, the relative contributions depending on the tip radius. Recently, PIERSON and WHITAKER (1976) and WHITAKER (1976) showed that the method is also applicable to surfactant solutions. They determined the time required for the surface to reach 95% of the equilibrium state (normally much lower than the life time of the drop) and showed that the stability of a pendant drop is not dependent on the surface viscosity or elasticity but only on its shape.

The shape of a liquid drop, being acted upon by gravitational and interfacial forces, is governed by an exactly known differential equation. ANDREAS et al. (1938) showed that the interfacial tension γ can be calculated from the pendant drop profile by:

$$\gamma = (\rho_1 - \rho_2) g d_e^2 / H \qquad (3.3\text{–}30)$$

where d_e is the largest diameter of the drop and H is a correction factor that depends on the shape of the drop and can be calculated exactly. Andreas et al., however, preferred to relate the shape of the drop with $1/H$ by empirical evaluation of $1/H$ using liquids of known surface tension. Later, Fordham, and Niederhauser and Bartell (see ADAMSON, 1967 p. 33) independently solved the differential equation by using numerical integration techniques. This provides a theoretically sound basis to the method. The shape of a drop can be characterized by $S_n = d_n/d_e$. Here, d_n is the diameter at the height $(n/10) \times d_e$ from the bottom of the drop. The tables in ADAMSON (1967) were determined for $n = 10$; ROE et al. (1967) calculated $1/H$ vs. S_n for $n = 8, 9, 10, 11,$ and 12. As indicated by ROE, the experimental errors are not simply additive. The highest accuracy is obtained with drops having a shape that corresponds to low $1/H$ values, using $n = 12$.

3.3.5.2. Experimental

The experimental arrangement, identical for both methods, is shown in fig. 3.3–8. A light beam from a 12 Volt, 100 Watt iodine lamp (1) entered the measuring cell (2) through a blue filter (3). A 35 mm Nikkormat camera (4) with a Nikkor-H lens of 50 mm focal length was fixed on a bellows of 120 mm. The whole set-up was mounted on an optical bench (5) that was placed on an anti-vibration table. The windows of the cell could not be glued to the double-walled glass cylinder, as the adhesive would have been affected by chromic acid. Therefore, they were clamped parallel to one another with a butyl rubber O-ring between the window and the cylinder. The lower entrance of the cell could be used for a thermometer, the upper one was closed by a cover with a hole just large enough for the dropforming tip to enter. A modified ultra-precision micrometer syringe (Gilmont) (6) was used to feed the solution to the tip. It was found that the widely used Agla syringe was unsuitable for these
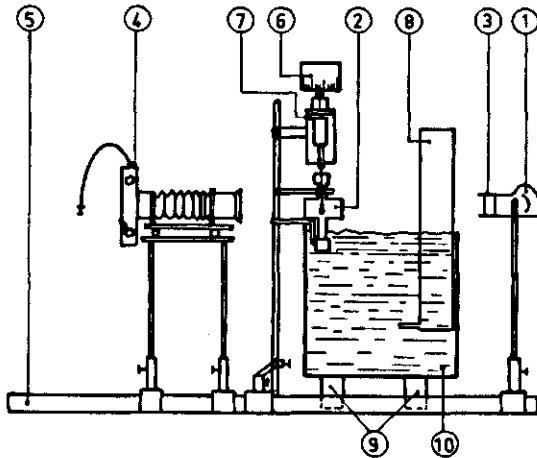
FIG. 3.3–8. Experimental set-up for the interfacial tension measurements (explanation of the numbers is given in the text).

measurements, as evaporation through the space between the piston and the syringe could be detected after a few minutes. A special micrometer was mounted on the syringe, so that we could obtain an accuracy in drop volume better than 10^{-5} ml. The piston of the syringe that determines the expelled volume of the wabu solutions was found to have the appropriate cross-sectional area within $1^{0}/_{00}$. The syringe with adapter was kept in a doublewalled brass tube (7). In order to guarantee constant temperature, water was pumped from a thermostat (8) through both doublewalled cylinders ($25.00 \pm 0.02\,°C$). Vibrations caused by the pump were absorbed by flexible rubber hosepipes and by the plugs (9) that sustained the thermostatted bath (10). Just before a measurement (a dropfall or a picture), the thermostat was stopped. The cylindrical cell always contained buwa and wabu on top of each other, to guarantee saturation.

For the highest precision, a set of tips with various diameters is required. We used five stainless steel hypodermic needles. Their ends were ground flat and perpendicular to the vertical axis by means of a whetstone. Their tip radius was measured with a micrometer in eight different directions (table 3.3–7).

All measurements were performed with at least two different tips, chosen in such a way that the correction factors f and H were most accurate ($0.5 < r/V^{1/3} < 0.9$; $0.3 < H < 0.5$). For f, we used the relation given by STRENGE (1969) as a third order polynomial of $r/V^{1/3}$. H was determined from the proper average of S_{10} (ADAMSON, 1967 p. 36) and S_{12} (ROE et al., 1967). The formation of the drops was observed with the same camera that was used to take pictures of the drop shape. We always thoroughly checked that the tips were vertical, that no creep of the solution took place at the outside of the dropping tip, and that the whole tip was wet.

The measurements with the drop-volume method were performed as follows. After the approximate volume of a drop at a given time had been deter-

50   *Meded. Landbouwhogeschool Wageningen 77-7 (1977)*

TABLE 3.3-7. Details of the dropping tips.

tip no.:	diameter (cm):	standard deviation (cm):
1	0.1835	0.0003
2	0.1505	0.0004
3	0.1238	0.0002
4	0.1047	0.0002
5	0.0697	0.0003

mined, drops were formed successively up to about 95% of their final volume in 5–10 s. Approximately 30 s before the drop had to fall off, the volume was increased very slowly. For each determination, the average of 10–20 successively formed drops was taken (the first three values were always excluded). When γ changed rapidly with time, the procedure was different. A fixed volume was expelled and the time until detachment was measured. By varying the volume, $\gamma(t)$ could be determined. With this method, the standard deviation in γ was 0.02 mN.m^{-1} at most.

For the drop-shape method, the light beam was directed parallel to the optical axis of the camera, perpendicular to the windows of the cell. When the interfacial tension was rather independent of time, one drop with a proper volume could be photographed after 1, 5 and 10 minutes. When the drop shape changed quickly with time, different volumes were required to get a proper shape after these periods. In order to guarantee a fresh interface, always two drops were expelled quickly before a measurement. For each measurement, at least three pictures were taken from different drops. The optimum resolving power of the lens is obtained with diaphragm 5.6 (about 150 lines per mm; VORST, 1972). We used Agfaortho 25 professional films (better than 300 lines per mm). The measurement of d_e, d_n and r from the negatives was performed with a Quantimet 720 (Imanco), connected with a Leitz microscope. The magnification of the negative was so adjusted, that the resolving power was at least 0.5%. The total magnification (approximately a factor 50) was determined from the ratio between the diameter of the magnified image of the tip and the actual diameter.

With these precautions, we could obtain a standard deviation in γ of 0.03 mN.m^{-1} at most.

3.3.5.3. Results and discussion

Although interfacial tension measurements are not a very exploratory tool to measure polymer adsorption (see ch. 1), they may yield some qualitative information on the differences in interfacial activity between the copolymers at hand. Comparison of the different $\gamma(t)$ curves may elucidate the role of the acetate groups in the adsorption mechanism at the wabu – buwa interface.

Wabu solutions with a (co)polymer concentration of 5.0 g.l^{-1} were made up. Probably, the solution of B5 contained copolymers with an average acetate
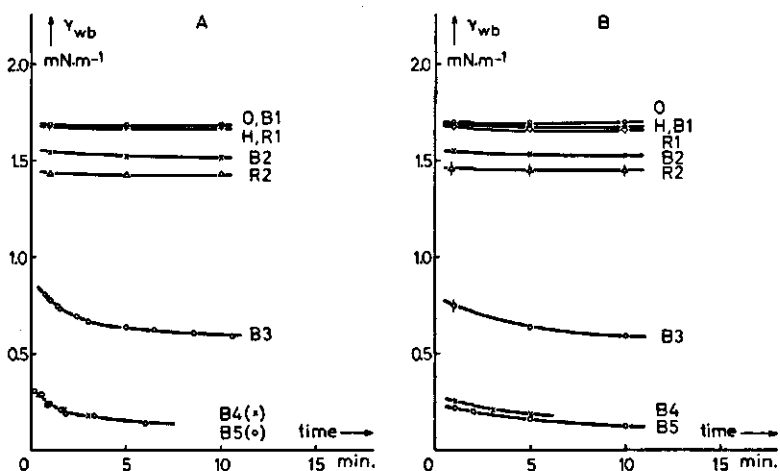
FIG. 3.3–9. Interfacial tensions between buwa and wabu ($= 0$), and between buwa and (co)polymer solutions in wabu (5.0 g.l^{-1}) as a function of time at $25.00 \pm 0.02°C$; A as determined with the drop-volume method, and B with the drop-shape method.

content less than given in table 3.3–1, as only 52 % of the sample was soluble in wabu at 25 °C. As γ appeared to be rather insensitive to the acetate content in the range of 22–26 % acetate groups, we did not determine the actual average acetate content of the dissolved copolymers. The interfacial tension measurements between wabu and buwa were carried out at $25.00 \pm 0.02°C$. The results are given as $\gamma(t)$ curves in fig. 3.3–9.

All $\gamma(t)$ values determined with the two methods are equal within their limits of accuracy. This is consistent with the findings of PIERSON and WHITAKER (1976) and WHITAKER (1976), who showed that the drop-volume method is also applicable to surfactant solutions. Because of its relative simplicity, the drop-volume method is very attractive for the measurement of interfacial tensions that change in time. We believe that, in the present case, this applicability is due to the fact that, at the concentration used, the diffusion relaxation time of the (co)polymers to the interface is negligible compared to its reconformation relaxation times. This diffusion relaxation time could be estimated to be much less than 1 s (PIERSON and WHITAKER, 1976), whereas the reconformation relaxation time, as can be estimated from the $\gamma(t)$ graphs, is at least in the order of minutes. Probably, this method is no longer applicable at very low (co)polymer concentrations. In that case, the reconformation relaxation process may be faster than diffusion of material from the bulk to the interface, resulting in a different conformation of the adsorbed (co)polymers at the point of detachment.

The decrease in interfacial tension varies substantially with acetate content and distribution. Generally, an increase in the acetate content causes a lower γ at each point in time; but γ is reduced much more effectively by blocky than by random copolymers (compare e.g. B3, R2 and B4!). From these results it can be inferred that the vinylacetate segments adsorb preferentially at this interface.

This fits in with the view that VAc is more hydrophobic than VA. The second effect is even more interesting. Several VAc monomers grouped together make the molecule much more interface-active than when they are statistically spread over the chain. From this we infer that interjacent VA groups prevent the formation of longer trains in random copolymers.

Comparison of these results with the solvent quality of wabu for the copolymers as deduced from viscometry yields another interesting result. Apparently, there is no distinct connection between the solvent quality that can be inferred from viscosimetry (ch. 3.3.4.3) and the decrease in interfacial tension. According to the theories of reversible homopolymer adsorption, the adsorbed amount will be smaller in a better solvent. Qualitatively, we find the opposite for B2, R1 and R2 if we infer the solvent quality from α_{wabu}. At the first stage of adsorption (before reconformations start to play a part), it is obvious that the peripheral solvent quality of a macromolecular coil will primarily determine the interfacial activity of the adsorbing coils. From the values of the Huggins coefficients. we inferred that this peripheral solvent quality is almost equal for all samples except B4 and B5. Therefore, only slight differences in interfacial activity would have to be expected. However, this is in contrast with the experiments; therefore, only those adsorption theories that take into account the amphipathic character originating from the sequences of the different monomers will be applicable to copolymer adsorption.

At any rate, the observed time effects can partly be caused by unfolding of the copolymer coils at the interface. This unfolding may be explained by the higher internal acetate content of the coil as compared to that at its periphery (ch. 3.3.4.3).

In fact, the wabu-buwa interface is a very peculiar one with smaller differences in hydrophilic-hydrophobic character than most oil-water interfaces. Besides, the interfacial tension is very low, so adsorption at this interface will only result in a small gain in free energy. Perhaps this is the reason for the distinct differences in adsorption behaviour of the copolymers. The observed anchor effect of VAc blocks does not have to be so pronounced at other interfaces where a higher free energy gain is also possible for the VA monomers.

The time scale of our measurements is, of course, too small to predict the steady state values of γ. The relaxation times are in the order of minutes, much smaller than found by LANKVELD and LYKLEMA (1972) for the water-paraffin interface. This may also be related to the small absolute change in γ that is possible in our system.

3.3.6. *Preparation of PVA and PVA-Ac solutions and their stability*

As PVA is hygroscopic, all samples were stored in flasks in a dessiccator above $CaCl_2$. Solutions were prepared by dissolving a weighed amount in water. The (co)polymer concentration of the solution was based on this amount, taking into account the moisture content of the sample. To achieve complete dissolution, the solutions of samples with less than 17 mole % VAc were stirred for two hours at 95–98 °C. B4 and B5 could only be dissolved by repeat-

ed heating and cooling of the solution during stirring. The elevated temperatures are apparently necessary to dissolve the micro-crystalline regions still present, while the copolymers as a whole are only soluble at low temperatures. The dissolution was always performed under N_2 to prevent oxidation of the samples.

All aqueous solutions were stable at 25°C, except those of PVA-H and B5. Small flakes had been formed in PVA-H solutions after about 24 hours. We only used aqueous PVA-H solutions for viscosimetric experiments, and care was taken to measure the efflux time directly after preparing the solution. The differences in η_r between the first and the second series of measurements (about 5 hours later) were never significant. Sample B5 exhibited phase separation at 25°C but was soluble in water at lower temperatures. Therefore, this solution was never used for experiments in water.

For the interfacial tension and viscosimetric measurements we used (co)polymer solutions in wabu. These were prepared from aqueous solutions by adding 8.6 ml buOH per 100 ml wabu solution at 25°C. At this temperature, buOH has a stabilizing effect on the copolymers which have an acetate content lower than about 16.4 mole %: PVA-H solutions did not exhibit flakes even after weeks. The influence of buOH on R2 was negligible, but it destabilized B4 and B5 (ch. 3.3.4). B4 was fully soluble, but formed flakes after several days. This solution was always used directly after preparation. Only 52% of B5 stayed in solution in wabu at 25°C.

The solutions used to spread copolymers at the interface (ch. 4 and 6) were prepared from an aqueous solution by adding 7 ml buOH, 5 ml 1-propanol and water up to 100 ml. Addition of 1-propanol improves the spreading capacity of the solution (CRISP, 1946). The composition of the solution of B5 was slightly different: 4 ml buOH and 8 ml 1-propanol were added. All these solutions were stable for months.

Although PVA-H is insoluble in buOH, we determined the distribution coefficient between wabu and buwa at 25.0°C for two copolymers. These amounted to 10^3 and 4×10^2 for B1 and B4 resp.. Therefore, it can be concluded that the copolymers are also practically insoluble in buwa.

The quantitative determination of (co)polymer concentrations was always performed either colorimetrically, as described by FLEER (1971), or interferometrically. The former method is applicable to solutions in water and wabu with (co)polymer concentrations between 0 and 40×10^{-4} weight %, the latter only to solutions in water, up to (co)polymer concentrations of 1 weight % (this was used in particular for the analysis of the GPC fractions).

3.4. CONCLUSIONS

The structure of PVA and PVA-Ac has been surveyed, especially with respect to possible structural irregularities, the acetate content and its distribution. These properties have been related to the rate of dissolution, the solubility of the (co)polymers in water, and to their interfacial activity.

Differences in adsorption between Poval and Polyviol copolymers containing 1–2 mole % acetate groups are mainly due to the presence of conjugated carbonyl structures, interface-active admixtures and a slightly more blocky acetate distribution in the Polyviol samples. The molecular weight distribution for all Poval samples is approximately the most probable or Flory distribution. The Polyviol samples have a broader distribution that varies with molecular weight.

Five blocky (B1–B5) and two random (R1 and R2) PVA-Ac copolymers have been prepared from a completely hydrolysed Poval sample. Therefore, these copolymers differ, irrespective of molecular weight, only in acetate content and distribution. Their acetate distribution has been analysed colorimetrically as well as with IR spectroscopy and thermal analysis.

The solution properties of these copolymers in water and wabu have been studied by viscosimetry. Special attention has been paid to the methods of processing the experimental data. For PVA(-Ac) in water and wabu, the generally applicable method suggested by Maron and Reznik and the Martin extrapolation yield the most reliable results.

For random copolymers, the linear expansion factor in water steadily decreases with acetate content, whereas it passes through a maximum for blocky copolymers. The decrease is related to the more hydrophobic character of the VAc groups. The initial increase of α for the blocky copolymers is explained by the incompatibility between longer VA and VAc sequences, that dominates the intramolecular interaction balance over that range of acetate content and distribution.

BuOH has a stabilizing influence on PVA in solution, probably due to preferential adsorption of buOH molecules onto the C–C backbone of the polymer. This stabilizing effect decreases with acetate content, which has been ascribed to a lower influence of the incompatibility in an expanded molecule and the prevention of buOH adsorption on those parts of the chain to which the acetate groups are attached.

An attempt has been made to determine the peripheral solvent quality for the (co)polymers from the values of the Huggins coefficient. Probably, the mean peripheral acetate content is less than the mean overall content for all copolymers studied.

The interfacial activity of PVA and of the copolymers has been studied by measuring the interfacial tension between a (co)polymer solution in wabu and buwa. The dynamic drop-volume and the static drop-shape method have been compared together. It has been shown experimentally, that the more accurate and much more simple drop-volume method is also applicable to (co)polymer solutions, provided their concentrations are not too low.

The interfacial activity of PVA-Ac increases with acetate content, especially for the blocky copolymers. It has been concluded that longer VAc sequences are the anchors that adsorb at the wabu-buwa interface. The time effects have been ascribed to unfolding of adsorbed copolymers, so that the longer VAc sequences of the inner part of the coil can adsorb.

4. A SEMI-EMPIRICAL STUDY ON MASS TRANSFER BETWEEN TWO LIQUID PHASES

4.1. INTRODUCTION

One of the simplest model systems that has ever been proposed to investigate the permeability of biological membranes is the solute transfer through a water-oil interface (e.g. ROSANO et al., 1961; TING et al., 1966; SCHULMAN, 1966; ROSANO, 1967; SHANBAG, 1973). A slightly more realistic simulation of this very complex process was obtained by the introduction of a protein at the interface (KUIPER, 1968; MOORE, 1968).

In all these studies, a transport vessel was used containing an aqueous phase, usually comprising the transferring material, with on top of it an oil layer (often buwa). These phases were stirred relatively slowly (20–50 min^{-1}). Thus, the transport to the interface was increased without disturbing the interface too much. It was always assumed, without any convincing proof, that the rate-determining step of this mass transfer process was the actual transfer through the interface. The diffusional resistances to the solute transport to and from the interface were, thus, considered to be negligible. This substantially unsupported hypothesis was used to relate the measured transport rate (usually determined at only one stirring speed) to the activation free energy of passage through the interface. By variation of the temperature, some investigators even went so far as to separate the free energy into an enthalpic and an entropic contribution (TING et al., 1966; SCHULMAN, 1966).

This very speculative but frequently used hypothesis is in contrast to observations of DE JONGE-VLEUGEL and BIJSTERBOSCH (1973), who investigated the transport rate of electrolytes through the wabu-buwa interface, also in such a stirred vessel. However, they observed an appreciable dependence of the transfer rate on the stirring speed. They proposed an improved rate equation by introducing two diffusional resistances for the 'unstirred layers' in the vicinity of the interface. Nevertheless, they were unable to estimate the actual magnitudes of both the resistance to transfer and the two diffusional resistances. They also found that the introduction of PVA in the aqueous electrolyte solution decreased the transfer rate drastically. An analysis of the quotient of the transport rate without and with PVA present, caused them to relate this quotient to the fraction of the interface covered with polymer segments. However, by this approach they had also assumed implicitly (although they were unaware of it) that the diffusional resistances were negligible.

In our opinion, the precise mechanism of retardation can only be decided upon once the 'clean' transfer process is understood in all details. An essential problem that has to be solved is: *which is the rate determining step in the 'clean' transfer process*? Only if the resistance of passing the interface is at least comparable in magnitude to the diffusional resistances, will the explanation of the

retarding effect be possibly found in a simple covering of the interface. The basic problem can be tackled by an analysis of the influence of the rotation speed on the measured transport rate. This will be shown in the next section. Subsequently, this semi-empirical analysis will be applied to the actual transfer process. In addition, the influence of several macromolecular and low molecular weight substances on the transfer rate will be investigated.

4.2. PRINCIPLE OF THE METHOD

Assuming ideal mixing in both bulk phases, DE JONGE-VLEUGEL and BIJS-TERBOSCH (1973) derived a general rate equation for the solute transfer from one phase (wabu) to the other (buwa):

$$- V_b \ln (1 - c_b^t/c_b^e) = \frac{A(1 + am_{bw})t}{m_{bw}/k_w + m_{bw}/k_\sigma + 1/k_b} = AK_b t \qquad (4.2-1)$$

where V_b means the buwa volume, c_b^t the mean concentration of transferring solute in that phase at time t, c_b^e the same at equilibrium, A the cross-sectional area of the interface, a the ratio between the volumes of buwa and wabu, and m_{bw} the distribution coefficient of the solute between buwa and wabu; k_w and k_b are the liquid phase mass transfer coefficients in the wabu and buwa phase, k_σ is the interfacial mass transfer coefficient (for transfer from wabu to buwa) and K_b the overall mass transfer coefficient with respect to the buwa phase. In ch. 5.2.3. these mass transfer coefficients will be defined from the basic principles of mass transfer. There, it will also be indicated that the derivation of (4.2–1) is essentially analogous to the two-film theory of LEWIS and WHITMAN (1924), but including an interfacial resistance.

At the moment, it suffices to know that both liquid phase mass transfer coefficients constitute the rate constants of the solute transport to and from the interface in the respective phases. It can be shown that they are both dependent on the hydrodynamics in the vicinity of the interface. A semi-empirical approach was proposed by SCHOLTENS and BIJSTERBOSCH (1976) by writing k_w and k_b as a function of the rotation speed, N (equal for both phases):

$$k_w = b_w N^\alpha \; ; k_b = b_b N^\alpha \qquad (4.2-2)$$

b_w and b_b are proportionality constants that depend on the diffusion coefficients in and the kinematic viscosities of both phases and, in addition, on the geometry of the transport vessel and the hydrodynamics in the vicinity of the interface. The value of α depends on the stirring conditions (often $0.6 < \alpha < 1.5$ is found; the more turbulent the flow, the higher the value of α; DAVIES, 1972 ch. 5). Substitution of (4.2–2) in (4.2–1) yields:

$$- V_b \ln (1 - c_b^t/c_b^e) = A \frac{C}{m_{bw}/k_\sigma + BN^{-\alpha}} t = AK_b t \qquad (4.2-3)$$

with

$$C = 1 + am_{bw} \tag{4.2-4}$$

$$B = m_{bw}/b_w + 1/b_b \tag{4.2-5}$$

B and C are constants provided the variation in solute concentration during a transport experiment is not too large (since D, m and v are alle functions of c). By keeping the stirring speed low enough so that the interface is not severely disturbed by waves, A can be considered a constant too. Under these assumptions, K_b can be determined from the slope of the plot of $-V_b \ln(1 - c_b^t/c_b^\delta)$ against t, provided A is known. From (4.2–3), we obtain then:

$$(K_b)^{-1} = m_{bw}/(Ck_\sigma) + (B/C) N^{-\alpha} \tag{4.2-6}$$

This means that, provided the value of α is known, a plot of $(K_b)^{-1}$ against the corresponding $N^{-\alpha}$ will yield an intercept that can provide k_σ directly.

This approach might enable us to separate the interfacial transfer coefficient, k_σ, from the overall transfer coefficient K_b, and to establish experimentally which part of the total process is rate determining. In the same way, the influence of any adsorbed material can be analysed: a change in the intercept of (4.2–6) can be explained by assuming a barrier at the interface, whereas a change in the slope must mean different hydrodynamic conditions near the interface. In the next section, we shall apply an empirical method to determine α for the electrolyte transfer through the wabu-buwa interface. In addition, we shall attempt to examine the influence of some copolymers and low molecular weight surfactants on the separate coefficients.

4.3. EXPERIMENTAL, RESULTS AND DISCUSSION

The transport rate of KCl from wabu to buwa was measured at $25.00 \pm 0.01\,^\circ\text{C}$. The experimental arrangement as drawn schematically in fig. 4.3–1 is
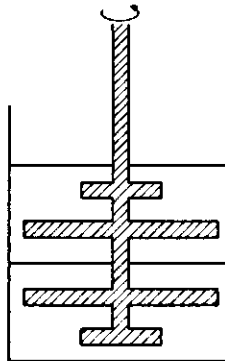

FIG. 4.3–1. Outline of the experimental arrangement for the mass transfer measurements, consisting of a 600 ml beaker that contains 225 ml 0.102 M KCl in wabu and on top of it 225 ml buwa; the glass stirrer is symmetrical with regard to the interface.

essentially equal to that of TING et al. (1966). The dimensions and the measuring technique have been described by DE JONGE-VLEUGEL and BIJSTERBOSCH (1973). Here, it suffices to mention that c_b^{KCl} was measured conductometrically as a function of time during 15–60 minutes. All the relevant properties of the wabu and buwa solutions have been described in ch. 2.2 and 2.3. From the values of the time-dependent c_b^{KCl}, K_b could be calculated with (4.2–3), since the rotation speed was always kept so low that A was not increased considerably by waves. Usually, the measured value of c_b^{KCl} varied between 0.2 and 1.0 mM (the starting value of c_w^{KCl} was always 0.1017 M). Thus B and C of (4.2–3) can safely be taken constant during the measurements (see also ch. 2.3).

In spite of all precautions, the transport measurements were not very reproducible. Since for most rotation speeds the standard deviation in K_b was rather large (approximately 5 %), the average values of several determinations were taken. These results, with their standard deviation, are collected in the first two columns of table 4.3–1.

In order to be able to use (4.2–6), α must be known. Since the hydrodynamics in this transport vessel are very complex, α cannot be predicted theoretically. Therefore, it must be determined experimentally; it seems reasonable to use that value of α that gives the best straight line for the $(K_b)^{-1}$ against $N^{-\alpha}$ plot. However, not each value of α is acceptable: its physical significance and consequences must be sound. For example, a negative intercept in the plot has no physical meaning for this system. It might be caused by spontaneous instabilities in the interface (ch. 5.4), but these will be proved to be absent (ch. 6.1). Therefore, the intercept must be at least zero.

The line with the highest correlation factor yielded a large negative intercept. Thus, no unambiguous value of α could be obtained experimentally. Two reasonable alternatives remained: either that value of α that gave relatively the best line with a physically sound value for the intercept, or the value that resulted in the smallest standard deviation in the intercept. These values of α appeared to be close together, 0.61 and 0.67 respectively. The former value gave

TABLE 4.3–1. Overall mass transfer coefficients as a function of the rotation speed.

N min^{-1}	$10^6 \times K_b$ m.s^{-1}	$10^6 \times K_b^s$ m.s^{-1}	K_b/K_b^s
15	5.9 ± 0.1	0.91 ± 0.05	6.5 ± 0.4
20	6.7 ± 0.2	1.07 ± 0.05	6.3 ± 0.4
25	7.9 ± 0.2	1.32 ± 0.05	6.0 ± 0.3
30	8.9 ± 0.2	1.54 ± 0.06	5.8 ± 0.3
35	9.5 ± 0.2	2.12 ± 0.09	4.5 ± 0.2
40	10.7 ± 0.2	2.69 ± 0.08	4.0 ± 0.2
45	11.4 ± 0.2		
50	12.1 ± 0.2		
60	13.3 ± 0.2		

an intercept deviating insignificantly from zero, and thus no measurable interfacial resistance; the latter yielded as intercept $(1.0 \pm 0.25) \times 10^4$ s.m^{-1} and $k_\sigma = (1.7 \pm 0.4) \times 10^{-6}$ m.s^{-1}. Although this method did not provide an unambiguous value for k_σ, it could still be inferred that the actual influence of k_σ on the transfer rate was negligible. As a first approximation we can further assume $b_w \approx b_b$ (equation (4.2–2)). Since m_{bw} is only 1.72×10^{-2} (ch. 2.3), we come to the conclusion that the transfer rate is almost completely determined by the value of k_b. Closer analysis leads to $b_w > b_b$, as the viscosity of the buwa phase is higher than that of the wabu phase. This only makes the role of k_b still more dominant. Our conclusion that the contribution of k_σ is negligible is in sharp contrast to the usual assumption as mentioned in ch. 4.1, namely that k_σ is the rate-determining factor.

Measurements of DE JONGE-VLEUGEL and BIJSTERBOSCH (1973) demonstrated that very small amounts of PVA, present in the wabu phase, could decrease K_b down to 1/6 of its original value. In fact, they used copolymers (PVA-Ac), containing 2 or 12 mole % vinyl acetate monomers. In their interpretation, they assumed implicitly that k_σ was rate-determining in this process, in contrast to the present results.

Although the method we have applied did not provide unambiguous values for k_σ, it can still be used to analyse the influence of any adsorbed material at the interface. A priori it seems rather improbable that the observed retarding effect can be explained by a barrier mechanism at the interface, as that barrier will only decrease by far the largest transfer coefficient, and this will hardly affect K_b (see equation (4.2–6)). However, it may still be possible that the extrapolations as described above will yield higher values for the intercept. In that case, the change in k_σ can, as yet, be interpreted in terms of a fractional covering of the interface.

To elucidate the effect of PVA-Ac, we determined, for different values of N, the overall mass transfer coefficient at constant amount of PVA-Ac present, K_b^s. For that purpose, PVA-Ac V 03/140 was used, the relevant properties of which have been treated in ch. 3.2. At the beginning of an experiment, an wabu PVA-Ac solution was poured very slowly down the stationary stirrer shaft, in order to allow it to spread most effectively at the interface. The final PVA-Ac concentration in wabu was 1 ppm, whereas its concentration in buwa was negligibly small (ch. 3.3.6).

Average values of K_b^s are collected in column 3 of table 4.3–1, and the ratios of K_b and K_b^s in column 4. From this last column we can already infer that $(K_b^s)^{-1}$ against $N^{-\alpha}$ will not yield a straight line for $\alpha = 0.61$ or 0.67. This is illustrated in fig. 4.3–2, where $(K_b)^{-1}$ and $(K_b^s)^{-1}$ are plotted against $N^{-0.67}$. This rather poor result might have been caused by the stirring rod that sticks through the interface. Especially at higher values of N, the rod will disturb the adsorption layer, thereby decreasing its retarding influence. This effect is still stronger at lower PVA-Ac concentrations: at 0.13 ppm, K_b/K_b^s varies from 5.5 at 15 min^{-1} down to 1.3 at 50 min^{-1}.
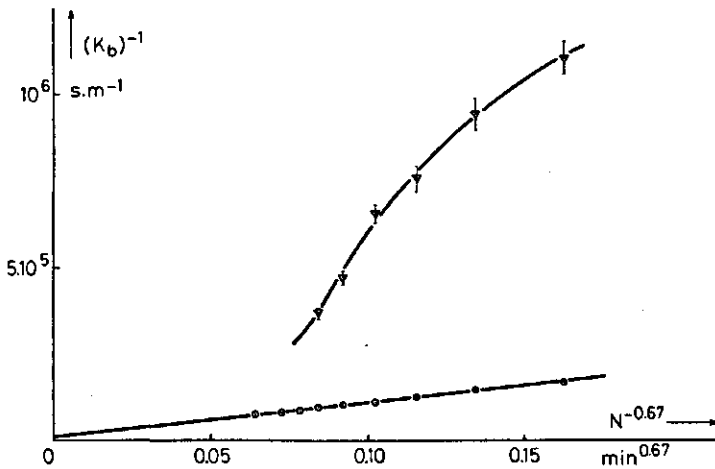
FIG. 4.3–2. $(K_b)^{-1}$ and $(K_b^s)^{-1}$, $\bigcirc$ and ∇ respectively, as a function of $N^{-0.67}$.

However, from the results at very low N, where K_b/K_b^s is almost constant, we can still infer qualitatively that mainly the liquid phase mass transfer coefficients are changed since the slope of the curve has been increased strongly. We showed above that, very probably, k_b is the rate determining factor in a 'clean' experiment. Therefore, we must primarily ascribe the observed effects of PVA-Ac to its influence on k_b. From the present results, however, we cannot draw any definite conclusion about the influence of PVA-Ac on k_σ. To that end, we would need an experimental set-up with an undisturbed interface and probably also a flow situation that is amenable to approximate calculations. This might also provide a more sound theoretical basis for the semi-empirical method used. A thorough knowledge of mass transfer phenomena seems indispensible both to decide which is the most promising flow field for these model measurements, and to be able to predict the hydrodynamic contributions theoretically. Therefore, we made a study on the fundamentals of mass transfer, which will be discussed in ch. 5.

Up to now, the retardation of mass transfer has been ascribed to PVA-Ac adsorption at the wabu-buwa interface, but without any direct proof. However, the very low PVA-Ac concentrations used, as well as the inferred change in k_b (whereas PVA-Ac is almost insoluble in buwa) both point strongly in the direction of adsorption as the cause of the retardation. Of course, the best proof would be to demonstrate adsorption for retarding agents and no retardation for non-adsorbing agents.

Therefore, we performed some exploring measurements with several 'interface-active' agents. It appeared that a lot of these agents did not influence K_b, whether they were dissolved originally in one of the phases or spread directly at the interface (e.g. PEG 4000, 1-octanol, 1-decanol, Span 80, stearic acid,

ω-aminocaproic acid and sodium oleate)*). Interfacial tension measurements with these substances present in either the wabu or the buwa phase showed that none of them decreased γ_{wb} (the drop-weight method was applied, as described in ch. 3.3.5). Sodium dodecylsulphate was able to decrease K_b down to about 2/3 of its original value, and it did feature a decrease in γ_{wb} of 20% (both at 10^{-4} M in wabu). All Polyviol samples used (ch. 3.2) were able to decrease K_b ultimately to approximately 1/6 of its original value; the PVA-Ac concentrations needed were the lower the more interface-active the samples were (as inferred from their effect on γ_{wb}, that was stronger for the preparations with the higher VAc content).

A very interesting result was obtained with Poval PVA-Ac preparations. Two samples with low acetate content (Poval 105 and 124, see ch. 3.2) neither adsorbed, nor retarded the mass transfer. This is in contrast to Polyviol V 03/20 and V 48/20, two preparations that closely resemble the Poval samples, both in acetate content and in molecular weight. The cause of this intriguing discrepancy in interfacial activity has been analysed further in ch. 3.2. During that investigation, the hypothesis was introduced that not only the acetate content would influence the interfacial properties of PVA-Ac, but also the acetate distribution. This has been investigated more systematically in ch. 3.3.

From all these results together, we can safely conclude that the retardation is indeed caused by an adsorption layer of PVA-Ac, spread or adsorbed at the interface. However, any explanation of this retardation on a molecular scale requires first of all a thorough understanding of the principles of both mass transfer, together with interfacial and polymer chemistry. After a short introduction to the first discipline (ch. 5), we shall combine these three aspects in ch. 6 in order to interpret the more quantitative investigation described there.

4.4. Conclusions

In this chapter, the KCl transport from wabu to buwa has been investigated. With a semi-empirical procedure, we have attempted to separate the interfacial from the overall mass transfer coefficient. Although this method does not provide an unambiguous value for k_σ, it can be inferred that k_b and not k_σ is the rate-determining factor in the transfer process.

The retarding influence of PVA-Ac is most likely to be of a hydrodynamic nature. With the present experimental set-up, more quantitative results cannot be obtained, but the hypothesis that adsorption is the cause of retardation has been confirmed.

---

*) Transport measurements in the presence of ionic interface-active agents were analysed by withdrawing regularly small samples of buwa. The K^+ concentration of these was determined with an Eppendorf flamephotometer.

5. FUNDAMENTALS OF LIQUID-LIQUID MASS TRANSFER

5.1. INTRODUCTION

The main objective of the transfer measurements being described in this study is to gain a better understanding of the retarding effect of adsorbed (co)-polymers on the transfer rate. In ch. 4, it appeared impossible to draw correct conclusions from the measurements without a thorough insight in the fundamentals of mass transfer. Therefore, these will be treated in this chapter.

Since mass transfer is an irreversible process by its very nature, we cannot use classical thermodynamics to describe it. However, phenomenological laws exist that relate any flux with its driving force(s). We shall confine ourselves to isothermal liquid-liquid mass transfer studies without chemical reaction. In addition, the transfer of only one solute between two mutually saturated phases will be treated. Thus, the relevant laws are: Fick's diffusion law that relates the flow of matter of a component in a mixture with its concentration gradient, and Newton's friction law that relates the shear stress with the velocity gradient in a fluid.

In this chapter, we shall first focus our attention on the basic principles of these two laws and introduce the terms mass transfer coefficient and resistance. Next, we shall indicate how these principles can be applied to experimental situations. We shall review the current theories of mass transfer in static, laminar- and turbulent-flow systems, and check their applicability with experimental results found in the literature. In addition, the effects of interface-active molecules (IAMs) on these transport processes will be discussed. Finally, we shall pay attention to spontaneous instabilities that may arise during mass transfer as a result of the non-equilibrium situation of the system. Within the restrictions of our system, density- or interfacial-tension-driven disturbances may occur, which increase mass transfer processes drastically. We shall outline their effect, their conditions of occurrence, and the influence that IAMs exert upon them.

5.2. BASIC PRINCIPLES

5.2.1. *Diffusion in liquid mixtures*
In an isothermal and isobaric system, any difference in chemical potential across both sides of a boundary causes a net mass flux through that boundary. This is due to the statistical Brownian motion of all molecules: the bruto flux from the side with the higher concentration will override that from the other side.

In general, a difference in chemical potential for any component i implies a driving force for all components of the system (Gibbs-Duhem). Therefore, all

components are diffusing, and it is necessary to define the rate of diffusion of each species relative to a local velocity of the mixture (BIRD et al., 1960 ch. 16). We shall use the molar-average velocity v^*, defined by:

$$v^* = \left(\sum_{i=1}^{n} c_i v_i \right) / c \tag{5.2-1}$$

c_i is the molar concentration ($kmol.m^{-3}$) of species i that moves with a velocity v_i ($m.s^{-1}$); $c = \sum_{i=1}^{n} c_i$ and n is the number of components of the mixture.

Now Fick's first law of diffusion is defined by:

$$J_i^* = c_i(v_i - v^*) = -c \sum_{k=1}^{n-1} D_{ik} \nabla x_k \tag{5.2-2}$$

J_i^* ($kmol.m^{-2}.s^{-1}$), is the molar flux relative to v^*, D_{ik} the diffusion coefficient that corresponds to the diffusional flow of i (relative to v^*) caused by the difference in chemical potential of species k, and x_k is the mole fraction of component k ($x_k = c_k/c$). In a two-component system, D_{12} is well defined, but in an n-component system, D_{ik} is a complex function of the partial derivatives of the chemical potentials of all species with respect to the concentration of component k (e.g. FITTS, 1962 ch. 8).

We can write the total molar flux of component i relative to stationary coordinates. ϕ_i'' ($kmol.m^{-2}.s^{-1}$), as the sum of a diffusional flux (J_i^*) and a convective flux ($c_i v^*$):

$$\phi_i'' = c_i v_i = c_i(v_i - v^*) + c_i v^* = J_i^* + c_i v^* \tag{5.2-3}$$

and since

$$cv^* = \sum_{i=1}^{n} \phi_i''$$

$$\phi_i'' = -c \sum_{k=1}^{n-1} D_{ik} \nabla x_k + x_i \sum_{i=1}^{n} \phi_i'' \tag{5.2-4}$$

In a two-component system with equimolar diffusion (this means that $\phi_1'' + \phi_2'' = 0$, so that $v^* = 0$), this equation reduces, at constant c, to the more familiar formalism of Fick's first law:

$$\phi_i'' = -D_{12} \nabla c_1 \tag{5.2-5}$$

At small concentration differences of component i in a mixture, (5.2-4) can also be approximated by (5.2-5) as $v^* \approx 0$ in that case. Then, D_{12} must be replaced by D_m^i, the diffusion coefficient of species i in that mixture (analogous to e.g. BIRD et al., 1960 p. 571).

Application of the law of conservation of mass of species i to a volume element results in the equation of continuity for component i:

$$\frac{\partial c_i}{\partial t} + \nabla \cdot \phi_i^r = 0 \qquad (5.2\text{--}6)$$

as we only consider systems with zero rate of production of i. Insertion of (5.2–2) and (5.2–3) in (5.2–6) yields:

$$\frac{\partial c_i}{\partial t} + \nabla \cdot (c_i \, \mathbf{v}^*) = \nabla \cdot \left(c \sum_{k=1}^{n-1} D_{ik} \, \nabla x_k \right) \qquad (5.2\text{--}7)$$

This equation describes the concentration profile of component i in an n component mixture. Assuming c and D_{ik} to be constant, which holds approximately in dilute solutions of i at constant temperature and pressure, (5.2–7) reduces to:

$$\frac{\partial c_i}{\partial t} + \mathbf{v}^* \cdot \nabla c_i = \sum_{k=1}^{n-1} D_{ik} \, \nabla^2 c_k \qquad (5.2\text{--}8)$$

At small concentration differences of component i in the mixture, this equation may be approximated by:

$$\frac{Dc_i}{Dt} = \sum_{k=1}^{n-1} D_{ik} \, \nabla^2 c_k \qquad (5.2\text{--}9)$$

where $\dfrac{Dc_i}{Dt}$, the substantial derivative, is given by:

$$\frac{Dc_i}{Dt} = \frac{\partial c_i}{\partial t} + \mathbf{v} \cdot \nabla c_i \qquad (5.2\text{--}10)$$

and $\mathbf{v}$ is the mass-average or barycentric velocity.

In a binary mixture with zero velocity, (5.2–9) reduces to Fick's second law:

$$\frac{\partial c_1}{\partial t} = D_{12} \, \nabla^2 c_1 \qquad (5.2\text{--}11)$$

5.2.2. *Fluid flow*

From (5.2–8) or (5.2–9) it can be inferred that the velocity of the fluid plays a very important part in the equation of conservation of mass, the master equation for the description of mass transfer processes. In a large number of mass transfer studies, some kind of convective transport is present. We shall distinguish between laminar and turbulent flow.

During laminar flow, fluid elements with different velocities move along parallel streamlines. The Brownian motion of the molecules then results in a net flux of momentum from the faster flowing to the slower flowing parts. This momentum flux can be interpreted as a stress at the boundary of two different

streamlines. Newton's law of viscosity relates the momentum flux to the velocity gradient by:

$$\tau_{yx}\Big|_{y_o} = -\eta \frac{\partial v_x}{\partial y}\Big|_{y_o} \tag{5.2–12}$$

τ_{yx} (N.m^{-2}) represents the flux of x-momentum in the y-direction at y_o caused by the velocity gradient $\partial v_x/\partial y$ at that position, η is the viscosity (kg.m^{-1}.s^{-1}) and v_x (m.s^{-1}) the velocity in the x-direction.

Laminar flow of a pure isothermal incompressible fluid can, in principle, be completely described by the equations of conservation of momentum and continuity. For liquids with constant ρ and η, this results in the Navier-Stokes equations (BIRD et al., 1960; SCHLICHTING, 1968). In multicomponent systems, a full description of flow is obtained from the equations of conservation of momentum and of continuity of each chemical species (equation (5.2–6)). Usually, even the Navier-Stokes equations cannot be solved because of their enormous mathematical complexity. In practice, the equations must be simplified by careful consideration of the relative magnitudes of the various terms, before a solution can be obtained for a simplified flow system.

In mass transfer studies, the flow in the immediate vicinity of the interface requires special attention. For the description of viscous flow in that region, we may take recourse to the boundary layer approaches, as given by SCHLICHTING (1968), LEVICH (1962), BIRD et al. (1960) and BEEK and MUTTZALL (1975).

In turbulent flow, the velocity fluctuates about its mean value. Momentum is not only transmitted by molecular interactions, but also by the velocity fluctuations (eddies). It is useful to introduce here the Reynold's number, Re, defined by:

$$Re = \bar{v} \, \rho \, L/\eta \tag{5.2–13}$$

where $\bar{v}$ is the mean bulk velocity and L a characteristic length of the system. When, in a given situation, Re exceeds a critical value (approximately 3×10^3 for flow in pipes, 5×10^5 for the boundary layer along a flat plate), the ordered laminar flow is no longer maintained. An additional, rapidly fluctuating velocity arises, perpendicular to the streamlines. Thus, turbulent transport of longitudinal momentum occurs, perpendicular to the flow direction and characterized by the turbulent momentum flux $\bar{\tau}$. The tensor $\bar{\tau}$ can only be handled semiempirically (HINZE, 1959; SCHLICHTING, 1968; DAVIES, 1972). Therefore, the momentum balance cannot be solved exactly: only time-averaged equations can be obtained that contain a term with $\bar{\tau}$.

A number of theories have been proposed to approximate the complex hydrodynamic situations for turbulent flow in the vicinity of the interface by more or less simple physical models. The main concepts of these models and their relevance to mass transfer studies will be discussed in ch. 5.3.3.

66

5.2.3. *Definitions of mass transfer coefficients and resistances*

Let us consider a solute A, dissolved in phase 1, that is in contact with an immiscible phase 2, in which A is soluble too. The essential quantity in mass transfer studies is the average flux of A through the interface, $\bar{\phi}''_A$. Henceforth, we shall omit the superscript – and the subscript A for the sake of simplicity. However, it must be borne in mind, that, throughout this section, average quantities are treated, referring to solute A.

Now, we define the average partial mass transfer coefficient of A in phase 1, k_1 (m.s^{-1}), by:

$$k_1 = \frac{\phi''}{c_1 - c_{1\sigma}} \tag{5.2-14}$$

Thus, ϕ'' is the experimentally accessible average molar flux of A through the interface, and c_1 and $c_{1\sigma}$ are the average molar concentrations of A in the bulk and at the interface, respectively. Since we confine ourselves to systems with very small values of x_A, insertion of (5.2–4) and omission of negligible terms yields:

$$k_1 = \frac{-D_1 \, (\partial c_1/\partial z)_{z=0}}{c_1 - c_{1\sigma}} \tag{5.2-15}$$

where the plane $z = 0$ is the interface and D_1 is the diffusion coefficient of A in phase 1.

Completely analogously, the partial mass transfer coefficient of A in phase 2 reads:

$$k_2 = \frac{-D_2 \, (\partial c_2/\partial z)_{z=0}}{c_{2\sigma} - c_2} \tag{5.2-16}$$

In general, there may also exist a finite average interfacial transfer coefficient, k_σ. It may be caused by a kinetically slow process during the transfer of A crossing the interface from phase 1 to phase 2 (desolvation, permeation through a monolayer, or desorption), and it is defined by:

$$k_\sigma = \frac{\phi''}{c_{1\sigma} - m_{12} \, c_{2\sigma}} \tag{5.2-17}$$

where m_{12} is the distribution coefficient of A between phase 1 and 2 at equilibrium conditions ($m_{12} = c^e_{1\sigma}/c^e_{2\sigma}$).

As the average interfacial concentrations of A are generally unknown, we eliminate them from the expressions of k_1, k_2 and k_σ. Provided m_{12} is constant for the studied concentration range of A, this results in:

$$\phi'' = \frac{m_{12} \, (c_{2*} - c_2)}{(k_1)^{-1} + (k_\sigma)^{-1} + m_{12}/k_2} = K_2(c_{2*} - c_2) \tag{5.2-18}$$

where c_{2*} is defined by:

$$c_{2*} = c_1/m_{12}$$

and K_2 is the mean overall mass transfer coefficient of A with respect to phase 2. Completely identically we can derive:

$$\phi'' = \frac{(c_1 - c_{1*})}{(k_1)^{-1} + (k_\sigma)^{-1} + m_{12}/k_2} = K_1(c_1 - c_{1*}) \qquad (5.2\text{--}20)$$

It must be remarked that this quite general approach is, in fact, similar to the derivation of the two-film theory by Lewis and Whitman (discussed in ch. 5.3.3).

In analogy with an electrical circuit, we can also introduce average mass transfer resistances, defined by the ratio of the average driving force (the concentration difference) and the average molar current density ($= \phi''$). So, they are just the reciprocals of the partial mass transfer coefficients*) (s.m^{-1}):

$$r_1 = (k_1)^{-1} \qquad (5.2\text{--}21)$$

$$r_\sigma = (k_\sigma)^{-1} \qquad (5.2\text{--}22)$$

$$r_2 = (k_2)^{-1} \qquad (5.2\text{--}23)$$

Thus, the overall mass transfer resistance with respect to phase 2, R_2 ($= 1/K_2$), can be represented by a series of the three partial mass transfer resistances.

$$R_2 = r_1/m_{12} + r_\sigma/m_{12} + r_2 \qquad (5.2\text{--}24)$$

From this equation we can infer that, provided r_1, r_σ and r_2 are of the same order of magnitude, at large values of m_{12}, R_2 (and R_1 analogously, of course) will be mainly determined by r_2 and, at small values of m_{12}, by r_1 and r_σ. So, the partial resistance of the phase in which A is least soluble is relatively the most important factor.

The liquid phase resistances (r_1 and r_2) can be considered as diffusional resistances governed by the diffusion coefficient of A and the effective diffusion path δ, over which the concentration difference is present:

$$r_1 = \delta_1/D_1 \qquad (5.2\text{--}25)$$

$$r_2 = \delta_2/D_2 \qquad (5.2\text{--}26)$$

Although we can infer qualitatively from these equations that the liquid phase resistances are, amongst others, a function of the hydrodynamics near the interface, it must be stressed that δ is not a hydrodynamic layer, as δ represents the thickness of a mathematically equivalent layer through which stationary diffusion is assumed. The value of δ can only be obtained from the solution of the equation of conservation of mass for that phase under the appropriate boundary conditions. In ch. 5.3, we shall treat more quantitatively the influence of the interfacial hydrodynamics on the solution of that equation.

---

*) It should be borne in mind that r_σ refers to the interfacial resistance that A meets with during the transfer through the interface from phase 1 to phase 2.

5.3. REVIEW OF LIQUID-LIQUID MASS TRANSFER STUDIES

5.3.1. *Introduction*

In the following sections, we shall indicate how, for some particular cases, the basic principles of mass transfer may be used to relate the liquid phase mass transfer coefficients with the diffusion coefficients, time, system geometry and the hydrodynamic conditions in the vicinity of the interface. For convenience, we shall distinguish between mass transfer studies in static as well as in laminar- and turbulent-flow systems, mainly with plane interfaces.

In discussing the methods and results found in the literature, we shall emphasize two subjects: the suitability of each method for the detection of an interfacial resistance (see equation (5.2–22)) and the influence of IAMs on the transfer process. Where possible, an explanation will be given on molecular scale. We shall restrict ourselves here to systems that do not exhibit any interfacial instabilities. It will be seen that many conflicting results have been published even on identical systems. This only indicates that our knowledge and understanding of these processes is still far from complete.

As to the interfacial resistance, even its presence, not to mention its magnitude, can hardly be predicted for a given system. In general, an interfacial resistance can only be determined by comparing the measured overall mass transfer coefficient, K_{exp}, with the partial liquid phase mass transfer coefficients derived from theory. In static systems, one can test, in addition, whether or not equilibrium exists on both sides of the interface. For that purpose, optical methods can be applied (WARD and BROOKS, 1952; DAVIES and WIGGIL, 1960; MUDGE and HEIDEGER, 1970; TRAHER and KIRWAN, 1973). When equilibrium prevails at the interface, it must be concluded that $r_\sigma = 0$. In systems where convective transport is present, on the contrary, the variation of K_{exp} with the hydrodynamic conditions near the interface may provide a means to estimate r_σ (this study, ch. 4 and 6).

5.3.2. *Static systems*

The concentration profile, necessary to calculate k_1 and k_2 (with equations (5.2–15) and (5.2–16)) is obtained by solving Fick's second law, equation (5.2–11). As an instructive, simple example, we shall treat the diffusion of A out of the plane $z = 0$ into an infinite stagnant liquid, assuming a constant interfacial concentration of A, c_σ, during the process. Thus, the boundary conditions are:

$c = c_o$ for $z \geqslant 0$ at $t \leqslant 0$

$c = c_\sigma$ for $z = 0$ at $t > 0$

$c = c_o$ for $z = \infty$ at $t > 0$

Equation (5.2–11) reduces to:

$$\frac{\partial c}{\partial t} = D \frac{\partial^2 c}{\partial z^2}$$

The solution of this homogeneous second order partial differential equation under the given boundary conditions is (CRANK, 1964):

$$c(z, t) = c_\sigma - (c_\sigma - c_o)\, \text{erf}\,(z/\sqrt{4tD})$$

with

$$\text{erf}\, a = \frac{2}{\sqrt{\pi}} \int_0^a \exp(-x^2)\, dx$$

Therefore,

$$\left.\frac{\partial c}{\partial z}\right|_{z=0} = -(c_\sigma - c_o)/\sqrt{\pi t D}$$

This leads to the following equation for the liquid phase mass transfer coefficient and resistance of A (equations (5.2–15) and (5.2–21)):

$$k = \frac{1}{r} = \left(\frac{D}{\pi t}\right)^{1/2} \tag{5.3–1}$$

Thus, r increases with $\sqrt{t}$. Approximate values for r in water are, assuming $D \approx 10^{-9}$ m^2.s^{-1}, 5×10^4 s.m^{-1} at $t = 1$ s, increasing to 5×10^5 s.m^{-1} after 100 s.

Many hundreds of problems described by Fick's second law have been solved (CRANK, 1964; CARSLAW and JAEGER, 1947; SCOTT et al., 1951; AUER and MURBACH, 1954; DAVIES and WIGGIL, 1960; VIGNES, 1960). So, in most cases the liquid phase resistances can be predicted from theory. Still, the determination of an interfacial resistance is almost impossible when its value is lower than approximately 5×10^4 s.m^{-1} (MUDGE and HEIDEGER, 1970). This is caused by two reasons: the liquid phase resistances become very large after short time, and there exists a 'blind' zone near the interface, for which concentrations can only be obtained by extrapolation.

Static liquid-liquid mass transfer processes have been studied only occasionally, mainly on account of the extreme accuracy required to obtain reliable results. Their main objective has been the investigation of the interfacial resistance and the influence of IAMs on it. However, it seems very difficult to draw any definite conclusions from the very different and sometimes even completely conflicting results of these studies.

This will be illustrated for the most frequently studied transfer process, acetic acid transferring from water to toluene. The results for the interfacial resistance vary from not detectable (WARD and BROOKS, 1952; DAVIES and WIGGIL, 1960) via 4×10^4 s.m^{-1} (VIGNES, 1960) up to 10^6 s.m^{-1} (CHANDRASEKHAR and HOELSCHER, 1975). The influence of IAMs varies from not measurable (DAVIES and WIGGIL, 1960) to an increase in r_σ up to 3 times its original value (VIGNES, 1960). These conflicting results must be caused by differences in experimental conditions or interpretation. The claimed inaccuracy of the

methods also varies considerably: from 2×10^3 s.m^{-1} by Vignes up to 10^5 s.m^{-1} by Davies and Wiggil, although their reported accuracy in observations and control of experimental conditions would suggest an opposite order of inaccuracy. There is not even agreement as to whether or not spontaneous instabilities occur during this static transfer process (DAVIES and WIGGIL, 1960; VIGNES, 1960).

The results for other systems do not offer more clarity: very high interfacial resistances have been reported (TUNG and DRICKAMER, 1952; SINFELT and DRICKAMER, 1955), but also zero resistances (BOGUE et al., 1975). In some cases, spontaneous turbulence has been observed that was eliminated by low concentrations of IAMs (HUTCHINSON, 1948; MUDGE and HEIDEGER, 1970).

From the foregoing, we conclude that, in principle, the static system can be used to determine interfacial resistances, but the demanded extreme accuracy in experiment and interpretation have not been attained in all cases. Any general conclusions on the existence of an interfacial resistance and on the influence of IAMs thereupon seem unpermitted.

It is worth mentioning here some results obtained for interfacial resistances to evaporation: with the most sensitive methods, these can be determined to be very small, even in the presence of insoluble monolayers ($r_\sigma \leqslant 5 \times 10^2$ s.m^{-1}; BARNES and LAMER, 1962; BLANK, 1972). It seems improbable that r_σ for liquid-liquid transfer differs orders of magnitude as compared to liquid-gas transfer, unless, in a special case, a very slow process takes place at the liquid-liquid interface (slow desorption due to interfacial activity, or a slow chemical reaction).

5.3.3. *Systems with laminar boundary layers*

Laminar boundary layers exist in all laminar flow situations where the critical value of Re (equation (5.2–13)) is not reached. We shall define the term boundary layer to be that layer over which 99% of the gradient exists (as in SCHLICHTING, 1968). Since diffusion usually penetrates much less deeply into the bulk of the liquid phases than momentum does, the diffusion boundary layer of species A diffusing into liquid 1, δ_{D1}, is much smaller than the hydrodynamic or momentum boundary layer, δ_{v1}. For laminar boundary layers, it can be shown (e.g. BIRD et al., 1960 p. 606) that:

$$\frac{\delta_{v1}}{\delta_{D1}} = \left(\frac{v_1}{D_1}\right)^{1/3} = (Sc_1)^{1/3} \tag{5.3–2}$$

where v is the kinematic viscosity, defined by $v = \eta/\rho$, and Sc_1 represents the Schmidt number for the transferring material in phase 1. Therefore, solutes with different values of D_1 will have different values for δ_{D1} under identical hydrodynamic conditions.

The presence of a liquid-liquid interface (say at $z = 0$), has a pronounced influence on the hydrodynamics by implication of the following boundary conditions:

1) the tangential velocity components are equal in both phases at $z = 0$;

2) the normal velocity components vanish at $z = 0$;

3) the momentum flux perpendicular to the interface is continuous, thus $(\tau_{zx})_{1,z=0} = (\tau_{zx})_{2,z=0}$.

The interfacial tension can only influence the motion when the interface is curved, or when its value varies from point to point along the interface. The second mechanism is mainly of importance either when IAMs are transferred, which may give rise to spontaneous interfacial convections (ch. 5.4), or when IAMs are compressed at the interface by flow phenomena in either of the phases. In the latter case, the interfacial pressure that is induced opposes the fluid movement (Marangoni-effect), resulting in an increase in kinetic energy dissipation in the boundary layers and a decrease in both the interfacial velocity and the momentum transport through the interface. Similar effects may be brought about by the excess interfacial shear viscosity of a monolayer. However, in most cases the latter effect is of minor importance, as only a very small part of the total energy is dissipated by the viscous monolayer.

For a number of relatively simple laminar flow configurations, solutions of equation (5.2–9) are available in the literature (e.g. BIRD et al., 1960; LEVICH, 1962; BEEK and MUTTZALL, 1975). Here, we will treat two cases that are relevant to flat liquid-liquid interfaces: a uniform velocity parallel to the interface and, secondly, a flow parallel to the interface with a constant velocity gradient. More complicated cases, e.g. with an interfacial velocity, can often be approximated by one of these, without introducing serious errors (BEEK and BAKKER, 1961; UEYAMA et al., 1972).

In fact, the non-stationary diffusion of solute A out of the interface ($z = 0$) into a liquid element with uniform velocity v parallel to the interface has been solved by HIGBIE (1935). He used the result for the development of the penetration theory (ch. 5.3.3), but his result can also be applied to flow with a uniform velocity parallel to the interface. In that case, the local mass transfer coefficient for A, k_x, is a function of the contact time, t_x, at any point of the interface:

$$k_x = \left(\frac{D}{\pi t_x}\right)^{1/2} = \left(\frac{Dv}{\pi x}\right)^{1/2} \tag{5.3–3}$$

where x is the length of the path covered by the liquid element from the point of first contact with the interface.

LÉVÊQUE (1928) treated the case in which a constant velocity gradient exists ($v_x = az$, $v_z = 0$). The solution reads:

$$k_x = 0.538 \left(\frac{aD^2}{x}\right)^{1/3} \tag{5.3–4}$$

The advantage of laminar flow situations is obvious for studies on the presence of any interfacial resistance: the possibility to predict the liquid phase resistances with some accuracy (if the exact boundary conditions for the flow system can be defined) is combined with much smaller values of these resistances (compare (5.3–3) with (5.3–1)). Therefore, much lower interfacial resistances

are detectable (down to approximately 5×10^3 s.m^{-1}), as can be derived from (5.2–24).

Although laminar liquid-liquid interfaces have been studied extensively (free falling drops, laminar jets, the dropping mercury electrode), they have not frequently been used to determine the presence of interfacial resistances without or with IAMs present.

Most laminar flow studies have been performed with drops. One of the first attempts to explain the drastic reduction in K_{exp} by poorly soluble IAMs was based on a barrier mechanism. The barrier was assumed to be proportional to the fraction of the interface covered (GARNER and HALE, 1953; LINDLAND and TERJESEN, 1956). However, it is now generally accepted that the inhibition of internal circulation and, if present, of spontaneous turbulence, constitute the main retarding effects of IAMs (LINTON and SUTHERLAND, 1957; DAVIES, 1963; BROWN, 1965; JOHNS et al., 1965; DAVIES, 1972 ch. 8). This inhibition is mainly induced by the compressibility modulus of the monolayer. At higher bulk IAM concentrations, this effect decreases, as the interfacial pressure is being cancelled out by diffusion of IAMs from the solution to the uncovered spots of the interface (LEVICH, 1962; DAVIES and RIDEAL, 1961).

Several studies have been performed with laminar jets or similar equipment (QUINN and JEANNIN, 1961; WARD and QUINN, 1964 & 1965; BAKKER, 1966; FOSBERG and HEIDEGER, 1967). Quinn et al. determined a small interfacial resistance for the transfer of isobutanol from isobutanol saturated with water into water, but is it very likely that the theoretical values for the interfacial velocity they used were too high (FOSBERG et al., 1967). This results, of course, in an apparent r_σ, see equation (5.3–3). The presence of IAMs had no effect. Ward et al. studied some binary and ternary transfer systems with a modified laminar jet set-up. For none of these systems, an appreciable resistance could be detected ($r_\sigma < 10^3$ s.m^{-1}). Fosberg et al. studied three binary systems with the laminar jet (one also comprising isobutanol-water). They arrived at the conclusion that interfacial equilibrium prevails in all those systems. Bakker also investigated the transfer of isobutanol into water. The measured transfer rates agreed well with the theoretical ones, again supporting the existence of equilibrium at the interface.

Dynamic interfacial tension measurements with a laminar contracting liquid jet have also been proposed as a means to measure the influence of adsorption accumulation and adsorption or desorption barriers on the diffusion rate of IAMs (ENGLAND and BERG, 1971). Analytical solutions were given for a static system. However, although the measurements were made with a laminar jet, they were still interpreted on the basis of these analytical solutions. Thus, whereas in several cases no appreciable barrier could be detected, this might have been caused by the higher transfer rate as a consequence of the liquid flow.

A method that also seems useful for mass transfer studies is the dropping mercury electrode (MILLER and GREAT, 1970). However, its applicability to this field of research seems to have received relatively little attention up to the present time.

Perhaps the only extensive investigation on mass transfer through a flat interface with laminar boundary layer flow is being performed by Nitsch and coworkers (NITSCH, 1968; RAAB, 1971; NITSCH et al., 1972; NITSCH et al., 1973a & b; KNIEP, 1974; NITSCH et al., 1976a & b). They showed that an interfacial resistance is detectable when the transferring agent undergoes a very slow chemical reaction at the interface. Unfortunately, the influence of IAMs on this interfacial resistance has never been measured. The influence of IAMs on transfer processes in which interfacial resistances were assumed to be absent, could be shown to be a purely hydrodynamic effect. This result was obtained from heat transfer measurements and from application of the analogy between heat and mass transfer. The conclusions drawn from the measured effects of IAMs are interesting, but of a speculative nature as they still lack sufficient proof (e.g. KNIEP, 1974).

5.3.4. *Systems with turbulent boundary layers*

Forced turbulence in the vicinity of a flat liquid-liquid interface may be set up in different ways, e.g. when the velocities of both phases differ in magnitude and direction; then, couples arise at the interface, which may cause rotation of the interfacial layers (e.g. KAFAROV, 1961). Another source of turbulence is a rapidly flowing liquid injected in the same slow moving liquid (e.g. from a stirrer blade). This causes eddies in the bulk liquid which may reach the interface when they are strong enough. Movement of the stirrer blade also causes eddies in its wake. Finally, the transition of a laminar to a turbulent boundary layer always occurs after Re has reached a certain critical value.

As turbulent single phase flow can only be handled semi-empirically, turbulent boundary layer flow can also at best be described in that way. We shall now review briefly the main theories that describe mass transfer in turbulent boundary layers, the hydrodynamics of which can, from necessity, only be treated approximately. Thus, most theories contain at least one empirical parameter, or make simplifying assumptions on the spectrum of turbulence near the interface. Rather comprehensive descriptions of these theories have been given by LEVICH (1962), ROZEN and KRYLOV (1966) and DAVIES (1963 & 1972).

LEWIS and WHITMAN (1924) proposed a model in which the turbulent bulk phase maintains a homogeneous concentration. Two laminar sublayers extend to a distance δ from the interface, the thicknesses of which are solely determined by the hydrodynamics of the bulk phases (analogous to the Prandtl-Taylor sublayers). Through these laminar sublayers, steady state diffusion is assumed to take place, while equilibrium is assumed at the interface. In this simple picture, the two values for δ are empirical parameters. Although this two-film theory has been proven to be physically incorrect, its conclusion as to the additivity of the liquid phase resistances still retains its value in most cases (deviations of this additivity have been treated by KING (1964) and SZEKELY (1965)).

HIGBIE (1935) assumed that eddies penetrate into the interfacial region, constantly renewing it with fresh liquid from the interior of the phase. He proposed an equal residence time, t^*, for all eddies at the interface, which is mostly quite unrealistic, and no influence of the eddy velocity on the diffusion process. Insertion of t^* in (5.3–3) and integration over t^* yields the time averaged partial mass transfer coefficient:

$$k = 2\left(\frac{D}{\pi t^*}\right)^{1/2} \tag{5.3–5}$$

where t^* is an empirical parameter.

KISHINEVSKI et al. (1949) and DANCKWERTS (1951) independently proposed modifications of the penetration theory. Kishinevski et al. developed a model for the limit of extreme turbulence, where diffusion is no longer rate-controlling. They assumed that the liquid phase mass transfer coefficients are practically only determined by the average velocities normal to the interface and not by the diffusion coefficient. Danckwerts improved the penetration theory by proposing a more realistic distribution of residence times for the eddies at the interface. He assumed that the possibility of removal of a liquid element at any instant is independent of the contact time of that element with the interface. However, the empirical character of the theory was not altered by this often more reasonable picture. The main drawback of both improved renewal theories remains, that they still contain an unknown parameter. For small values of the Fourier number ($Fo = Dt/d^2 < 0.05$, where d is the eddy size), the Danckwerts' theory seems justified, whereas the extreme turbulence in Kishinevski's theory is almost never reached in practice.

TOOR and MARCHELLO (1958) proposed the film-penetration theory, in which the film and the penetration theory are actually assumed to be complementary. At high Sc-values and short contact times, the penetration theory holds for the liquid elements at the interface, whereas at lower Sc-values and longer residence times the material is not accumulated any more in that element, but only transferred through it. In the latter case, the (stationary) film theory applies to the elements at the interface.

Some attempts have been made to relate the renewal frequency-distribution with the bulk turbulence, either on the basis of empirical correlations (DAVIES et al., 1964, 1965 & 1974; BRAGINSKII and PAVLUSHENKO, 1965), or on the basis of assumptions as to the structure of the turbulent field (PROCHÁZKA and BULIČKA, 1971). However, these theories can at best give only relations for the very special stirring conditions and geometry of the transport vessel used.

Levich and Landau (LEVICH, 1962 ch. 3) developed a hydrodynamic theory of a gradual damping of eddies (and thus of turbulent diffusion) in the vicinity of a solid-liquid interface. It was assumed that, in contrast to the film theory, the turbulent motion does not suddenly disappear in the viscous sublayer. In the vicinity of the wall, the theory distinguishes between 3 regions with different effective diffusion coefficients (see also fig. 5.3–1):
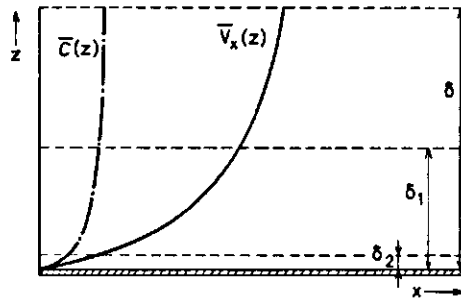
FIG. 5.3–1. Time averaged concentration and velocity profile in a turbulent boundary layer.

1. The 'turbulent boundary layer' ($\delta_1 < z < \delta$), a zone where all mass transport is provided by eddy diffusion, identical to the bulk phase, but where the turbulence is damped yet.
2. The 'viscous sublayer' ($\delta_2 < z < \delta_1$), a zone where all mass is still transported by eddy diffusion, but where the Prandtl-Taylor mixing length of the eddy is taken proportional to the distance from the wall (this proportionality has been examined by DEVANATHAN et al., 1973).
3. The 'diffusion sublayer' ($0 < z < \delta_2$), the innermost part of the viscous sublayer, where molecular diffusion dominates over eddy diffusion.

As molecular and turbulent diffusion are compared in this model, the thickness of the diffusion sublayer for each component is a function of the diffusion coefficient of that species, in contrast with the thickness of δ and δ_1. The smaller the diffusion coefficient, the smaller also is the ratio δ_2/δ. At high Sc values, the diffusional resistances for these three regions can be approximated separately. They can be related to the overall resistance through the mass flux, that must be the same in all three zones at steady state (LEVICH, 1962; DAVIES, 1972 app. 2). In this way, the liquid phase mass transfer coefficient can be estimated as a function of measurable hydrodynamic and physical quantities.

DAVIES (1972 ch. 5) extended the use of this method to liquid-liquid interfaces. Thus, both liquid phase resistances can also be estimated from measurable (time-averaged) quantities.

Since turbulent boundary layers have the smallest liquid phase resistances as compared to laminar-flow or static systems, turbulently stirred systems should, from this point of view, be most suitable for the measurement of r_σ and the influence of IAMs on its value. However, as can be inferred from the different theoretical approaches, the hydrodynamic conditions near an interface are very complex and they vary widely for different experimental set-ups. In addition, even if it is yet known which theory describes the transfer process correctly, the empirical parameter which is inherent to that theory must be estimated from the experiments. Thus, it is very difficult to predict turbulent flow liquid phase resistances theoretically.

Therefore, K_{exp} has often been expressed as an empirical function of the

stirring speeds, geometry, diffusion coefficients and kinematic viscosities of both phases by using several liquid-liquid(-solute) combinations in the same experimental set-up (LEWIS, 1954; GORDON and SHERWOOD, 1954; McMANA-MEY, 1961; MAYERS, 1961; OLANDER and BENEDICT, 1962; SAWISTOWSKI and AUSTIN, 1967). These authors all obtained different functions which described their experiments best, probably due to experimental inaccuracies and to differences in the geometry of the transport vessel and in the spectrum of turbulence. Usually, this relation described the transfer rate for the different liquid-liquid(-solute) combinations to within 20–40%.

Thus, an interfacial resistance could only be ascribed to liquid-liquid(-solute) systems for which the transfer rate was appreciably lower than the empirical functions predicted. Therefore, also with this method only relatively large inter-facial resistances could be detected. Rates appreciably lower than predicted were only found to occur in a few cases where the solute might reasonably be expected to be involved in a slow chemical reaction at the interface (e.g. LEWIS, 1954; BLOKKER, 1957; KREMNEV et al., 1965).

In general, most of the proposed theories can, because of the presence of an empirical parameter, only be verified experimentally from the dependence of K_{exp} on D. On this basis, it can be concluded that the very simple two-film concept is incorrect, and that Kishinevski's theory is also almost never applicable. As to the other theories (e.g. the surface renewal theory of Danckwerts), their empirical parameter (e.g. renewal frequency) can, in principle, be approximated from a comparison with the empirical equations for K_{exp}. This parameter is, of course, a function of the very geometry of the set-up and of the spectrum of applied turbulence. Most empirical equations for K_{exp} are also approximately of the type expected according to the Levich-Landau-Davies approach (DAVIES, 1972 ch. 5). This treatment has been further confirmed by results of McMANAMEY et al. (1973 & 1975).

As r_σ has been found to be negligible in most cases, IAMs can, in general, mainly affect the K_{exp} by their influence on the hydrodynamics in the vicinity of the interface, and thus on k_1 and k_2 (equations (5.2–14) and (5.2–15)). The damping influence of a monolayer on penetrating eddies can be explained analogously to its inhibiting effect on small waves, on circulation in drops, and on spontaneous turbulences (DAVIES and RIDEAL, 1961 chs. 5 & 7; LEVICH, 1962 ch. 11; DAVIES, 1972 chs. 6 & 8). The pressure fluctuation of an eddy approaching a covered interface is resisted not only by the capillary pressure resulting from the deformed interface and by a gravitational force, but also by the elastic stress that originates from the interfacial pressure, set up at the interface when an eddy renews the interface (Marangoni-effect). DAVIES (1966) formulated a quantitative theory for this phenomenon. On the basis of this theory, it can be predicted that, at higher bulk concentrations of film-forming IAMs, this monolayer effect becomes short-circuited by diffusion to the clean areas. Thus, with increasing bulk concentration of IAMs, K_{exp} passes through a minimum. It can also be shown that the reduction of mass transfer by the film

decreases with increasing degree of turbulence. Thus, at very high turbulence, even an insoluble monolayer is without effect: all the material is swept out of the interface. However, also at very low turbulence the effect decreases, as there are almost no eddies penetrating into the stagnant interface.

Experimental evidence for this retarding mechanism by IAMs has frequently been obtained: the value of K_{exp} may be reduced by as much as 80% by an insoluble monolayer (LEWIS, 1954; BLOKKER, 1959; DAVIES and MAYERS, 1961; DAVIES and DRISCOLL, 1974). The effect becomes negligible at low degree of turbulence or high IAM bulk concentrations (ultimately, all static systems, ch. 5.3.2; SJÖLIN, 1942; GORDON and SHERWOOD, 1954; DAVIES and MAYERS, 1961; MAYERS, 1961; DAVIES et al., 1964). However, a completely quantitative verification of the theory of the damping of eddies, as proposed by Davies, has not yet been given.

5.4. SPONTANEOUS INSTABILITIES

Up to this moment, we have only been dealing with forced convection in stable systems. However, a vast amount of systems exists that may show spontaneous instabilities during mass transfer (a historical review has been given by SCRIVEN and STERNLING, 1960). These instabilities are caused by the non-equilibrium state of the system and may increase the mass transfer rate up to more than ten times. Of course, they are very inconvenient during the mass transfer measurements which are used to relate K_{exp} with external hydrodynamics, diffusion and interfacial resistances (HUTCHINSON, 1948; LEWIS, 1954; SIGWART and NASSENSTEIN, 1956; BLOKKER, 1957; BAKKER et al., 1966; SAWISTOWSKI and AUSTIN, 1967).

In general, we may distinguish between density- and interfacial-tension-driven instabilities as well as spontaneous emulsification. Firstly, we shall indicate the conditions of their occurrence, and how they are influenced by the presence of IAMs; secondly, we shall discuss how their existence can be demonstrated.

During mass transfer, *density-driven instabilities* may occur due to a considerable change in density of one of the phases either with the concentration of transferring material or with the temperature (as a result of the heat evolved during solvation of that material). It can easily be shown that concentration-driven density instabilities may occur when A diffuses from (the lower) phase 1 to (the upper) phase 2, provided that $\partial\rho_1/\partial c_1^A > 0$ or $\partial\rho_2/\partial c_2^A < 0$. The opposite conditions hold for the transfer from (the upper) phase 2 to (the lower) phase 1, whereas a completely analogous reasoning can be applied to temperature-driven density instabilities.

IAMs will particularly influence the onset of these density gradients, that arises at the interface, as well as the flow of liquid along the interface that

78   *Meded. Landbouwhogeschool Wageningen 77-7 (1977)*

replaces the moving liquid elements. Thus, density-driven instabilities will be diminished by IAMs, but not completely eliminated.

The dynamic interfacial tension of an interface through which mass transfer takes place can vary from point to point. This can be brought about not only by the influence of flow on a monolayer, but also by the variation of the static interfacial tension with solute concentration or temperature. The two latter effects may both be responsible for interfacial convections, better known as *Marangoni instabilities*. As the gradients in the interfacial tension (γ) due to temperature fluctuations are usually at least one order of magnitude smaller than those caused by concentration fluctuations, we shall confine ourselves to the instabilities that arise from concentration-driven interfacial tension gradients.

These concentration variations are caused by the ever present fluctuations, that can, under certain conditions, be self-amplifying in a non-equilibrium system. Qualitatively, a great deal is known about the factors that amplify these fluctuations into 'roll cells', 'oscillatory instabilities', 'eruptions' or 'interfacial turbulence' (see e.g. the reviews of SAWISTOWSKI, 1971 & 1973). Factors that are of primary importance for the self-amplification of instabilities during the transfer of A from phase 1 to 2 are:
1) the sign of the interfacial tension gradient ($\partial\gamma/\partial c^A$);
2) the ratio $D_1^A/D_2^A = r^2$;
3) the ratio $v_1/v_2 = e^2$.
Secondary factors that mainly influence the intensity are:
a) the magnitude of $\partial\gamma/\partial c^A$;
b) the concentration levels of A in phase 1 and 2;
c) the value of the distribution coefficient of A, m_{12}^A;
d) the values of D_1^A, D_2^A, v_1 and v_2;
e) the presence of IAMs at the interface.

For small initial disturbances, hydrodynamic stability theories have been applied (STERNLING and SCRIVEN, 1959; BRIAN and ROSS, 1972; GOUDA and JOOS, 1975), from which the conditions of their occurrence may be predicted. However, these predictions do not always agree with experiment, as can be anticipated from the approximate character of the theories. A completely different approach has been made by OSTROVSKII et al. (1967, 1968 & 1973) who assumed that convections arise when the driving force of mass transfer exceeds the interfacial free energy. However, this model is unrealisticly simple: it does not even predict the existence of any 'growth constant' of the instabilities. Due to the approximate character of all these theories, the most convincing proof of absence or presence of instabilities still remains the experiment.

The presence of an equilibrium amount of IAMs at the interface has a pronounced damping influence on interfacial-tension-driven instabilities: primarily, the IAMs will resist gradients in γ by the compressional modulus that arises (Marangoni effect), but their presence may also decrease the magnitude

of $\partial\gamma/\partial c^A$. This problem has been analysed theoretically by BERG and ACRIVOS (1965), and by BRIAN and ROSS (1972). Of course, when the transferring substance itself is a strong interface-active substance, the instabilities may be very large as a result of the high value of $\partial\gamma/\partial c^A$.

In a three-component mass transfer process, spontaneous emulsification frequently occurs either by the mechanism called 'diffusion and stranding' (DAVIES and RIDEAL, 1961 ch. 8; DAVIES and WIGGIL, 1960), or by violent interfacial turbulence.

These mechanisms can be affected by IAMs in several ways. IAMs reduce the boundary layer flow, thus the diffusion rate of transferring material will be decreased and therefore also the rate of emulsion formation. However, the emulsion that is formed will be stabilized by the IAMs. It is obvious, that IAMs will reduce the violent interfacial turbulences that cause emulsification analogously to what has been described before.

decreased and therefore also the rate of emulsion formation. However, the

The existence of interfacial instabilities can be proven either optically or from the value of K_{exp}. A liquid-liquid interface undergoing spontaneous instabilities is optically non-uniform; the refractive index, being a function of composition and temperature, varies from point to point. Thus, interfacial instabilities can be demonstrated with interferometry or with the Schlieren method (see e.g. BERG et al., 1966; SAWISTOWSKI, 1971). However, the fact that no instabilities can be seen is not yet a waterproof evidence that they are not operative: they may very well be invisibly small.

Fortunately, their existence can also be inferred from the value of K_{exp}, particularly in the following ways:

1) Provided that K can be estimated a priori, interfacial instabilities are operative when $K_{exp} >> K$.

2) The spontaneous convections are weaker at smaller concentration differences. Thus, when K_{exp} is dependent on the concentration level, or when K_{exp} changes more strongly with time during an experiment than according to theory, instabilities are operative.

3) In the presence of interfacial turbulences, the value of K_{exp} is primarily governed by the intensity of these convections, and less so by the hydrodynamics of the bulk phases.

4) As the occurrence of instabilities depends on the direction of transfer, the equality of K_{exp} in both directions may be an indication that instabilities are absent.

5) IAMs that are present in high concentrations may affect the instabilities by changing the value of $\partial\gamma/\partial c^A$, whereas their influence on the hydrodynamics is negligible due to the mentioned short-circuiting effect of diffusion on the compressibility modulus of the monolayer.

5.5. CONCLUSIONS

The total resistance to mass transfer of a substance A through a liquid-liquid interface can be described phenomenologically as a series of three separate resistances: two diffusional resistances for both phases and an interfacial resistance. The latter refers to any slow transfer process of A through or at that interface: desolvation, permeation through a monolayer, chemical reaction or desorption. The presence of an interfacial resistance implies that the interfacial concentrations of A are not in equilibrium with each other. In all cases, the liquid phase resistance of that phase, in which A is less soluble, dominates.

Whereas the liquid phase resistances can be predicted for a number of systems with simple geometry and boundary layer flow, the value of the interfacial resistance is unknown a priori and is neglected in most cases. In principle, its value can be obtained from comparison of the experimentally determined overall resistance with the calculated values of both liquid phase resistances. In practice, however, either the experimental accuracy must be extremely high (static systems) or the boundary layer flow very well known to make this procedure successful. For only a few special cases in the literature could a resistance be determined unambiguously.

Model mass transfer measurements can be severely disturbed by spontaneous instabilities that may arise as a consequence of the non-equilibrium situation. The conditions that favour their occurrence have been treated, and a few methods have been proposed to demonstrate their existence during the transfer process.

In most cases, IAMs may reduce mass transfer rates drastically. Either the *hydrodynamics* of the boundary layer are changed (a reduced momentum transport through the interface or the damping of spontaneous instabilities), or a *physico-chemical* retardation may occur (blocking of the interface or a chemical interaction with the transferring material). Only in liquid-gas systems, the latter mechanism has been proven unambiguously by special, very accurate techniques.

Obviously, the most suitable system for mass transfer studies would feature a flat phase boundary with laminar liquid flow that has exactly known velocity profiles. This makes the transfer process amenable to model calculations, whereas the liquid phase resistances are not too high to detect any appreciable interfacial resistance. In addition, the absence of any spontaneous convection during the transport process must be checked thoroughly.

It will also be clear now, that completely wrong conclusions have indeed been drawn in the model studies on biological membranes, as mentioned in ch. 4.1. In fact, purely hydrodynamic effects have been measured, but these have been attributed to the transfer process at the interface. Therefore, the interpretation of those results in terms of a free energy of activation for the transfer itself are also completely wrong. Apparently, our approach of estimating the diffusional liquid phase resistances from their dependence on the rotation speed (ch. 4.2) constitutes a semi-empirical method of separating the very

important hydrodynamic effects from the contribution of the actual transfer process through the interface.

It seems very probable that the retardation of mass transport which has been observed in ch. 4.3, is primarily caused by a change in the hydrodynamics near the interface, as already proposed there. This hypothesis will be further tested in ch. 6, where we shall describe transport measurements in a system that is more suitable to model calculations. This enables us to determine more unambiguously the value of r_σ without and with PVA-Ac present at the interface. In addition, the results may provide a deeper insight into the behaviour of (co)polymers at a liquid-liquid interface that is not in mechanical equilibrium. Therefore, this method may become a useful tool in investigating the dynamical properties of adsorption layers.

6. MASS TRANSFER BETWEEN TWO LIQUID PHASES AND ITS RETARDATION BY PVA-Ac COPOLYMERS

In this last chapter, we shall apply the results of the experimental and theoretical investigations described in the preceding chapters to explore the influence of copolymers on mass transfer between the two phases. First, the stability of the experimental system will be analysed in several ways. Then, a transport vessel will be described that features more of the attributes necessary for a model system than the one used in ch. 4. The use of this vessel guaranteed a better defined liquid flow in the vicinity of the interface. This will enable us to predict, with some accuracy, liquid phase resistances from a simple physical model and from liquid-flow measurements. These results, combined with a higher reproducibility of the transport rate measurements, will allow us to make more definite conclusions on the value of the interfacial resistance.

After analysis of the experiments with a clean interface, we investigated the influence of PVA-Ac copolymers on the transport process. For that purpose, the random and blocky copolymers described and characterized in ch. 3.3 were used. An attempt will be made to analyse the effects of VAc content and distribution on the (dynamic) interfacial properties of the copolymers. The dependence of the observed effects on the hydrodynamic conditions in the vicinity of the interface will be shown to contain a key to understanding the relevant interfacial phenomena in a more conclusive manner.

6.1. STABILITY ANALYSIS OF THE SYSTEM USED

One very important requirement for model mass transfer studies is the absence of any interfacial instability (ch. 5.4). In principle, our system may exhibit density- as well as interfacial-tension-driven instabilities, and that because of the following reasons:

1. Since $\partial \rho_b / \partial c_b^{KCl}$ is negative, density-driven instabilities may arise during transfer of KCl from wabu to buwa. From the measured value of $\partial \rho_b / \partial c_b^{KCl}$ (ch. 2.3) and the maximum possible value of $(c_{b\sigma}^{KCl} - c_b^{KCl})$, it can be calculated that $\rho_{b\sigma}$ may be decreased by at most $1\%_{00}$.

2. Interfacial tension measurements (with the drop-weight method, described in ch. 3.3.5) yielded $\partial \gamma / \partial (\ln a_w^{KCl}) = 0.13$ mN.m^{-1} for $0.04 < c_w^{KCl} < 0.15$ mol.l^{-1}, and thus $\partial \gamma / \partial c_w^{KCl} = 1.3 \times 10^{-3}$ mN.m^2.mol^{-1} at $c_w^{KCl} = 0.1$ mol.l^{-1} (this means that a 'fluctuation' of 10% in c_w^{KCl} results in $\Delta \gamma = 0.013$ mN.m^{-1}). Since $v_w/v_b = e^2 < 1$ and $D_w^{KCl}/D_b^{KCl} = r^2 > 1$, the instability theory of STERN-LING and SCRIVEN (1959) predicts that interfacial-tension-driven instabilities (oscillatory cells) may occur for KCl transfer from wabu to buwa, whereas the reverse transfer direction corresponds to a stable system. Application of the

instability theory of GOUDA and JOOS (1975) yields that instabilities are possible for transfer in both directions.

Although, theoretically, both kinds of instabilities are thus possible, their driving forces ($gV\Delta\rho$ and $l\Delta\gamma$, respectively, where V is the relevant volume and l the interfacial periphery of the fluctuation) are so extremely small that it is doubtful whether they will develop during the experiments.

Fortunately, all experimental investigations led to the conclusion that these spontaneous instabilities were not operative at the concentration levels used, provided both solutions were properly saturated with the relevant component. Thus, the retarding influence of PVA-Ac can certainly not be ascribed to its inhibiting effect on spontaneous instabilities. The most convincing arguments supporting these conclusions are:

1. Schlieren observations in a thermostatted cell (controlled within $0.05\,^{\circ}C$) only showed instabilities in the buwa phase when the starting $c_w^{KCl} > 0.2$ mol.l^{-1} (their intensity increased with c_w^{KCl}, but at $c_w^{KCl} = 0.5$ mol.l^{-1} no instabilities were visible when a starting c_b^{KCl} of 0.003 mol.l^{-1}, instead of 0, was used).
2. Since spontaneous convections are very dependent on the existing concentration difference, the following observed facts are pertinent:
a) K_b appeared to be time-independent.
b) K_b appeared to be independent of the starting value of c_w^{KCl} for $0.04 \leqslant c_w^{KCl} \leqslant 0.2$ mol.l^{-1}.
c) Some experiments were performed with NaCl instead of KCl. In these cases, K_b was first determined in the usual conductometric way, after which both phases were equilibrated. Next, K_b was determined for Na^{22}Cl, after injection of a very small amount of Na^{22}Cl in the wabu phase (c_w^{NaCl} was increased with less than 0.1$^{\circ}/\text{oo}$, so chemical equilibrium could be assumed for this case). Both values appeared to be equal within their limits of accuracy, and also in the latter experiment K_b was decreased similarly by the addition of small amounts of PVA-Ac.
3. As has been shown in ch. 4.3, K_b was positively dependent on N, contrary to what would be expected if interfacial instabilities were dominant.
4. The K_b value for KCl transfer in the opposite direction appeared to be equal to that for a normal experiment, and also an equal retardation was observed due to the presence of PVA-Ac (the starting c_b^{KCl} was 10 mmol.l^{-1}).
5. During the Schlieren experiments, it was observed that, when instabilities were visible, saponin was effective at damping their onset at the interface: instead of rather violent convection currents, only slow rising density instabilities remained. At the same concentration (5 g equilibrated between 500 ml wabu and 500 ml buwa), no effect at all was observed on K_b (probably because of the short-circuiting effect of saponin diffusion from the bulk to the interface, as mentioned in ch. 5).
6. Since interfacial instabilities are influenced by the values of v and m, some experiments were performed with isobuOH instead of buOH. While v of the

organic phase is higher ($v_{ib} = 4.1 \times 10^{-6}$ m^2.s^{-1}; QUINN and JEANNIN, 1961) and m_{bw}^{KCl} lower (ch. 2.3). a similar retarding effect of PVA-Ac was still observed; only the absolute values of K_{ib} and K_{ib}^{p} were about 35% lower. In this case, no instabilities were observed with the Schlieren set-up, not even at starting values of c_w^{KCl} as high as 0.4 mol.l^{-1}.

6.2. EXPERIMENTAL

In order to fulfil the demands of a suitable model system as much a possible, a new transport vessel was designed, rather similar to the one used by NITSCH et al. (1972). We selected large propellers to obtain relatively high overall flow rates with little turbulence. Draft tubes with baffles guaranteed the most systematic flow patterns near the interface and the most complete participation of all liquid elements of both phases in the exchange process. The construction onto which two vessels, identical within the given limits of accuracy, were fixed, is drawn to scale in fig. 6.2–1 together with a scaled-up cross-section of a vessel; all parts are described in the legends.

Two Motomatic D.C. motors (Electrocraft Co.), fixed rigidly against a wall, were used to drive the propellers by means of toothed belts (Synchroflex). The rotation speeds were independently adjustable between 0 and 100 min^{-1} by two ten-turn potentiometers. The reproducibility of their rotation speeds was very good. while a servo-amplifier ensured a very high stability. In order to suppress interfering vibrations in the vessels as much as possible, the whole construction was mounted on a heavy concrete slab that rested on rubber plugs. The glass jackets were connected to a thermostat (Tamson TX 100), controlling the temperature to within 0.01 °C.

Both vessels were always used simultaneously. However, it appeared to be very difficult to obtain identical and reproducible mass transfer rates. Therefore, all parts that could influence the velocity profiles in both phases were fixed in the same place. Before an experiment was started, the positions of the plugs, draft tubes and propellers were always checked with a cathetometer.

After installation of the clean and dry apparatus, both vessels were filled with 225 ml wabu of 25.0 °C, with $c_w^{KCl} = 0.1016$ mol.l^{-1}. With a special device, 210 ml buwa of 25.0 °C was pipetted very carefully on top of the wabu phase, so that mixing was avoided as much as possible. These volumes fix c_b^t at 1.72 mmol.l^{-1}.

The value of c_b^{KCl} was always determined conductometrically. Two conductance cells (Philips PR 9510) were used. with their protecting glass jackets removed to increase the buwa flow between both plates; the cell constants were checked regularly. A modified conductance transmitter (Electrofact, type 43000) with a low measuring frequency (73 s^{-1}) could be connected subsequently with any of these conductance cells (and with a known resistance for control) by means of a relay box. All measuring cables were screened separately. The transmitter signal was fully processed by an automatic data
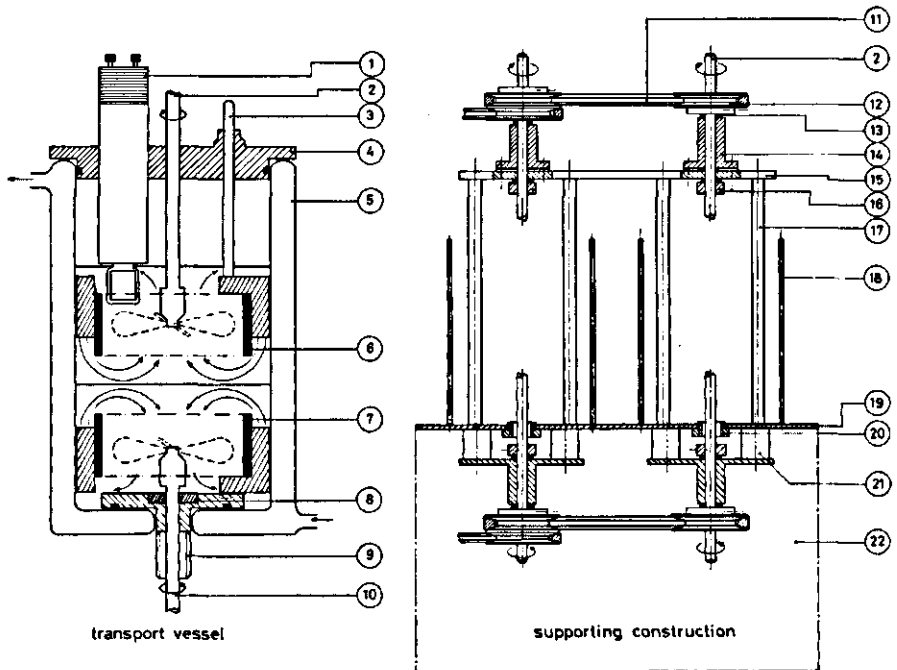
FIG. 6.2-1. Vertical cross section of one transport vessel and the supporting construction; 1: conductance cell; 2: upper stirring shaft ($\emptyset = 0.60$ cm) with a three-blade, right-hand propeller ($\emptyset = 5.1$ cm, 2.7 cm above the interface), both stainless steel; 3: stainless steel shaft connected to a baffle of the draft tube; 4: PVC cover with butyl rubber O-ring; 5: thermostatted double-walled Pyrex glass vessel (inside $\emptyset = 8.08 \pm 0.02$ cm); 6: upper draft tube (inside $\emptyset = 5.90$ cm, outside $\emptyset = 6.36$ cm, height $= 2.50$ cm) with six baffles (2.60 $\times$ 0.75 cm²), the lower edge 1.2 cm above the interface; 7: identical lower draft tube, resting with three baffles in holes in the plug; 8: butyl rubber gasket ring; 9: stainless steel plug ($\emptyset = 5.8$ and 1.5 cm, height $= 0.6$ and 3.4 cm) with a butyl rubber O-ring, fixed by a PVC nut (20); 10: lower stirring shaft, identical to 2; 11: toothed belt (Synchroflex), tooth $= 0.5$ cm; 12: toothed pulley ($\emptyset = 3$ cm); 13: Teflon slide ring; 14: brass slide bearing, fixed on 15 with insulating material; 15 upper aluminium plate (thickness 0.6 cm); 16: locking ring; 17: brass column ($\emptyset = 1.0$ cm, height $= 20$ cm); 18: shaft with nut to fix the cover (length $= 15$ cm); 19: lower aluminium plate (33 $\times$ 22 $\times$ 0.3 cm³) with two insulating rubber mats; 20: PVC nut; 21: insulating PVC columns; 22: aluminium support (33 $\times$ 20 $\times$ 0.3 cm³).
Both propellors and draft tubes are situated symmetrically with regard to the interface.

acquisition system, consisting of a PDP 11/10 minicomputer (Digital) and a Camac Crate Interface (Borer). This system will be described by DE KEIZER (1977). By using an average value of 70 conductance measurements (obtained within 5 s), the accuracy and reproducibility of these measurements were within 1⁰/oo.

Before an experiment, it was always checked that no conducting parts of the vessel were connected to the earthed aluminium construction, which screen-ed both vessels. When the mean conductance in the two (homogeneous) upper

86

phases corresponded approximately with $c_{\xi}^{KCl} = 0.2$ mmol.l^{-1}, both motors were started, driving the propellers with a fixed and specified speed. In order to achieve comparable hydrodynamic conditions at both sides of the interface, we kept $N_b/N_w = 2.78$, so that the values of Re were equal. The propellers were always counterrotating, in order to obtain the most systematic, mainly radial, flow patterns (as sketched in fig. 6.2–1). Both pumped the fluid away in the centre of the interface, which was usually very flat. By precoating the glass wall with traces of silicone spray (Ambersil), the contact angle between the interface and the wall was almost 90°. Only at the highest rotation speeds were some small waves visible, but the increase in interfacial area could be estimated to be always less than 1 %. During an experiment, the jacket temperature was kept between 24.94°C for $N_b = 90$ min^{-1} and 24.99°C for $N_b = 40$ min^{-1}, to compensate the frictional heat that evolved in the vessel.

Subsequently, the conductance in both vessels and the control resistance were measured as a function of time. At the end of a series, the specific conductances were calculated from the data. and from these the values of c_{ξ}^{KCl}, using equation (2.3–3). The terms $-V_b \ln(1-c_b/c_{\xi})$ were also determined automatically, and finally, a linear regression analysis yielded K_b. Accurate values of K_b were obtained by measuring 12–24 combinations of c_{ξ}^{KCl} and t over a period of 10–40 minutes. The measurements were always performed at $0.2 < c_{\xi}^{KCl} < 1.3$ mmol.l^{-1}; at lower concentrations $\partial c_{\xi}^{KCl}/\partial t$ was too high, while at higher values the absolute error in $-V_b \ln(1-c_b/c_{\xi})$ became too large. During one run, K_b values for at least six different rotation speeds could be determined. After each experiment, the vessels and devices were cleaned very thoroughly and dried in an oven at 40°C.

The effect of PVA-Ac on the transfer process was always investigated by spreading the copolymers at the wabu-buwa interface, so that at least a maximum vale of Γ could be estimated. Spread macromolecular layers exhibit still another advantage over adsorption layers, namely that their relaxation times are usually shorter (LANKVELD, 1970; BÖHM, 1974). In addition they may enable us to investigate the reversibility of (co)polymer adsorption, because the spread layer is usually not the equilibrium situation.

In order to facilitate this spreading process, the solutions had a special composition (ch. 3.3.6), while their densities were always between that of wabu and buwa. In all cases, the (co)polymer concentration of these solutions was between 0.025 and 25 g.l^{-1}. An Agla micrometer syringe with a very thin needle, filled with the solution, was stuck through the interface by means of a micromanipulator, and then pulled back to maintain the outlet of the needle precisely in the raised interface. A step motor mounted on the micrometer caused the solution to spread very slowly at the interface (approximately 0.006 ml.min^{-1}). Usually, the total volume expelled amounted to between 0.02 and 0.2 ml.

Whereas literature values for the spread amount often vary between 0.1 and 5 mg.m^{-2}, we went as high as 2.5×10^3 mg.m^{-2}. It was found that

only the total amount of (co)polymer was relevant and not its concentration in the spreading solution. Since we were unable to detect any significant change in retardation during a series of measurements of 7 hours at most, we suspect the relaxation times of the spread layers are either very short or extremely long (usually, the first measurement was started 10–60 minutes after spreading).

6.3. Theoretical relations for the liquid phase mass transfer coefficients

A fundamental requirement to decide on the presence of an interfacial resistance is the knowledge of both liquid phase resistances, or at least, how they vary with the applied hydrodynamic conditions. In the present transport vessel, flow visualization experiments with suspended particles showed that a rather systematic radial flow pattern existed in both phases, provided the propellers were rotating as described in ch. 6.2. By approximating the real flow situations in the vicinity of the interface by two simple but realistic models, we were able to solve the equation of conservation of mass for the component transferred (5.2–7). From this solution, in turn, the concentration profiles could be estimated, and from these, ultimately, the approximate liquid phase mass transfer coefficients were calculated.

Let us consider an axially symmetric, flat liquid-liquid interface at $z = 0$, extending arbitrarily between r_0 and r_1 ($r_0 > r_1$), with a laminar boundary layer for $z \geqslant 0$. If we assume that the flow is stationary ($\partial/\partial t = 0$), that the density in this boundary layer is constant, and that only a radial velocity component is present ($\partial/\partial\theta = \partial/\partial z = 0$), the equation of continuity, in cylindrical coordinates (e.g. Bird et al., 1960 p. 83), can be integrated to:

$$rv_r = \text{constant} \tag{6.3-1}$$

In the experimental set-up, v_r is pointing to $r = 0$, thus we shall only consider negative constants. However, these constants may still be a function of z. We shall examine two cases (see fig. 6.3–1):

$$v_r = \frac{-az}{r} \tag{6.3-2}$$

and

$$v_r = \frac{-b}{r} \tag{6.3-3}$$

where $a(\text{m.s}^{-1})$ and $b(\text{m}^2.\text{s}^{-1})$ are positive constants. In fact these cases are similar to those treated respectively by Lévêque and Higbie (ch. 5.3.3).
    For diffusion of A, out of the interface into this laminar boundary layer, the equation of continuity of A must hold. For the present situation, this equation,
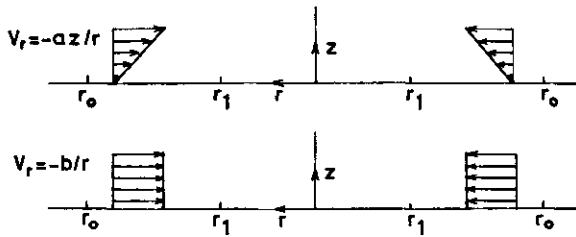
FIG. 6.3-1. Schematic representation of the two hydrodynamic boundary layers.

also in cylindrical coordinates (e.g. BIRD et al., 1960 p. 559), can be approximated by:

$$v_r \frac{\partial c_A}{\partial r} = D_A \frac{\partial^2 c_A}{\partial z^2} \qquad (6.3\text{–}4)$$

provided a very large bulk phase is in contact with the interface, so that a pseudo-steady state approximation can be made: $\partial c_A/\partial t = 0$. In addition we have assumed that ϕ_A^x is so small that the velocity profile in the boundary layer is not affected by ϕ_A^x, and we have neglected any radial diffusion, because it is much smaller than the convective transport in that direction. The boundary conditions for the solution of (6.3–4) with either (6.3–2) or (6.3–3) are:

$$c_A = c_{A0} \text{ at } z > 0 \quad \text{and} \quad r = r_0$$

$$c_A = c_{A\sigma} \text{ at } z = 0 \quad \text{and } r_1 \leqslant r \leqslant r_0$$

$$c_A = c_{A0} \text{ at } z = \infty \text{ and } r_1 \leqslant r \leqslant r_0$$

Inserting (6.3–2) into (6.3–4) yields

$$-\frac{az}{r} \frac{\partial c_A}{\partial r} = D_A \frac{\partial^2 c_A}{\partial z^2} \qquad (6.3\text{–}5)$$

In order to solve equation (6.3–5) we use the dimensionless variable

$$\xi = z \left(\frac{2a}{D_A (r_0^2 - r^2)} \right)^{1/3} \qquad (6.3\text{–}6)$$

Insertion into (6.3–5) leads to:

$$\frac{\partial^2 c_A}{\partial \xi^2} + \frac{\xi^2}{3} \frac{\partial c_A}{\partial \xi} = 0 \qquad (6.3\text{–}7)$$

whereas the boundary conditions are now formulated as:

$$c_A = c_{A0} \text{ at } \xi = \infty$$

$$c_A = c_{A\sigma} \text{ at } \xi = 0$$

The solution of (6.3–7) satisfying these boundary conditions, is:

$$\frac{c_{A\sigma} - c_A}{c_{A\sigma} - c_{A0}} = \frac{\int\limits_0^\xi \exp\left(-\xi^3/9\right) d\xi}{\int\limits_0^\infty \exp\left(-\xi^3/9\right) d\xi} = P\left(^1/_3, \xi\right) \tag{6.3–8}$$

where $P(1/3, \xi)$ is the incomplete Γ – function (ABRAMOWITZ et al., 1968 p. 260).

From this concentration profile, the local molar flux ϕ''_{Ar} can be calculated with (5.2–5):

$$\phi''_{Ar} = -D_A \left(\frac{\partial c_A}{\partial z}\right)\bigg|_{z=0} = \frac{(c_{A\sigma} - c_{A0})}{\Gamma(^1/_3)} \left(\frac{6aD_A^2}{r_0^2 - r^2}\right)^{1/3} \tag{6.3–9}$$

The average mass transfer coefficient for the area between r_0 and r_1, k_A, is obtained from:

$$k_A = \frac{\int\limits_{r_1}^{r_0} \phi''_{Ar} 2\pi r\, dr}{\pi(r_0^2 - r_1^2)(c_{A\sigma} - c_{A0})} = \frac{3\,(6aD_A^2)^{1/3}}{2\Gamma(^1/_3)\,(r_0^2 - r_1^2)^{1/3}} = \frac{1.017(aD_A^2)^{1/3}}{(r_0^2 - r_1^2)^{1/3}} \tag{6.3–10}$$

Since k_A is independent of any concentration, it is obvious that this derivation also applies to situations in which c_{A0} changes slowly with time.

In case the velocity profile is given by (6.3–3) rather than by (6.3–2), an analogous treatment, using identical boundary conditions, leads to:

$$k_A = \frac{2(2bD_A)^{1/2}}{\Gamma(^1/_2)\,(r_0^2 - r_1^2)^{1/2}} = \frac{1.596(bD_A)^{1/2}}{(r_0^2 - r_1^2)^{1/2}} \tag{6.3–11}$$

As a clean liquid-liquid interface can not resist any tangential shear stress, the wabu-buwa interface will be set into motion by both flowing liquids. Now it will be clear that (6.3–3) is applicable to this situation, where $(-b/r)$ refers to the interfacial velocity. In ch. 5 we have seen that IAMs can decrease this interfacial motion drastically due to the interfacial pressure that results from their compression by the liquid flows. The ultimate case of zero interfacial velocity of the complete interface can thus be approximated by (6.3–2). It must be remarked that these models will probably only be approximate, because in the experimental set-up the 'end' effects at the periphery and the centre of the interface will influence the average mass transfer coefficients.

Since $m_{bw}^{KCl} << 1$ and since $D_b^{KCl} << D_w^{KCl}$, as can be inferred from the equivalent conductance of KCl in buwa (ch. 6.5.1), we have, in practice, only to calculate the liquid phase mass transfer coefficient for KCl in buwa, k_b (see equation (5.2–18)). With reasonable approximations for D_b^{KCl}, a, b, r_0, and r_1, we can now thus predict not only the power α of the semi-emperical relation (4.2–2), but even the values of k_b with and without PVA-Ac present (with (6.3–10) and (6.3–11) respectively). Ultimately the comparison of experimental

90

and theoretical values will enable us to decide on the presence of any appreciable interfacial resistance, and on the mechanism of the retarding effect of PVA-Ac.

6.4. RESULTS

6.4.1. *Liquid-velocity measurements in the bulk phases*

In order to make a good estimate for the value of k_b, the boundary layer flow at the wabu-buwa interface should be known precisely. In the present experimental set-up this very complex problem can probably only be tackled with an advanced laser doppler apparatus. However, when reasonable assumptions can be made on the structure of the boundary layers, approximate information on the hydrodynamic conditions near the interface can be gained from the bulk flow velocities. Here we shall describe these velocity measurements, the results of which will be used in ch. 6.5.1 to approximate the values of a and b (of equation (6.3–10) and (6.3–11), respectively).

Coagulated polystyrene latex particles were suspended in either phase under the usual experimental stirring conditions ($N_b/N_w = 2.78$ and $40 \leqslant N_b \leqslant 90$ min^{-1}). Near the interface, pictures were taken of the flowing liquids, the times of exposure varying between $^1/_4$ and 1 s (see photo 6.4–1). A narrow parallel band of side light was used and a dark background. From the lengths of the stripes, the bulk velocities could be estimated at different N_b (and corresponding N_w) values. Allowance was made for the total magnification of the stripes by also measuring a reference distance in the vessel; in addition we corrected for the magnitude of a stationary particle, assuming spherical particles. At four different rotation speeds we measured 30–50 particles flowing in radial direction in the volume confined by $2 \times 10^{-2} < r < 3 \times 10^{-2}$m and $3 \times 10^{-3} < |z| < 9 \times 10^{-3}$m. In this way, we determined the average radial velocities in both phases at $r = 2.5 \times 10^{-2}$m and $|z| = 6 \times 10^{-3}$m. The measurements were not accurate enough to establish significant differences in velocities within this volume. A curve fitting analysis yielded:

$$v_{wr} = 2.3 \times 10^{-5} N_b^{1.4} \text{ m.s}^{-1} \tag{6.4–1}$$

and

$$v_{br} = 6.3 \times 10^{-5} N_b^{1.4} \text{ m.s}^{-1} \tag{6.4–2}$$

PHOTO 6.4–1. Liquid flow visualization in the wabu phase; at the left: $N_b = 40$ min^{-1} ($^1/_2$ s); at the right: $N_b = 80$ min^{-1} ($^1/_2$ s); 1: upper draft tube; 2: buwa phase; 3: interface; 4: wabu phase; 5: lower draft tube.

TABLE 6.4–1. Experimental K_b values for three different 'clean' interfaces and the retardation of K_b^{plate} and K_b^{ring}, respectively, caused by $S^{B4} = 195$ mg.m^{-2}.

N min^{-1}	$10^6 \times K_b$ m.s^{-1}	$10^6 \times K_b^{plate}$ m.s^{-1}	$10^6 \times K_b^{ring}$ m.s^{-1}	$(R_N^{B4})^{plate}$	$(R_N^{B4})^{ring}$
40	8.6 ± 0.1	7.4 ± 0.5	9.3 ± 0.4	4.7 ± 0.15	5.3 ± 0.17
50	10.5 ± 0.1	9.5 ± 0.8	10.9 ± 0.4	5.2 ± 0.15	5.7 ± 0.18
60	12.1 ± 0.1	11.6 ± 0.6	12.5 ± 0.4	5.3 ± 0.17	6.0 ± 0.20
70	13.7 ± 0.1	13.5 ± 0.7	14.1 ± 0.3	5.4 ± 0.17	5.9 ± 0.18
80	15.5 ± 0.1	15.8 ± 0.5	15.6 ± 0.3	5.5 ± 0.18	5.8 ± 0.23
90	17.0 ± 0.1	17.5 ± 0.6	16.8 ± 0.2	5.6 ± 0.17	5.8 ± 0.20

6.4.2. *The interphase transport rate measurements*

As in ch. 4.3, the overall mass transfer coefficients of KCl from wabu to buwa were measured at 25.0°C. Usually, the average K_b^g of at least 4 different experiments was taken, while regularly measurements with a 'clean' interface were performed as a check. Henceforth we shall only mention the value of N_b pertaining to an experiment, since the ratio N_b/N_w was always kept constant (at 2.78). At values of $N_b < 40$ min^{-1} the reproducibility of the K_b values was rather poor and at $N_b > 90$ min^{-1} the disturbances of the interface became appreciable; therefore all experiments were performed at $40 \leqslant N_b \leqslant 90$ min^{-1}.

For the experiments without PVA-Ac present, the average values of K_b (and their standard deviations) are collected in column 2 of table 6.4–1 as a function of N_b. In addition some measurements were performed with a reduced interfacial area: either a circular plate ($r = 2.85 \times 10^{-2}$m) or a ring ($2.85 \times 10^{-2} < r < 4.04 \times 10^{-2}$m), both stainless steel and 0.5 mm thick, was placed in the interface concentric to the vessel. Either of these reduced the interfacial area to half of its original value. The resulting K_b^{plate} and K_b^{ring} values are collected in columns 3 and 4 of table 6.4–1. Although the plate or ring might change the hydrodynamics of the uncovered interface, some extra information on the hydrodynamics may be obtained from these measurements, as will be attempted in ch. 6.5.2.

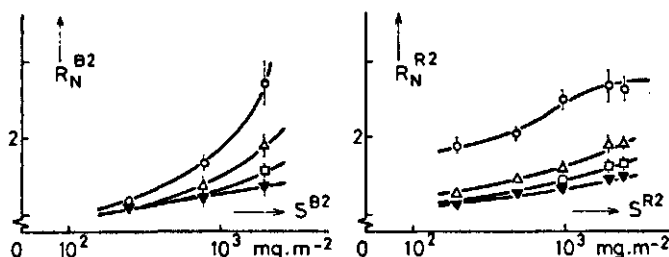For that same purpose, some experiments were performed with $N_w \neq$

FIG. 6.4–1. The experimental retardation R_N as a function of the amount of B2 and R2 spread at the interface;
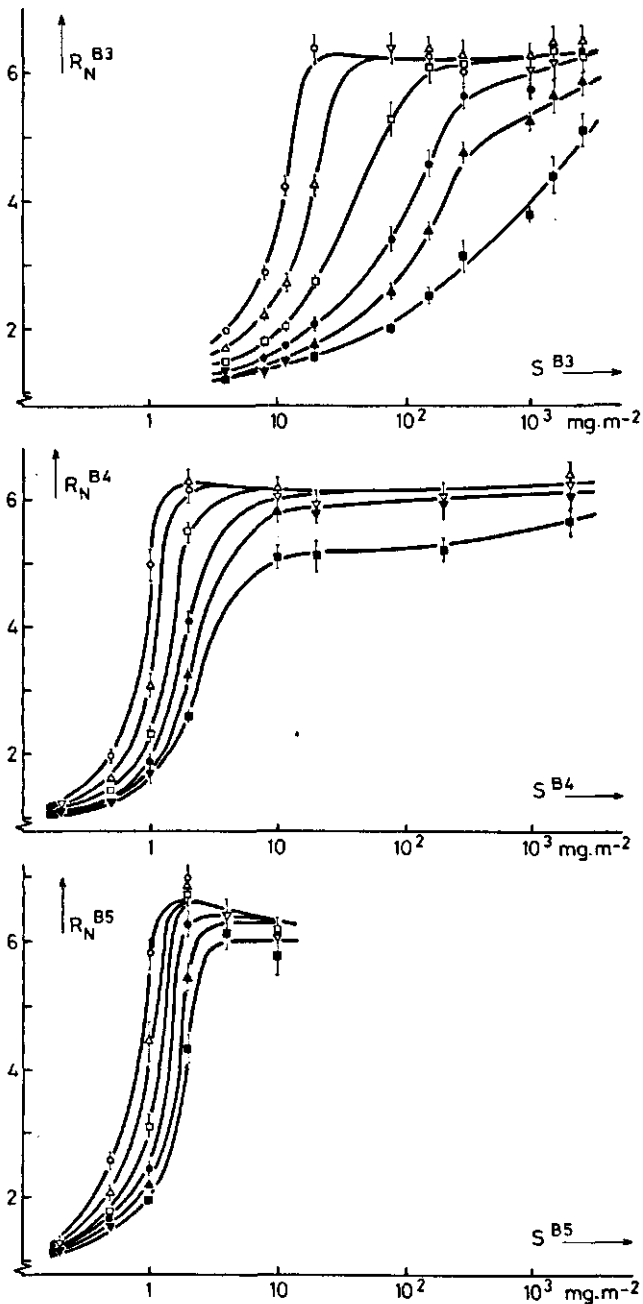○ refers to $N_b = 40$, △ to $N_b = 50$, □ to $N_b = 60$ and ▼ to $N_b = 70, 80$ and 90 min^{-1}.

FIG. 6.4-2. The experimental retardation R_N as a function of the amount of B3, B4 and B5 spread at the interface; ○ refers to $N_b = 40$, △ to $N_b = 50$, □ to $N_b = 60$, ● to $N_b = 70$, ▲ to $N_b = 80$ and ■ to $N_b = 90$ min^{-1};
∇ represents a coinciding point for at least two of the four lowest rotation speeds and ▼ for at least two of the four highest rotation speeds.

$N_b/2.78$: K_b was measured with $N_b = 50$ and $N_w = 32.4$ min^{-1} and in addition with $N_b = 90$ and $N_w = 18$ min^{-1}. In the first case K_b was 8% higher than with the usual $N_w = 18$ min^{-1}, in the second case 6% lower than with $N_w = 32.4$ min^{-1}.

The influence of the spread (co)polymers was diverse, and appeared to depend on the amount applied, the acetate content and the intra-molecular acetate distribution of the (co)polymers. The amount of (co)polymer spread at the interface varied between 0.2 and 2500 mg.m^{-2}.

Even at that highest quantity, no significant influence was observed at any rotation speed for PVA-H and R1, while B1 retarded the transfer rate with maximally 15% (at the lowest rotation speeds and the highest amount of copolymer spread). All other samples caused a significant retardation of the transport rate; henceforth, this retardation will be indicated by $R_N = (K_b/K_b^0)_N$, where N represents N_b in min^{-1}. In fig. 6.4–1, R_N for B2 and R2 is plotted against the amount of copolymer spread, S. These graphs show similar trends although their acetate contents (6.8 and 16.6 mole % respectively) differ substantially. The samples B3, B4 and B5 gave quite different results, as can be seen in fig. 6.4–2. For the S values that cause a certain R_N which is lower than the maximum R_N, the following holds: $S^{B2} \approx S^{R2} > S^{B3} > S^{B4} > S^{B5}$. Furthermore, the resemblance of the shapes of R_N^{B2} and especially R_N^{B2} to the other graphs at much lower S is striking. In addition, the value of S at which R_N reaches its maximum decreases from B3 to B5, the stronger so, the higher N. At high S, the value of R_N seems to become ultimately independent of both N and the kind of copolymer. The last notable feature is, that in some cases, R_N decreases with increasing S after having reached its maximum; this effect is most pronounced at low N_b, particularly for B5.

Finally, some experiments were performed using either the ring or the plate with $S^{B4} = 195$ mg.m^{-2}. The R_N^{B4} values for both cases are collected in the last two columns of table 6.4–1. As can be seen $(R_N^{B4})^{plate}$ is always lower than R_N^{B4} at the same S^{B4}, while $(R_N^{B4})^{ring}$ is almost equal to it (compare to fig. 6.4–2).

6.5. Discussion

6.5.1. *Estimation of the parameters that govern the theoretical mass transfer coefficients*

By substituting approximate values of D^{KCl}, a and b in, respectively, equations (6.3–10) and (6.3–11), we can estimate the values of the liquid phase mass transfer coefficients, an essential requirement to separate the retarding effect of PVA-Ac into a *hydrodynamic* and a *physico-chemical* part.

The value of D_b^{KCl} at infinite dilution (thus D_o of equation (2.3–1)) can be determined using the Nernst equation for completely dissociated electrolytes (Handbook, 1972 p. F. 47). As was shown in ch. 2.3 KCl is probably completely dissociated in buwa at $0.2 \leqslant c_b^{KCl} \leqslant 1.3$ mmol.l^{-1}. From the limiting

molar conductance of KCl in buwa ($23.6\ cm^2\ .\Omega^{-1}.mol^{-1}$ at $25.0°C$) and the assumption that the anionic and cationic limiting equivalent conductances also are almost equal in buwa, we estimated $D_b^{KCl} = 3 \times 10^{-10}\ m^2.s^{-1}$ for the relevant concentration range. Although some (reasonable) assumptions were necessary to arrive at this approximate value, it will be shown that the retardation predicted by our model is hardly dependent on the absolute value of D_b^{KCl} (a variation of 50% in D_b^{KCl} will change the theoretical value of R with only 7%!). Therefore, only the absolute values of the predicted partial mass transfer coefficients will be sensitive to the precise value of D_b^{KCl}.

To obtain approximate values for a and b, we consider a particular part of the interface and of the two adjacent phases, namely $2 \times 10^{-2} < r < 3 \times 10^{-2}$ m, which is the region investigated in ch. 6.4.1. To estimate the radial interfacial velocity, v_{ar}, in that region, we can use a relation derived by LOCK (1951) for the interfacial velocity between two parallel laminar streams; v_{ar} appears to be only a function of the ratio of both viscosities, densities and bulk velocities (his equations 32 and 42). Application to the present situation yielded: $v_{ar} = -0.12\ N_b^{1.4}/r$ (m.s^{-1}) and thus $b_a = 0.12\ N_b^{1.4}$ (m^2.s^{-1}). For a rigid interface the most realistic model to estimate a_w and a_b in the same region can be derived from the description of the flow in the vicinity of a stagnation point (SCHLICHTING, 1968 p. 88). From the known solution of this problem, $\partial v_r/\partial z$ at $z = 0$ can be estimated at $r = 2.5 \times 10^{-2}$ m and from these values, it follows ultimately that $a = 0.025 \times 0.227\ v^{3/2}/(0.2 \times (v \times 0.015)^{1/2})$, where v is the bulk velocity (measured in ch. 6.4.1).

In our models, a and b are constants, and they are thus supposed to be suitable to describe the complete liquid flow in the vicinity of the interface. In table 6.5-1, we have collected the relevant hydrodynamic characteristics, which enable us, together with the value of D_b^{KCl}, to estimate the partial liquid phase mass transfer coefficients. Combination of these with the experimental results may provide us with a sound basis to decide on the presence of an appreciable interfacial resistance and on the effect of the copolymers upon K_b.

6.5.2. KCl transfer through the wabu – buwa interface

As indicated in ch. 6.3, equation (6.3-11) can be used to estimate the theore-

TABLE 6.5-1. Approximate values for the hydrodynamic parameters in the vicinity of the interface.

N_b min^{-1}	$10^2 \times v_{br}$ m.s^{-1}	$10^2 \times v_{wr}$ m.s^{-1}	$10^2 \times v_{ar}$ m.s^{-1}	$10^4 \times b_a$ m^2.s^{-1}	a_b m.s^{-1}	a_w m.s^{-1}
40	1.1	0.4	0.8	2.1	0.15	0.06
50	1.5	0.5	1.2	2.9	0.24	0.09
60	1.9	0.7	1.5	3.7	0.34	0.13
70	2.4	0.9	1.9	4.7	0.47	0.17
80	2.9	1.1	2.2	5.6	0.63	0.23
90	3.4	1.3	2.6	6.6	0.80	0.29

TABLE 6.5–2. Theoretical values of the overall mass transfer coefficients for a 'clean' interface, and the comparison of them with the experimental results.

N_b	$10^6 \times K_b^t$ *)	K_b^t/K_b ^{0})	$10^6 \times K_b^{t,plate}$ $10^6 \times K_b^{t,ring}$ *)	$(K_b^t/K_b)^{plate\,0}$)	$(K_b^t/K_b)^{ring\,0}$)
min^{-1}	m.s^{-1}		m.s^{-1}		
40	10.0	1.16	14.1	1.91	1.52
50	11.7	1.11	16.5	1.73	1.51
60	13.2	1.09	18.7	1.62	1.50
70	14.8	1.08	20.9	1.55	1.48
80	16.2	1.05	23.0	1.45	1.48
90	17.6	1.04	24.9	1.42	1.48

*) theoretical K_b value calculated with equation (6.3–11).

^{0}) ratio of theoretical and experimental K_b values.

tical overall mass transfer coefficient, K_b^t, for a clean interface, neglecting any interfacial resistance. But also experimental proof was obtained that justified this assumption: in the absence of any PVA-Ac, talc particles that were distributed over the interface, rapidly collected at the centre of the interface by the radial interfacial flow, even at $N_b = 40$ min^{-1}. Although in the derivation of (6.3–11) plug flow was assumed, this is, of course, not the actual velocity profile, since $v_{wr} \neq v_{br}$. But application of (6.3–11) with b_σ will not introduce a serious error (actually less than 1% in our case), because $a_b^2 D_b^{KCl}/rv\frac{3}{\sigma r} << 1$ (e.g. BEEK and BAKKER, 1961; or BEEK and MUTTZALL, 1975 p. 250).

In columns 2 and 3 of table 6.5–2, we have collected K_b^t data for a clean interface and the ratio of the theoretical and experimental values. Taking into account the approximate nature of the model and the approximate values of D_b^{KCl} and b_σ, the agreement between theory and experiment is excellent. The largest deviations occur at the lowest N_b, just contrary to what would be expected if an interfacial resistance was operative. We ascribe this to a less developed flow at the periphery and in the centre of the interface than assumed in our model. This hypothesis was supported qualitatively by several different flow visualization experiments, using suspended particles or buOH in stead of buwa (so that spontaneous instabilities were visible in the buOH phase during transfer). From the particle streamlines and the penetration depth of the instabilities we inferred that, at low N_b, the flow along the interface was less effective for $r \gtrsim 3.5 \times 10^{-2}$m, and particularly for $r \lesssim 2 \times 10^{-2}$ m, than for the region in between these two.

Since the interface available for transfer in the presence of the plate or the ring was equal, identical values were obtained for $K_b^{t,plate}$ and $K_b^{t,ring}$ (column 4 of table 6.5–2). The agreement between theory and experiment is less satisfactory, as appears from columns 5 and 6 of table 6.5–2. It is remarkable that $(K_b^t/K_b)^{plate}$ decreases steadily with increasing N_b, whereas the same quantity for the ring remains almost constant. Part of this disagreement will probably be

caused by the influence of the metal plates on the average interfacial velocity. But we can infer from column 5, that at higher N_b the flow along the interface at the outer edge becomes more effective, whereas it seems that in the centre a less effective flow remains even at high N_b. This conclusion is completely consistent with the above mentioned visualization experiments and with our conclusion on the deviations of the flow models from the actual flow.

The experiments in which N_b/N_w was varied (p. 92) provide more support for the applicability of the present model: at $N_b = 50$ min^{-1}, a change in N_w from 18 to 32.4 min^{-1}, results in an increase in b_σ of 20% (calculated with Lock's solution for $v_{\sigma r}$). Thus K_b' would increase with 10%, which is close to the experimental result. The theoretical decrease in K_b' for the other case ($N_b = 90$ and $N_w = 18$ min^{-1}) is 5%, also in good agreement with the experiment.

All things considered, we can state that the present model describes the complete KCl transfer process through the wabu-buwa interface satisfactorily. In all cases, the agreement between experiment and theory improves with increasing N, contrary to what would be expected if an interfacial resistance (r_σ) would be present (see equation (5.2–18)). From theory we find that $K_b' \sim b^{1/2} \sim N^{0.7}$, so $\alpha' = 0.7$ (see equation (4.2–6)). A plot of log (K_b) against log (N_b) yields $\alpha = 0.84$. Since the presence of any positive r_σ will always yield a slope that is lower than α', this means that only an r_σ is operative when the experimental $k_b \sim N^\alpha$ with $\alpha > 0.84$. But even in this case is r_σ much smaller than the overall resistance.

We attribute the deviation of α' from α to the less well developed interfacial flow at the boundaries (at $r \gtrsim 3.5 \times 10^{-2}$m and $r \lesssim 2 \times 10^{-2}$m) at low N_b. Our empirical method to obtain the best α from experiment did not work, because the correlation factor of the plots hardly changed with α: a variation from $\alpha = 0.7$ to $\alpha = 1.0$ changed the correlation factor by only 0.0003.

It must be remarked that even for different absolute values of D_b^{KCl} and b_σ, the same reasoning applies, resulting in $K_b' \sim N^{0.7}$ (which is quite reasonable for the assumed laminar flow). Only when the average b_σ would vary with N very differently from what was observed for part of the interface, a small interfacial resistance might be operative.

We can conclude from this analysis that no indications are present that suggest the presence of an interfacial resistance for the KCl transfer from wabu to buwa. This same conclusion can also be inferred qualitatively from the average diffusion time $\bar{t}$ for the total transfer process: $\bar{t} = (\delta_D)^2/2D = D_b^{KCl}/2K_b'^2$. Even at $N_b = 90$ min^{-1} $\bar{t}$ is still approximately 0.5 s; however, the relaxation time of a partial dehydration of K$^+$ and Cl$^-$, a possible mechanism causing an r_σ, is in the order of 10^{-8}s (e.g. KAVANAU, 1964 p. 29). Therefore it must be concluded that the resistance caused by dehydration is negligible compared to the diffusional resistance in the buwa phase.

6.5.3. *The effect of PVA-Ac on the mass transfer process*

As a consequence of our conclusion that r_σ is negligibly small, it is impossible to interpret our results in terms of a fractional coverage of the interface with

copolymer train segments. Since it is k_b that almost completely determines the value of K_b, it is obvious that the explanation of the retarding effect of PVA-Ac must be primarily ascribed to a change in k_b. This may be brought about by a modification of the concentration profile in the buwa phase (see equation (5.2–15)) either due to a change in D_b^{KCl} or due to a different flow profile in the vicinity of the interface (see equation (5.2–8)).

A decrease in D_b^{KCl} caused by the presence of PVA-Ac is rather improbable for the following two reasons. Firstly, it is well known that even in concentrated polymer solutions or gels the diffusion coefficients of small molecules are not necessarily much lower than in the pure solvent. HOSHINO and SATO (1967), e.g., found hardly any variation in D_{water}^{NaCl} with PVA concentrations up to 6 weight % polymer. The same result was found by LEYTE (1974) for the self-diffusion coefficient of NaCl in wabu solutions containing 6% PVA 205. Secondly, even if the PVA-Ac molecules would extend in the buwa phase for a considerable part, which is not likely because they are almost insoluble in that phase, still D_b^{KCl} could only be decreased over the distance of the adsorption layer (at most about 10^{-8} m), whereas the mean overall diffusion boundary layer is at least three orders of magnitude larger. Therefore PVA-Ac cannot have any significant influence on k_b by its effect on D_b^{KCl}.

The hydrodynamic conditions near the wabu-buwa interface can be changed either by an excess interfacial shear viscosity or by an interfacial pressure gradient $(\partial\Pi/\partial r)$ set up by compression of the copolymer layer. Experiments with a modified surface shear viscometer according to DE BÉNARD (1957) showed that any excess interfacial shear viscosity was absent in our system (DE FEIJTER, 1976). Therefore the drastic influence of PVA-Ac on K_b must be attributed to the dynamic interactions between the shear stress at the interface and the (partly) compressed copolymer layer. This results in a non-homogeneous copolymer layer at the interface, for which $\partial\Pi/\partial r = |\tau_{zr}||_{z=0,w} + |\tau_{zr}||_{z=0,b}$ holds, so that in this region $v_{ar} = 0$. The ultimate situation is that the whole interface is immobilized so that the flow near the interface can be described by (6.3–2) in stead of (6.3–3), and k_b thus by (6.3–10).

We have estimated the influence of a complete immobilization of the interface on K_b, based on the model proposed in ch. 6.3 and on the values of D_b^{KCl} and a. The maximum theoretical retardation, R_N', is obtained directly from the ratio of the k_b values calculated with (6.3–11) and (6.3–10) respectively. Since we have found that $b_\sigma \backsim v_b$ and $a_b \backsim v_b^{3/2}$, the value of R_N' is independent of v_b and thus of N (R_N is proportional to $(D_b^{KCl})^{-1/6}$ and also to the available area to the power $-{}^1/_6$). In table 6.5–3 we have collected the values of R_N' for four different interfaces: the interface met with in the experimental set-up, the interface available when the plate or ring is present, and in addition the interface in the region where v_b and v_w have been measured.

Comparison of these theoretical values with the experimental maximum values of R_N (fig. 6.4–2 and table 6.4–1) indicates that R_N' for the total interface is about 20% lower. The prediction that R_N' is independent of N and of the

98

TABLE 6.5–3. Theoretical values for the maximum retardation.

interfacial area	R_N' *)
$0 \leqslant r \leqslant 4.04 \times 10^{-2}$ m	4.9
$\left.\begin{array}{l} 0 \leqslant r \leqslant 2.85 \times 10^{-2}\,\text{m} \\ 2.85 \times 10^{-2} \leqslant r \leqslant 4.04 \times 10^{-2}\,\text{m} \end{array}\right\}$	5.5
$2 \quad \times 10^{-2} \leqslant r \leqslant 3 \quad \times 10^{-2}$ m	6.0

*) R_N' was calculated from: $R_N' = \dfrac{1.596\,(b_\sigma D_\beta^{KCl})^{1/2}/(r_\delta^3 - r_1^3)^{1/2}}{1.017\,(a_b^{1/2} D_\beta^{KCl})^{2/3}/(r_\delta^2 - r_1^2)^{1/3}}$.

kind of copolymer adsorbed holds for B3, B4 and B5 for most rotation speeds at (very) high S. R_N' for the interface with the ring fits the experiments rather well, whereas the agreement for the interface with the plate is excellent except for the two lowest N_b's. The value of R_N' calculated for $2 \times 10^{-2} \leqslant r \leqslant 3 \times 10^{-2}$ m fits the experimental results for the total interface very well, but is still slightly too low.

The observed differences between experiment and theory can again be explained by the deviations of the actual flow field from the one assumed. As shown in ch. 6.5.2, the theoretical flow profile only existed along a part of the interface, but the interfacial flow in that region will induce a radial interfacial flow along the parts that are not directly reached by it (by the demand of continuity). However, when the interface is stationary this indirect flow mechanism is less effective, so that the experimental $R_N > R_N'$. This mechanism must be particularly operative in the centre of the interface: although, even in the absence of PVA-Ac, a small region near the edge of the ring must exist where $v_{\sigma r} = 0$. R_N^{plate} is still larger than $R_N'^{plate}$.

The hypothesis of the reduction of $v_{\sigma r}$ could be demonstrated with talc particles at the interface. Whereas these particles were directed to the centre of a 'clean' interface very quickly, they did not move radially over a period of a few minutes when 10 mg.m^{-2} B5 was spread at the interface, even at $N_b = 90$ min^{-1}. This influence of PVA-Ac could not be visualized in the set-up described in ch. 4.3, probably because its flow patterns were neither radial nor systematic.

We can mention here another finding sustaining the usefulness of the proposed models. We have also solved equation (6.3–4) with $v_r = -b$ and $v_r = -az$, respectively. These cases do not take into account the convergence of the flow, so they would give identical results at very large r. Although the resulting individual K_N' values of the total interface are higher (because of a higher velocity at the outer edge), the value of R_N' is almost the same. So, although a different dependence of v_r on r was assumed, the models of plug flow and of a stationary interface have still resulted in comparable values of R_N'.

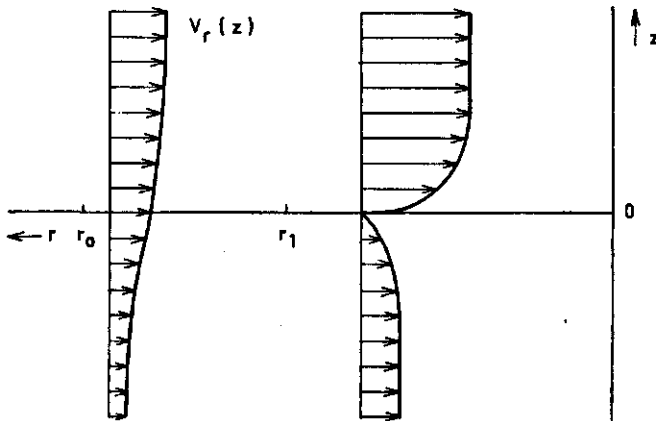Since the reason for the maximum retarding effect of PVA-Ac is clear now,

FIG. 6.5-1. The supposed hydrodynamic boundary layer flow of a partly covered interface (for $r < r_1$).

we can attempt to explain the differences in the experimental results as observed in ch. 6.4.2. However, first some general remarks must be made.

SAITO (1969) showed that 0.1 mol.l^{-1} KCl has a negligible effect on the solution properties of water for several PVA-Ac copolymers. Therefore, it is justified to assume that the presence of KCl will not change the trend in the interfacial activities of the (co)polymers which was found in ch. 3.3.5.

Because the shear stresses of both moving phases are minimal at the lowest N_b, the value of $\partial \Pi / \partial r$ necessary to oppose these stresses will also be at a minimum at the stirring speed. So, for a constant amount of copolymer at the interface, the polymers can cover the largest area (namely πr_1^2, see fig. 6.5–1), at the lowest N_b. Thus r_1 at $N_b = 40$ will be $> r_1$ at $N_b = 50$ min^{-1} etc.. This explaines why, at constant S, $R_{40} > R_{50}$, as found experimentally, but this supposed effect could also be demonstrated with talc particles at the interface: at $S^{B5} = 1$ mg.m^{-2}, the interface was completely immobilized at $N_b = 40$ min^{-1} whereas at 90 min^{-1}, the periphery was partly cleared.

From the experiments we could infer that no PVA-Ac desorbed completely anymore due to the above mentioned shear stresses. A series of measurements with N_b successively 40, 90, 40, 90 and 40 min^{-1} showed R_{40} and R_{90} to be constant. Thus, it can be concluded that the total amount of copolymer present at the interface, Γ, remains equal for all stirring speeds at one value of S. This means that either the copolymers adsorbed are irreversibly attached at the interface, or their relaxation time of desorption is very long (in the order of hours).

In ch. 3.3.5 we have found that PVA-H, B1 and R1 did not (or hardly) adsorb at the wabu-buwa interface. Therefore, the (co)polymers spread at the interface will desorb immediately, no interfacial pressure gradient can be induced by the flow, and thus no retardation will arise. This reasoning completely fits the experiments, except that, at very high S^{B1}, a small reduction was measured at

100

low N_b. We attribute this to the broader inter-molecular acetate distribution of the blocky PVA-Ac's (ch. 3.1). As a result, a small proportion of the B1 molecules contains an appreciably higher acetate content than the average value, and this proportion is more interfacially active. As a result of the short duration of the γ-measurements, these copolymers are unable to diffuse to the interface, but when they are spread at the interface they will remain there.

This same reasoning applies to B2, but to a higher extent, as its acetate distribution is more blocky (ch. 3.3.3). Whereas B2 demonstrated a systematically lower $\Pi(t)$ than R2 for adsorption layers (ch. 3.3.5), their effects after spreading are similar. By spreading, the most interfacially active copolymers will remain at the interface. But, since random copolymers have a relatively narrow inter- and intra-molecular acetate distribution (ch. 3.1 and ch. 3.3.3) this 'fractionation' will not be very effective for R2, in contrast to B2.

From the amounts of B2 and R2 required to obtain a significant R_N, we can infer that only a very small fraction of all copolymers remains adsorbed after spreading: usual values of Γ for a spread macromolecular layer amount to $0.1-5$ mg.m^{-2}.

The above mentioned 'fractionating effect' can also be inferred from the differences in $\partial R_N/\partial\ln(S)$ at $N_b = 40$ and 50 min^{-1} (see fig. 6.4-1). Whereas R_{40}^{R2}, and thus also Γ^{R2}, seems to have reached its maximum at the highest S^{R2}, R_{40}^{B2} can still reach higher values at higher S^{B2} (although $\Pi(t)^{B2} < \Pi(t)^{R2}$, see fig. 3.3-9).

We shall treat the more fascinating results of B3, B4 and B5 together. Firstly we must remind what is the main cause of a decrease in γ, and thus of an increase in Π, during polymer adsorption. It is very probable that, for a given polymer-solvent-interface system,Π is determined by θ, the fraction of the interface covered with train segments, and by the segment density distribution as a function of the distance to the interface, $\rho(z)$ (e.g. LANKVELD and LYKLEMA, 1972). It should be realized, however, that these parameters are interrelated, for $\theta \sim \rho(0)$. This $\rho(z)$ contains the interaction free energies of the segments in loops and trains, and the average loop length. Because $\rho(z)$ decreases exponentially, Π is almost completely determined by the first ten or twenty Å of the adsorption layer. Therefore it must be concluded that Π is not only determined by θ. Up to this moment, however, no satisfactory quantitative theory has been developed to estimate the different effects separately, and thus to determine the contribution of θ to Π.

The three graphs in fig. 6.4-2 have many 'corresponding' points: each R_N value (up to the maximum of R_N) corresponds to an equal $\partial\Pi/\partial r$ distribution, and therefore their $\int_0^{r_1} (\partial\Pi/\partial r) \, dr$ is equal. For one fixed combination of N_b and R_N the following inequality holds: $S^{B3} > S^{B4} > S^{B5}$ (still provided $R_N < $ the maximum value of R_N). Since the spreading technique was identical for all copolymers, this inequality must be due to an increasing desorption and a smaller θ and Γ, going from B5 to B3.

Several different attempts were made to determine the amount desorbed (and thus Γ, from the combination with S), but they all failed. The colorimetric method (ch. 3.3.6) and the detection of C^{14}-labelled PVA-Ac appeared to be insensitive in the relevant concentration range (0.01–0.1 ppm). In principle, H^3-labelled PVA-Ac can be used to tackle this problem, but H^3 of the CH_3 group exchanges with water (by keto-enol tautomers), particularly at the high temperatures that are necessary to dissolve the copolymers. In addition it appeared difficult to homogenize the very small wabu phase. Nevertheless, we inferred from the measurements with H^3-labelled copolymers, that for a PVA-Ac copolymer which resembled B3, only a small fraction of S remained adsorbed at the interface after spreading of both 1 and 20 mg.m^{-2}. From the facts that B5 is only about 50% soluble in wabu (ch. 3.3.6) and that $m_{5w}^{B5} \approx 2 \times 10^{-3}$ we can infer that at least 50% remained at the interface as long as R_{90} has not reached its maximum (at $S^{B5} \approx 4$ mg.m^{-2}). Thus we can draw the conclusion that in all cases $0.1 < \Gamma^{B5} < 4$ mg.m^{-2}. The following relation holds for the average VAc sequence length. L_{VAc}: $L_{VAc}^{B5} > L_{VAc}^{B4} > L_{VAc}^{B3}$ (fig. 3.3–4; table 3.3–2). Therefore the VAc train lengths of B5 will also be the largest, p (and thus θ) the highest, and thus the desorption after spreading (and the reversibility of its adsorption from solution) the lowest, as inferred.

The fact that, going from B3 to B5, $\partial R_N / \partial \ln(S)$ increases, particularly at high N_b, is closely related to these phenomena. Since R_N is related to $\int_0^{r_1} (\partial \Pi / \partial r)\, dr$, $\partial R_N / \partial \ln(S)$ is related to $\partial [\int_0^{r_1} (\partial \Pi / \partial r)\, dr] / \partial \ln(S)$, and thus to the variation of both the area covered by PVA-Ac ($= \pi r_1^2$) and the degree of coverage (related to Π), with ln (S). Thus, at decreasing γ, $-\partial \gamma / \partial \ln(S)$ becomes steadily lower for B3 than for B4 or B5, which is caused by the lower interfacial activity of B3 and, as a consequence, by the higher amount that desorbs. Whereas 25×10^2 mg B3.m^{-2} must be spread to arrive at the maximum of R_{70}, only 2 mg.m^{-2} is needed for B5. This is in contrast to the maximum of R_{40} for which 20 respectively 1.5 mg.m^{-2} is sufficient.

As we have observed before, all points with equal R_N value (for $R_N <$ the maximum value of R_N) have an equal interfacial area covered by copolymers. Yet $\partial R_N / \partial N$ decreases going from B3 to B5 for one particular S. This must be due to differences in compressibility. It is well known that, on water, a monolayer of PVA is more compressible than a PVAc monolayer (e.g. CRISP 1946; ISEMURA and FUKUZUKA, 1956). Thus one would expect a decreasing compressibility with increasing VAc train length. Add to this that at increasing Π the shortest VAc trains will desorb first, then it will be clear that B3 is more compressible than B4, and B4 more than B5. This explains qualitatively the large experimental differences in the effect of the three blocky PVA-Ac's.

The only unexplained result remains the decrease in R_N after having reached its maximum (fig. 6.4–2). R_{40}^{B3}, R_{50}^{B3}, R_{40}^{B4} and R_{50}^{B4} first decrease slightly, after which they increase again. For B5 it is unknown whether R_N will also increase again at still higher S^{B5}. A priori, two explanations can be proposed for this

phenomenon. For both we assume, as before, that the total interface is just covered with a PVA-Ac layer when R_N reaches its maximum, so that $\gamma = \gamma_0$ at $r = 4 \times 10^{-2}$m. A further increase in S will, therefore, result in a decrease of γ at the periphery of the interface, which in turn may cause a decrease in the contact angle between the interface and the glass wall and thus an increase in the interfacial area. The second possible mechanism is that at increasing Π, the Π-A curve for PVA-Ac shows a less steep or even horizontal section. In that case the monolayer will respond less quickly to fluctuations in the flow field, which in turn causes a higher average liquid velocity near the interface and thus a lower retardation. Since no decrease in contact angle could be observed during the experiments, we must conclude for the moment, that the last mentioned effect was operative. Because wabu and buwa are poor solvents for PVA and PVAc, respectively, the occurrence of a two dimensional condensation of the copolymers at the interface is clearly possible at a certain Γ. Verification of this hypothesis at the wabu-buwa interface is, however, very difficult, since Π can at most amount to 1.7 mN.m^{-1}.

The proposed mechanism of retardation can also be checked in another way. To that purpose we formulate the force balance for an interfacial area for which $v_{ar} = 0$. Since the flow near the interface is most effective for $2 \times 10^{-2} \lesssim r \lesssim 3.5 \times 10^{-2}$m we have worked out the balance for this region:

$$\left.|\tau_{zr}|\right|_{z\,=\,0,\,w} + \left.|\tau_{zr}|\right|_{z\,=\,0,\,b} = \left|\frac{\partial\Pi}{\partial r}\right| \tag{6.5-1}$$

Insertion of (5.2–12) and (6.3–2) in the left hand side and integration between r_1 and r_2 yields:

$$\frac{2\eta_w a_w}{r_1 + r_2} + \frac{2\eta_b a_b}{r_1 + r_2} = \frac{\Delta\Pi}{r_1 - r_2} \tag{6.5-2}$$

TABLE 6.5-4. Estimated values for the interfacial pressure difference necessary to oppose the shear stress of both flowing phases.

N_b min^{-1}	$\Delta\Pi$ *) mN.m^{-1}	$\Delta\Pi^0$) mN.m^{-1}
40	0.3	0.3
50	0.4	0.5
60	0.6	0.8
70	0.8	1.0
80	1.1	1.4
90	1.4	1.8

*) calculated for $2 \times 10^{-2} \leqslant r \leqslant 3.5 \times 10^{-2}$m.
^{0}) calculated for $2 \times 10^{-2} \leqslant r \leqslant 4 \times 10^{-2}$m.

where we thus have considered the region of $r_2 \leqslant r \leqslant r_1$. Since all parameters at the left hand side of equation (6.5-1) are known approximately, the value of $\Delta \Pi$ that is necessary to oppose the shear stress of both flowing bulk phases, can be estimated with (6.5-2). $\Delta \Pi$ has been calculated for two cases, namely $2 \times 10^{-2} \leqslant r \leqslant 3.5 \times 10^{-2}$m and $2 \times 10^{-2} \leqslant r \leqslant 4 \times 10^{-2}$m (table 6.5-4). The magnitude of $\Delta \Pi$ is in good agreement with the values that are possible for the wabu-buwa interface (see also fig. 3.3-9): B3 (that gave $\Pi \approx 1.1$ mN.m^{-1}) reaches the maximum of R_{70}, and B5 (that gave $\Pi \approx 1.6$ mN.m^{-1}) even seems to reach the maximum of R_{90}. Thus, this agreement in Π values is another support for the correctness of the proposed model.

The resemblance of the present results to those found in ch. 4.3 is striking. There it was also concluded, but on a more empirical basis, that m_{bw}/k_σ is negligible as compared to $1/k_b$.

The influence of PVA-Ac could not be interpreted unambiguously in ch. 4.3 (see fig. 4.3-2), but the analysis given here demonstrates the dominant influence of the adsorbed copolymers on the two-phase flow near the interface. To show the close agreement with ch. 4.3, we have plotted $(K_b)^{-1}$ against $N_b^{-0.84}$ for five different S^{B5} values (fig. 6.5-2). The curve of $S^{B5} = 2$ mg.m^{-2} is very similar to the one given in fig. 4.3-2, whereas the curve of $S^{B5} = 10$ mg.m^{-2} demonstrates the correctness of the theoretical prediction that α must be equal for a 'clean' and a completely covered interface (this must hold, since $b^{1/2} \backsim a^{1/3}$). The fact that no straight line is obtained at intermediate values of S^{B5} is caused by the dependence of the interfacial coverage (and thus of r_1, see fig. 6.5-1) on N_b, as indicated above.
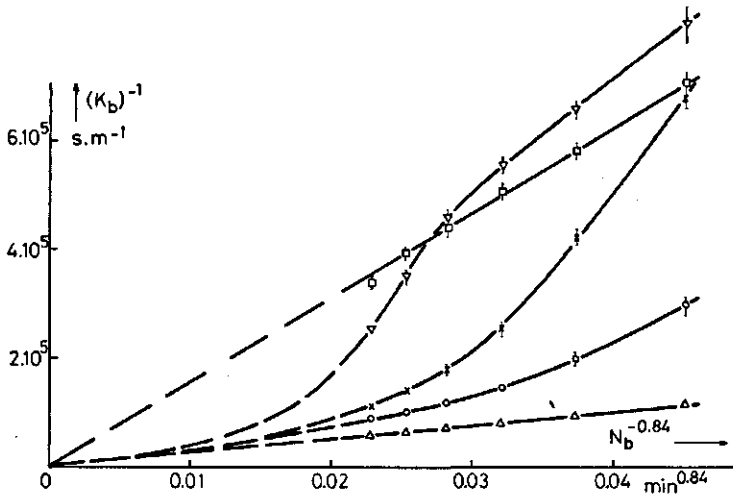

FIG. 6.5-2. The influence of B5 on the overall mass transfer coefficient at $S^{B5} = 0$ ($\triangle$), 0.5 ($\bigcirc$), 1 ($\times$), 2 (∇) and 10 ($\square$) mg.m^{-2}.

Provided we knew the exact flow profiles, we might even endeavour to calculate which area is covered by PVA-Ac. Suppose, e.g., an interface for $0 \leqslant r \leqslant r_0$, that is covered with PVA-Ac for $0 \leqslant r \leqslant r_1$ (see ch. 6.3 and fig. 6.5–1). Then K_b^p can be represented by:

$$K_b^p = \frac{5.01 \, (b_\sigma D_b)^{1/2} \, (r_0^2 - r_1^2)^{1/2} + 3.20 \, (a_b D_b^2)^{1/3} r_1^{2/3}}{\pi r_0^2} \tag{6.5–3}$$

as derived in appendix C. Under the given conditions, we are thus able to determine r_1 from the known values of K_b^p, D_b, a_b, b_σ and r_0 with a simple iterative method. This provides a new tool to study the structure of adsorbed (co)polymer layers under variable dynamic conditions, which are so very important during e.g. emulsification processes.

6.5.4. *Comparison of the present results with those found in the literature*

Our conclusions that r_σ is negligible, agrees with most chemical engineering literature (ch. 5.3) and is in contrast to the faulty hypothesis frequently met with in biochemical and colloid chemical literature (ch. 4.1). Two groups (Nitsch et al. and Davies et al.) are performing similar investigations, so that a comparison of our results with theirs is required. Although all three arrive at the same conclusion as to the importance of the hydrodynamic conditions near the interface, there are still considerable mutual differences.

NITSCH et al. (1973a & b, 1976a & b) used much higher rotation speeds (up to $1000 \, \text{min}^{-1}$), but they still assumed laminar flow profiles near the liquid-liquid interface (their maximal Re amounted to 3×10^4, which indicates turbulent flow, in contrast to our maximal value of 2×10^3). In addition they found that $v \sim N^2$, in contrast to the usual observations at completely developed turbulence, namely $v \sim N$ (e.g. DAVIES, 1972 p. 65). They mainly investigated the effect of low molecular weight IAMs, for which they had to assume a steady adsorption at the cleared periphery and a steady desorption of the compressed material in the centre of the interface (KNIEP, 1974). In fact, both processes short-circuit the effect of the IAMs on the transport rate. We have shown that no allowance for these phenomena has to be made for our copolymers: neither desorption took place during the experiments (due to irreversibility or to a very long desorption relaxation time) nor adsorption. The reason for this difference are both the low bulk concentrations of PVA-Ac (at most 50 ppm, but usually below 1 ppm) and the very small diffusion coefficients of these macromolecules.

The retarding effects measured by Nitsch et al. were lower (at most a decrease in K of 50% was found), while they were unable to verify quantitatively the proposed mechanism of retardation, as we did. They found that K was always proportional to N, which implies that a higher flow rate did not result in a higher compression of the IAMs, which sounds quite unrealistic for radial flow. Both differences suggest that their boundary layer flow was essentially different due to both the higher stirring speeds and the small-mesh wire-netting which they applied in their vessels.

Davies et al. have been mainly concerned with turbulently stirred liquid-liquid or liquid-gas systems. Consequently, either only semi-empirical treatments were possible (DAVIES et al., 1961, 1964, 1965 & 1974), or suppositions had to be made on the structure of the turbulent spectrum (DAVIES, 1966 & 1972). Because of the essentially different boundary layer flow, their results are not all comparable to ours. DAVIES et al. (1964) found, e.g., that the retarding influence of spread proteins increased with the stirring rate. But the maximal retardation R found by DAVIES et al. (1961) is of comparable magnitude. They assumed that the retardation was caused partly by the damping of turbulent eddies from the stirrer in the relevant phase and partly by a decrease in the momentum transfer across the interface. This is analogous to our assumption that v_σ becomes zero and that, consequently, the velocity profiles in both phases change.

From this comparison we must conclude that differences in hydrodynamic and geometric conditions may change the quantitative results considerably, and that they may even reverse a certain trend. Therefore it remains very risky to draw general conclusions based on one particular series of experiments.

6.6. CONCLUSIONS

It was shown theoretically that both density- and interfacial-tension-driven instabilities may occur during KCl transfer from wabu to buwa. All experiments supported the conclusion that the driving forces of these spontaneous convections were so small that they were not effective in practice.

A new transport vessel was designed to obtain a more systematic and better defined liquid flow near the interface in both phases. The transport rate measurements were fully automated by means of a data acquisition system, which made it possible to measure accurately several transport rates at different N_b during one experiment.

By assuming two simple but realistic models for the laminar boundary layer flow, the equation of conservation of mass was solved for both a mobile and a stationary interface. Approximate values of the diffusion coefficient and of the hydrodynamic parameters characterizing the liquid flow near the interface were obtained from the limiting equivalent conductivity and from liquid-velocity measurements, respectively. With these quantities, theoretical liquid phase mass transfer coefficients, K_b^t, were calculated for both models.

Comparison of K_b^t for a mobile interface with the experimental K_b for a 'clean' interface, as well as comparison of the theoretical and experimental values of $\partial \ln(K_b)/\partial \ln(N)$ yielded that the interfacial resistance is negligible for the present system. Therefore, any change in K_b due to adsorption has to be ascribed to a change in the liquid phase mass transfer coefficients.

Although the transport measurements could, therefore, not provide any direct information on the degree of coverage of the interface, they appeared to be a sensitive method to distinguish between the interfacial activities of the

(co)polymers. The effect of the blocky and random PVA-Ac copolymers on the transfer process was investigated after spreading them at the wabu-buwa interface. Very different results were obtained, depending on the total amount spread, the average VAc content and the intra-molecular VAc distribution of the (co)polymers. The retarding effect appeared to be positively related to the effect of PVA(-Ac) on γ during adsorption (ch. 3.3.5). In addition, it appeared that the average VAc sequence length rather than the overall VAc content determined the adsorption behaviour of PVA-Ac at the wabu-buwa interface.

The influence of PVA-Ac was proved to be mainly a hydrodynamic effect on the partial buwa mass transfer coefficient, k_b. The theoretical retardation, R'_N, calculated from the ratio of K'_b for a mobile and for a stationary interface and the experimental maximum R_N were in reasonable agreement. Deviations were attributed to the imperfectness of the actual flow near the interface, both in the centre and at the periphery.

The different effects of the individual (co)polymers were explained qualitatively in terms of the (ir)reversibility of their desorption processes and the compressibility of their adsorption layers, due to differences in the VAc train lengths at the interface. Finally, a method was suggested to determine more quantitatively the behaviour of adsorption layers in a variable stationary shear stress field.

SUMMARY

In this study we have investigated the interfacial properties of several polyvinyl alcohol-acetate (PVA-Ac) copolymers, which only differ in the content and the intra-molecular distribution of their vinyl acetate monomers (VAc).

In chapter 1 the relevant theoretical and experimental aspects of studies on polymer adsorption are reviewed. Because of experimental difficulties, studies on polymer adsorption at liquid-liquid interfaces have, up to this moment, only resulted in qualitative information on the adsorption mechanism and the structure of polymer adsorption layers. One of the objectives of the present study was to further elaborate a recently proposed method to determine the degree of coverage of a liquid-liquid interface from the retarding effect of polymers adsorbed at that interface, on mass transfer through it. To that end, KCl transfer measurements between water saturated with 1-butanol (wabu) and 1-butanol (buOH) saturated with water (buwa) have been performed, as described in the chapters 4 and 6.

With the exception of the PVA(-Ac) (co)polymers, all materials and their relevant physical properties are described in chapter 2.

In chapter 3, a short review is given on the properties of PVA-Ac, with special emphasis on the influence of the VAc monomers on the (dis)solution and interfacial properties of the copolymers. Since it was supposed that it is the intra-molecular VAc distribution that determines the interfacial properties of PVA-Ac to a large extent, this aspect has been investigated systematically. To that end, five blocky (B1–B5) and two random (R1 and R2) PVA-Ac copolymers have been prepared, the intra-molecular VAc distributions of which have been analysed in several ways (with complexometry, IR spectroscopy and thermal analysis).

The solution properties of these copolymers in water have been studied by viscosimetry. Particular attention has been paid to the methods of processing the experimental data. For the random copolymers, the linear expansion factor in water steadily decreases with increasing VAc content, whereas it passes through a maximum for the blocky copolymers. These differences can not be explained by the often assumed inhibition of inter- and intra-molecular H-bonding between VA segments due to the size of the acetate groups. It is suggested that the incompatibility of VA and VAc sequences causes the expansion of the blocky copolymers. The decrease in expansion with (a further) increase in VAc content is related to the more hydrophobic character of the VAc monomers.

BuOH has a stabilizing influence on PVA in aqueous solution, probably due to preferential adsorption of buOH molecules with their hydrophobic part onto the C–C backbone of the polymers. This influence decreases with increasing VAc content of the copolymers, which is ascribed to the prevention of

this adsorption on those parts of the chain to which the acetate groups are attached. An attempt is made to estimate the peripheral solvent quality for the copolymers from their Huggins coefficients. Probably the mean peripheral VAc content is less than the mean overall content of the copolymers.

The interfacial activities of the copolymers have been studied by measuring the interfacial tension between a copolymer solution of wabu and buwa, both with the static drop-shape and the dynamic drop-volume method. It is shown experimentally that the more accurate and much simpler drop-volume method is also applicable to these solutions, provided the copolymer concentration is not too low. In this system, the interfacial activity of PVA-Ac increases with the VAc content and, in particular, with the average VAc sequence length of the copolymers. It is concluded that these VAc sequences are the anchors that adsorb at the wabu-buwa interface. The observed time effects are ascribed to the unfolding of the adsorbed copolymers, so that the longer VAc sequences of the inner part of the coil can adsorb.

In chapter 4, the KCl transport from wabu to buwa is investigated. With a semi-empirical method it is attempted to separate the *hydrodynamic* from the *physico-chemical* contributions to the overall mass transfer coefficient, K_b. Although no unambiguous quantitative results are obtained, it can yet be concluded that the partial buwa mass transfer coefficient, k_b, is the rate determining step in the transfer process. This implies that the explanation of the retarding effect of PVA-Ac can not be found in a simple reduction of the interfacial area available for transfer. The effect is assumed to be mainly of a hydrodynamic nature. The experimental set-up used does not enable more quantitative results to be obtained, but the hypothesis that adsorption is the cause of the retardation is confirmed.

Since the effect of PVA-Ac can only be properly explained when the interphase mass transfer process itself is understood in all details, the fundamentals of those transport phenomena that are relevant to this process are treated in chapter 5. In addition, attention is paid to the experimental results found in the literature.

In chapter 6, a transport vessel is described that has more systematic and better defined flow patterns at both sides of the interface. By assuming two simple but realistic models for the laminar boundary layer flow, k_b is estimated theoretically for both a 'clean' (mobile) and a completely covered (stationary) interface. This makes it possible to draw more definite conclusions on the presence of any interfacial resistance.

The agreement between the theoretical and experimental mass transfer coefficients for a 'clean' interface allows the conclusion to be made that the interfacial resistance is negligible for the system studied. This must mean that k_b is changed drastically by the adsorption of PVA-Ac, which is confirmed by the agreement between the theoretical and experimental mass transfer coefficients for a completely covered interface. However, this method can not provide any direct information on the degree of coverage of a liquid-liquid interface.

Yet it appears a sensitive method to distinguish between the interfacial

activities of the blocky and random copolymers: the effects are diverse, depending on the total amount of PVA-Ac spread at the interface, on the VAc content and in particular on the average VAc sequence length. These differences are interpreted qualitatively in terms of the (ir)reversibility of the desorption processes and the compressibility of the adsorption layers. Finally, a method is suggested to investigate more quantitatively the behaviour of adsorption layers in a variable, stationary shear-stress field.

ACKNOWLEDGEMENTS

SAMENVATTING

In dit onderzoek hebben we de eigenschappen van verschillende polyvinyl alcohol-acetaat (PVA-Ac) copolymeren aan een vloeistof-vloeistof grensvlak bestudeerd. Deze copolymeren verschillen onderling slechts in het gehalte en de intra-moleculaire verdeling van hun vinyl acetaat monomeren (VAc).

In hoofdstuk 1 wordt een overzicht gegeven van de relevante theoretische en praktische kanten van het onderzoek aan polymeer-adsorptie. Vanwege experimentele moeilijkheden heeft de bestudering van polymeer-adsorptie aan vloeistof-vloeistof grensvlakken tot nu toe slechts geleid tot kwalitatieve kennis over het mechanisme van de adsorptie en de opbouw van de geadsorbeerde polymeerlagen. Het huidige onderzoek had gedeeltelijk tot doel een onlangs voorgesteld methode, om de bedekkingsgraad van een vloeistof-vloeistof grensvlak af te leiden uit de remmende invloed van polymeren, geadsorbeerd aan dat grensvlak, op de stofoverdracht daar door heen, verder uit te werken. Daartoe zijn in de hoofdstukken 4 en 6 KCl overdrachtsmetingen tussen water verzadigd aan 1-butanol (wabu) en 1-butanol (buOH) verzadigd aan water (buwa) beschreven.

Met uitzondering van de PVA(-Ac) (co)polymeren worden alle materialen en hun relevante fysische eigenschappen beschreven in hoofdstuk 2.

Hoofdstuk 3 wordt begonnen met een kort overzicht van de eigenschappen van PVA-Ac; met name wordt de invloed behandeld die de VAc monomeren hebben op de oplossnelheid en de oplosbaarheid van de copolymeren in water, en op de grensvlakactieve eigenschappen van de copolymeren. Omdat verondersteld werd dat de intra-moleculaire VAc verdeling de eigenschappen van PVA-Ac aan grensvlakken in belangrijke mate zou kunnen bepalen, hebben we dit facet systematisch onderzocht. Daartoe zijn vijf blokvormige (B1–B5) en twee statistische PVA-Ac copolymeren bereid, waarvan de intra-moleculaire VAc verdelingen op verschillende manieren zijn geanalyseerd (met complexometrie, IR spectorscopie en thermische analyse).

De eigenschappen van deze copolymeren in waterige oplossing zijn bestudeerd met viscosimetrie, waarbij bijzondere aandacht is besteed aan de verwerking van de experimentele resultaten. De lineaire expansie factor voor de statistische copolymeren daalt regelmatig met toenemend VAc gehalte, terwijl deze bij de blokvormige copolymeren door een maximum gaat. Omdat deze verschillen niet verklaard kunnen worden door de vaak veronderstelde belemmering van inter- of intra-moleculaire H-bruggen tussen VA segmenten door de omvang van de VAc groepen, wordt voor dit verschijnsel een andere oorzaak voorgesteld, namelijk de incompatibiliteit van VA en VAc reeksen. De inkrimping met (verder) toenemend VAc gehalte wordt toegeschreven aan het meer hydrofobe karakter van de VAc groepen.

BuOH heeft op PVA in waterige oplossing een stabiliserend effect, waarschijnlijk ten gevolge van preferente adsorptie van de buOH moleculen met

hun hydrofobe gedeelte aan de C–C keten van het polymeer. Deze stabilisatie neemt af met toenemend VAc gehalte van de copolymeren, hetgeen wordt toegeschreven aan verhindering van deze adsorptie op die plekken van de keten waaraan de acetaat groepen vast zitten. Er wordt ook een poging gedaan om de oplosmiddelkwaliteit voor de buitenkant van de copolymeren te schatten, en wel uit de Huggins coëfficiënt. Waarschijnlijk is de gemiddelde VAc dichtheid *in* de kluwen hoger dan aan de buitenkant ervan.

Met behulp van grensvlakspanningsmetingen tussen een (co)polymeer oplossing in wabu en buwa (met de statische druppel-vorm en de dynamische druppel-volume methode) is de grensvlakactiviteit van de (co)polymeren bestudeerd. Er wordt experimenteel aangetoond dat de nauwkeurigere en veel eenvoudigere druppel-volume methode ook voor deze oplossingen gebruikt kan worden, mits de (co)polymeer concentratie niet te laag is. De grensvlakactiviteit neemt, voor het gebruikte systeem, toe met het VAc gehalte en in het bijzonder met de gemiddelde VAc reeks lengte. Er wordt uit geconcludeerd dat deze VAc reeksen de ankers zijn die aan het wabu-buwa grensvlak adsorberen. De waargenomen tijdseffecten worden toegeschreven aan het ontvouwen van de geadsorbeerde copolymeren, zodat de langere VAc reeksen uit het binnenste van de kluwen kunnen adsorberen.

In hoofdstuk 4 wordt de KCl-overdracht van wabu naar buwa bestudeerd. Getracht wordt om met een semi-empirische methode de *hydrodynamische* bijdragen te scheiden van de *fysisch-chemische* bijdrage tot de totale overdrachtscoëfficiënt, K_b. Hoewel met deze methode geen ondubbelzinnige resultaten worden verkregen, kan toch geconcludeerd worden dat de partiële buwa overdrachtscoëfficiënt, k_b, de snelheidsbepalende factor is voor het overdrachtsproces. Dit betekent dat de verklaring voor het remmend effect van PVA-Ac niet gezocht kan worden in een eenvoudig 'dichtmetselen' van het grensvlak. Het effect wordt verondersteld voornamelijk van hydrodynamische aard te zijn. Meer kwantitatieve resultaten zijn met de gebruikte experimentele opstelling niet mogelijk, maar de hypothese dat adsorptie de reden van de remming is, wordt bevestigd.

Omdat het effect van PVA-Ac alleen op een juiste wijze kan worden verklaard, wanneer het stofoverdrachtsproces zelf tot in alle details begrepen wordt, zijn in hoofdstuk 5 die grondbeginselen van de transport verschijnselen behandeld die voor stofoverdracht van belang zijn. Bovendien wordt er aandacht besteed aan de experimentele resultaten die in de literatuur gevonden zijn.

In hoofdstuk 6 wordt een transport cel beschreven, die, dicht bij het grensvlak in beide fasen, meer systematische en beter gedefinieerde stromingsprofielen heeft. Door twee eenvoudige maar realistische modellen aan te nemen voor de laminaire grenslaag-stroming kan k_b theoretisch berekend worden, zowel voor een 'schoon' (mobiel) als voor een volledig bedekt (stilstaand) grensvlak. Dit maakt het mogelijk meer definitieve conclusies te trekken met betrekking tot de aanwezigheid van een grensvlakweerstand.

De overeenstemming tussen de theoretische en experimentele stofover-

drachtscoëfficiënten voor een 'schoon' grensvlak pleiten voor een verwaarloosbaar kleine grensvlakweerstand voor het onderzochte systeem. Dit moet betekenen dat k_b sterk verandert onder invloed van de PVA-Ac adsorptie, hetgeen bevestigd wordt door de overeenkomst van de theoretische en experimentele stofoverdrachtscoëfficiënten voor een volkomen bedekt grensvlak Deze methode kan echter geen rechtstreekse inlichtingen verschaffen over de bedekkingsgraad van een vloeistof-vloeistof grensvlak.

Toch blijkt het een gevoelige methode te zijn om tussen de grensvlakactiviteiten van de blokvormige en statistische copolymeren onderscheid te maken: de effecten zijn erg verschillend en hangen af van de totale hoeveelheid PVA-Ac die in het grensvlak wordt gespreid, van het VAc gehalte en in het bijzonder van de gemiddelde lengte van de VAc reeksen. Deze verschillen worden kwalitatief uitgelegd in termen van de (ir)reversibiliteit van de desorptie processen en van de compressibiliteit van de adsorptielagen. Tot slot wordt een methode voorgesteld om meer kwantitatief het gedrag van adsorptielagen in een variabel, stationair afschuif-druk veld te bestuderen.

REFERENCES

ABRAMOWITZ, M. and STEGUN, A. (1968) 'Handbook of mathematical functions', Dover Publ. Inc., New York.
ADAMS, D. J., EVANS, M. T. A., MITCHELL, J. R., PHILLIPS, M. C. and REES. P. M. (1971) J. Polym. Sci. Polym. Symp. 34, 167–179.
ADAMSON, A. W. (1967) 'Physical chemistry of surfaces', Interscience Publ., New York.
ADELMAN, R. L. and FERGUSON, R. C. (1975) J. Polym. Sci. Polym. Chem. Ed. 13, 891–911.
AMAYA, K. and FUJISHIRO, R. (1956) Bull. Chem. Soc. Japan 29, 361–3; 830–3.
ANDREAS, J. M., HAUSER, E. A. and TUCKER, W. B. (1938), J. Phys. Chem. 42, 1001–19.
AUER, P. L. and MURBACH, E. W. (1954) J. Chem. Phys. 22, 1054–9.
BAKKER, C. A. P. (1966) 'Grensvlakstroming en stofoverdracht tussen beweeglijke fasen', Universitaire Pers, Rotterdam.
BAKKER, C. A. P., BUYTENEN, P. M. VAN and BEEK, W. J. (1966) Chem. Eng. Sci. 21, 1039–46.
BARNES, G. T. and LAMER, V. K. (1962) in 'Retardation of evaporation by monolayers: transport processes', ed. LaMer, V. K., Academic Press, New York, 9–33; 35–39.
BAUR, H. (1966a) Kolloid-Z.u.Z. Polym. 212, 97–112.
BAUR, H. (1966b) Makromol. Chem. 98, 297–301.
BEEK, W. J. and BAKKER, C. A. P. (1961) Appl. Sci. Res. A10, 241–52.
BEEK, W. J. and MUTTZALL, K. M. K. (1975) 'Transport phenomena', J. Wiley and Sons Ltd., London.
BELTMAN, H. (1975) Thesis, Agricultural University, Wageningen, The Netherlands; Communic. Agric. Univ. Wageningen, 75–2.
BÉNARD, L. DE (1957) Proc. IInd Intern. Congr. on Surface Activity, ed. Schulman, J. H., Butterworths, London, Vol. 1, 7–12.
BERESNIEWICZ, A. (1959a) J. Polym. Sci. 35, 321–32.
BERESNIEWICZ, A. (1959b) J. Polym. Sci. 39, 63–79.
BERG, J. C. and ACRIVOS, A. (1965) Chem. Eng. Sci. 20, 737–45.
BERG, J. C., ACRIVOS, A. and BOUDART, M. (1966) Adv. Chem. Eng. 6, 61–123.
BIRD, R. B., STEWART, W. E. and LIGHTFOOT, E. N. (1960) 'Transport phenomena', J. Wiley and Sons Inc., New York.
BLANK, M. (1972) in 'Techniques of surface and colloid chemistry and physics', ed. Good, R. J., Stromberg, R. and Patrick, R. L., Marcel Dekker Inc., New York, Vol. 1, 41–88.
BLOKKER, P. C. (1957) Proc. IInd Intern. Congr. on Surface Activity, ed. Schulman, J. H., Butterworths, London, Vol. 1, 503–11.
BOGUE, B. A., MYERSON, A. and KIRWAN, D. J. (1975) Ind. Eng. Chem. Fund. 14, 282.
BÖHM, J. T. C., (1974) Thesis, Agricultural University, Wageningen, The Netherlands; Commun. Agric. Univ. Wageningen, 74–5.
BRAGINSKII, L. N. and PAVLUSHENKO, I. S. (1965) Zh. Prikl. Khim. 38, 1290–5.
BRANDRUP, J. and IMMERGUT, E. H. (1975) 'Polymer Handbook', J. Wiley and Sons. Inc., New York.
BRAVAR, M., ROLICH, J., BAN, N. and GNJATOVIC, V. (1974) J. Polym. Sci. Polym. Symp. 47, 329–34.
BRIAN, P. L. T. and ROSS, J. R. (1972) AIChE J. 18, 582–91.
BROWN, A. H. (1965) Br. Chem. Eng. 10, 622–6.
CARSLAW, H. S. and JAEGER, J. C. (1947) 'Conduction of heat in solids', Oxford.
CLARK, A. T., LAL, M. and TURPIN, M. A. (1975) Faraday Discuss. Chem. Soc. 59, 189–95.
CLAYFIELD, E. J. and LUMB, E. C. (1974) J. Colloid Interface Sci. 47, 6–26.
COHEN STUART, M. A. (1976) unpublished results.
COSGROVE, T. and VINCENT, B. (1977) to be published.
CRANK, J. (1964) 'The mathematics of diffusion', Clarendon Press, Oxford.
CRISP, D. J. (1946) J. Colloid Sci. 1, 49–70; 161–84.

DANCKWERTS, P. V. (1951) Ind. Eng. Chem. **43**, 1460–7.
DAVIES, C. W. (1962) 'Ion association', Butterworths, London.
DAVIES, J. T. and WIGGEL, J. B. (1960) Proc. R. Soc. London A**255**, 277–91.
DAVIES, J. T. and RIDEAL, E. K. (1961) 'Interfacial phenomena', Academic Press, New York.
DAVIES, J. T. and MAYERS, G. R. A. (1961) Chem. Eng. Sci. **16**, 55–68.
DAVIES, J. T. (1963) Adv. Chem. Eng. **4**, 1–50.
DAVIES, J. T., KILNER, A. A. and RATCLIFF, G. A. (1964) Chem. Eng. Sci. **19**, 583–90.
DAVIES, J. T. and KHAN, W. (1965) Chem. Eng. Sci. **20**, 713–5.
DAVIES, J. T. (1966) Proc. R. Soc. London A**290**, 515–26.
DAVIES, J. T. (1972) 'Turbulence phenomena', Academic Press, New York.
DAVIES, J. T. and DRISCOLL, J. P. (1974) Ind. Eng. Chem. Fund. **13**, 105–9.
DEVENATHAN, M. A. and GURUSVANI, V. (1973) Elektrokhimiya **9**. 1275–82.
DONAHUE, D. J. and BARTELL, F. E. (1952) J. Phys. Chem. **56**, 480–4.
DONDOS, A., REMPP, P. and BENOÎT, H. (1974) Makromol. Chem. **175**, 1659–63.
DREVAL, V. E., MALKIN, A. Y. and BOTVINNIK, G. O. (1973) J. Polym. Sci. Polym. Phys. Ed. **11**, 1055–76.
ENGLAND, D. C. and BERG, J. C. (1971) AIChE J. **17**, 313–22.
FEIJTER, J. A. DE (1976) unpublished results.
FINCH, C. A. (1968) 'Properties and applications of polyvinyl alcohol', S.C.I. Monograph no. 30, Soc. Chem. Ind., London.
FINCH, C. A. (1973a) 'Polyvinyl alcohol properties and applications', J. Wiley and Sons Inc., London.
FINCH, C. A. (1973b) in FINCH (1973a) 203–231.
FISCHER, L. (1971) 'Laboratory techniques in Biochemistry and Molecular Biology', Vol. 1, part II, 'An introduction to gel chromatography', North Holland Publ. Co., Amsterdam.
FLEER, G. J. (1971) Thesis, Agricultural University, Wageningen, The Netherlands; Commun. Agric. Univ. Wageningen, 71–20.
FLORY, P. J. (1953) 'Principles of Polymer Chemistry', Cornell University Press, Ithaca.
FLORY, P. J. (1955) Trans. Faraday Soc. **51**, 848–57.
FONTANA, B. J. and THOMAS, J. R. (1961) J. Phys. Chem. **65**, 480–7.
FOSBERG, T. M. and HEIDEGER, W. J. (1967) Can. J. Chem. Eng. **45**, 82–9.
FOX, K. K., ROBB, I. A. and SMITH, R. (1974) J.C.S. Faraday I, **70**, 1186–90.
FRANKS, F. and IVES, D. J. G. (1966) Q. Rev. **20**, 1–44.
FRIEDLANDER, H. N., HARRIS, H. E. and PRITCHARD, J. G. (1966) J. Polym. Sci. Polym. Chem. Ed. **4**, 649–64.
FUJII, K. (1971) Macromol. Rev. **5**, 431–540.
GARNER, F. H. and HALE, A. R. (1953) Chem. Eng. Sci. **2**, 157–63.
GARVEY, M. J., TADROS, T. F. and VINCENT, B. (1974) J. Colloid Interface Sci. **49**, 57–68.
GARVEY, M. J., TADROS, T. F. and VINCENT, B. (1976) J. Colloid Interface Sci. **55**, 440–53.
GLASS, J. E. (1968) J. Phys. Chem. **72**, 4450–8.
GORDON, K. F. and SHERWOOD, T. K. (1954) Chem. Eng. Progr. Symp. Ser. no. 10, **50**, 15–23.
GOUDA, J. H. and JOOS, P. (1975) Chem. Eng. Sci. **30**, 521–8.
GRUBER, E., SOEHENDRA, B. and SCHURZ, J. (1974) J. Polym. Sci. Symp. Ser. **44**, 105–18.
GULBEKIAN, E. V. and REYNOLDS, G. E. J. (1973) in FINCH (1973a) 427–60.
HAAS, H. C. (1957) J. Polym. Sci. **26**, 391–3.
HAAS, H. C., HUSEK, H. and TAYLOR, L. D. (1963) J. Polym. Sci. Part A **1**, 1215–26.
HAAS, H. C. (1973) in FINCH (1973a) 493–521.
HACKEL, E. (1968) in FINCH (1968) 1–15.
HAMADA, F. and NAKAJIMA, A. (1966) Kobunshi Kagaku **23**, 395–9; Chem. Abstr. (1966) **66**, 46701 v.
HANDBOOK OF CHEMISTRY AND PHYSICS (1972) ed. Weast. R.C., The Chemical Rubber Co., Cleveland, Ohio.
HARTLAND, S. and SRINIVASAN, P. S. (1974) J. Colloid Interface Sci. **49**, 318–20.

116   *Meded. Landbouwhogeschool Wageningen 77-7 (1977)*

HASTED, J. B. (1973) in 'Water a comprehensive treatise', ed. Franks, F., Vol. 2, ch. 7, Plenum Press, New York.
HAYASHI, S., NAKANO, C. and MOTOYAMA, T. (1963) Kobunshi Kagaku 20, 303–11; Chem. Abstr. (1964) 61, 5802.
HAYASHI, S., NAKANO, C. and MOTOYAMA, T. (1964a) Kobunshi Kagaku 21, 300–4; Chem. Abstr. (1965) 62, 9249 g.
HAYASHI, S., NAKANO, C. and MOTOYAMA, T. (1964b) Kobunshi Kagaku 21, 304–11; Chem. Abstr. (1965) 62, 9249 h.
HAYASHI, S., NAKANO, C. and MOTOYAMA, T. (1965a) Kobunshi Kagaku 22, 354–8; Chem. Abstr. (1965) 63, 16476.
HAYASHI, S., NAKANO, C. and MOTOYAMA, T. (1965b) Kobunshi Kagaku 22, 358–62; Chem. Abstr. (1965) 63, 16477.
HIGBIE, R. (1935) Trans. AIChE 31, 365–89.
HINZE, J. O. (1959) 'Turbulence', McGraw-Hill, New York.
HOSHINO, S. and SATO, K. (1967) Kagaku Kogaku 31, 961–6.
HUTCHINSON, E. (1948) J. Phys. Chem. 52, 897–908.
ISEMURA, T. and FUKUZUKA, K. (1956) Memoirs Inst. Sci. Ind. Res. Osaka Univ. 13, 137–44.
JACKSON, J. F. (1963) J. Polym. Sci. Part A 1, 2119–26.
JOHNS, L. E., BECKMAN, R. B. and ELLIS, W. B. (1965) Br. Chem. Eng. 10, 86–92.
JONGE, C. T. DE and BIJSTERBOSCH, B. H. (1973) Berichte vom VI Intern. Kongr. für grenz-flächenaktive Stoffe, Carl Hanser Verlag, München, Band 2, 469–82.
KAFAROV, V. V. (1961) Zh. Prikl. Khim. 34, 1061–5.
KAVANAU, J. L. (1964) 'Water and solute-water interactions' Holden-Day Inc., San Francisco.
KAWAI, T. (1958) J. Polym. Sci. 32, 425–44.
KEIZER, A. DE (1977) Thesis, Agricultural University, Wageningen, The Netherlands, to be published.
KENNEY, J. F. and WILLCOCKSON, G. W. (1966) J. Polym. Sci. Polym. Chem. Ed. 4, 679–98.
KILLMANN, E. and WINTER, K. (1975) Angew. Makromol. Chem. 43, 53–73.
KING, C. J. (1964) AIChE J. 10, 671–7.
KISHINEVSKY, M. and PAMFILOV, A. V. (1949) Zhurn. Anal. Khim. 22, 1183–90.
KLENIN, V. J., KLENINA, O. V., SHVARTSBURD, B. I. and FRENKEL, S. Y. (1974) J. Polym. Sci. Symp. Ser. 44, 131–40.
KNIEP, P. (1974) Thesis, T.U. Munich.
KOLNIBOLOTCHUK, N. K., KLENIN, V. J., MIKUL'SKII, G. F. and FRENKEL, S. Y. (1974) Kolloidn. Zh. 36, 865–71.
KOOPAL, L. K. and LYKLEMA, J. (1975) Faraday Discuss. Chem. Soc. 59, 230–41.
KOOPAL, L. K. (1977) Thesis, Agricultural University, Wageningen, The Netherlands, to be published.
KREMNEV, L. Y., SKVIRSKII, L. Y., OSTROVSKII, M. V. and ABRAMZON, A. A. (1965) Zhurn. Prikl. Khim. 38, 2496–505.
KUIPER, P. J. C. (1968) Plant Phys. 43, 1372–4.
KUL'MAN, R. A. (1965) Nature 207, 1289–90.
KURARAY CO. LTD., Osaka, Japan, prospectus.
KURARAY (1976) personal communication.
KURATA, M., TSUNASHIMA, Y., IWAMA, M. and KAMADA, K. (1975) in BRANDRUP and IMMERGUT (1975) ch. 4.
LANKVELD, J. M. G. (1970) Thesis, Agricultural University, Wageningen, The Netherlands; Commun. Agric. Univ. Wageningen, 70–21.
LANKVELD, J. M. G. and LYKLEMA, J. (1972) J. Colloid Interface Sci. 41, 454–83.
LEYTE, J. C. (1974) unpublished results.
LÉVÊQUE, M. A. (1928) Ann. des Mines 13, 201–99.
LEVICH, V. G. (1962) 'Physicochemical hydrodynamics', Prentice Hall Inc., Englewood Cliffs, New York.
LEWIS, W. K. and WHITMAN, W. G. (1924) Ind. Eng. Chem. 16, 1215–20.

LEWIS, J. B. (1954) Chem. Eng. Sci. **3**, 248–78.

LINTON, M. and SUTHERLAND, K. L. (1957) Proceedings IInd. Intern. Congr. on Surface Activity, ed. Schulman, J. H., Butterworths, London, Vol. 1, 494–502.

LIPATOV, Y. S. and SERGEEVA, L. M. (1974) 'Adsorption of polymers', Halstred Press, J. Wiley and Sons, New York.

LIPATOV, Y. S., and SERGEEVA, L. M. (1976) Adv. Colloid Interface Sci. **6**, 1–92.

LOCK, R. C. (1951) Q. J. Mech. Appl. Math. **4**, 42–63.

MACINNES, D. A. (1961) 'The principles of Electrochemistry', Dover Publ. Inc., New York.

MARON, S. H. and REZNIK, R. B. (1969) J. Polym. Sci. Polym. Phys. Ed. **7**, 309–24.

MATSUMOTO, M. and IMAI, K. (1957) J. Polym. Sci. **24**, 125–34.

MATSUMOTO, M., IMAI, K. and KAZUSA, Y. (1958) J. Polym. Sci. **28**, 426–8.

MATSUMOTO, M. and OHYANAGI, Y. (1960) Kobunshi Kagaku **17**, 191–6; Chem. Abstr. (1960) **55**, 19319 a.

MAYERS, G. R. A. (1961) Chem. Eng. Sci. **16**, 69–75.

MCMANAMEY, W. J. (1961) Chem. Eng. Sci. **15**, 251–4.

MCMANAMEY, W. J., DAVIES, J. T., WOOLEN, J. M. and COE, J. R. (1973) Chem. Eng. Sci. **28**, 1061–9.

MCMANAMEY, W. J., MULTANI, S. K. S. and DAVIES, J. T. (1975) Chem. Eng. Sci. **30**, 1536–8.

MILLER, I. R. and GREAT, H. (1970) Electrochim. acta, **15**, 1143–54.

MIYAMOTO, T. and CANTOW, H. J. (1972) Makromol. Chem. **162**, 43–51.

MONK, C. B. (1961) 'Electrolytic dissociation', Academic Press, London.

MOORE, J. T. (1968) J. Lipid Res. **9**, 642–6.

MOORE, W. R. A. D. and O'DOWD, M. (1968) in FINCH (1968) 77–87.

MUDGE, L. K. and HEIDEGER, W. J. (1970) AIChE J. **16**, 602–8.

MURAHASHI, S., NOZAKURA, S., SUMI, M., YUKI, H. and HATTADA, K. (1966) J. Polym. Sci. Polym. Lett. Ed. **4**, 65–9.

NAGAI, E. and SAGANE, N. (1955) Kobunshi Kagaku. **12**, 195–9; Chem. Abstr. (1957) **51**, 860 b.

NASH, G. R. and MONK, C. B. (1958) Trans. Faraday Soc. **54**, 1650–6.

NISHINO, Y. (1961) Bunseki Kagaku **10**. 656–8; Chem. Abstr. (1962) **57**, 4851 b.

NITSCH, W. (1968) Chem. Ing. Tech. **40**, 390–2.

NITSCH, W. and HILLEKAMP, K. (1972) Chem. Ztg. **96**, 254–61.

NITSCH, W., RAAB, M. and KNIEP, P. (1973a) Berichte vom VI Intern. Kongr. für grenzflächenaktive Stoffe, Carl Hanser Verlag, München, Band 2, 147–55.

NITSCH, W., RAAB, M. and WIEDHOLZ, R. (1973b) Chem. Ing. Tech. **45**, 1026–32.

NITSCH, W. and HECK, K. D. (1976a) Wärme- und Stoffübertragung **9**, 53–4.

NITSCH, W. and WEBER, G. (1976b) Chem. Ing. Tech. **48**, 715.

NORDE, W. (1976) Thesis, Agricultural University, Wageningen, The Netherlands; Commun. Agric. Univ. Wageningen, 76–6.

NORO, K. (1970) Br. Polym. J. **2**, 128–34.

NORO, K. (1973a) in FINCH (1973a) 67–89.

NORO, K. (1973b) in FINCH (1973a) 91–120.

NOZAKURA, S., MORISHIMA, Y. and MURAHASHI, S. (1972a) J. Polym. Sci. Polym. Chem. Ed. **10**, 2767–80.

NOZAKURA, S., MORISHIMA, Y. and MURAHASHI, S. (1972b) J. Polym. Sci. Polym. Chem. Ed. **10**, 2781–92.

OLANDER, D. R. and BENEDICT, M. (1962) Nucl. Sci. Eng. **14**, 287–94.

OSTROVSKII, M. V., FRUMIN, G. T., KREMNEV, L. Y. and ABRAMZON, A. A. (1967) Zh. Prikl. Khim. **40**, 1319–27.

OSTROVSKII, M. V., FRUMIN, G. T., and ABRAMZON, A. A. (1968) Zh. Prikl. Khim. **41**, 803–10.

OSTROVSKII, M. V., KALUGINA, S. K. and ABRAMZON, A. A. (1973) Teor. Osn. Khim. Tekhnol. **7**, 344–52.

PEYSER, P. and STROMBERG, R. R. (1967) J. Phys. Chem. **71**, 2066–74.

PIERSON, F. W. and WHITAKER, S. (1976) J. Colloid Interface Sci. **54**, 203–30.

PRITCHARD, J. G. (1970) 'Poly (vinyl alcohol) basic properties and uses', Polymer Mono-
    graphs, Vol. 4, Gordon and Breach, London.
PRITCHARD, J. G. and AKINTOLA, D. A. (1972) Talanta 19, 877–88.
PROCHÁZKA, J. and BULIČKA, J. (1971) Int. Solv. Extract. Conf., The Hague, paper 27.
QUINN, J. A. and JEANNIN, P. G. (1961) Chem. Eng. Sci. 15, 243–50.
RAAB, M. (1971) Thesis, T.U. Munich.
ROBB, I. D. and SMITH, R. (1974) Eur. Polym. J. 10, 1005–10.
ROE, R. J., BACHETTA, V. L. and WONG, P. M. G. (1967) J. Phys. Chem. 71, 4190–3.
ROSANO, H. L., DUBY, P. and SCHULMAN, J. H. (1961) J. Phys. Chem. 65, 1704–8.
ROSANO, H. L. (1967) J. Colloid Interface Sci. 23, 73–9.
ROZEN, A. M. and KRYLOV, V. S. (1966) Int. Chem. Eng. 6, 429–37.
SAITO, S. (1969) J. Polym. Sci. Polym. Chem. Ed. 7, 1789–802.
SAKAI, T. (1968a) J. Polym. Sci. Polym. Phys. Ed. 6, 1659–72.
SAKAI, T. (1968b) J. Polym. Sci. Polym. Phys. Ed. 6, 1535–49.
SAKURADA, I. and SAKAGUCHI, Y. (1956) Kobunshi Kagaku 13, 441–8; Chem. Abstr. (1957)
    51, 17365 g.
SAKURADA, I. (1968) Pure Appl. Chem. 16, 263–83.
SAWISTOWSKI, H. and AUSTIN, L. J. (1967) Chem. Ing. Tech. 39, 224–31.
SAWISTOWSKI, H. (1971) in 'Recent advances in liquid-liquid extraction', ed. Hanson, C.,
    Pergamon Press, Oxford.
SAWISTOWSKI, H. (1973) Ind. Chem. Eng. 15, 35–43.
SCHLICHTING, H. (1968) 'Boundary layer theory', Mc Graw-Hill, New York.
SCHOLTENS, B. J. R. and BIJSTERBOSCH, B. H. (1976) FEBS lett. 62, 233–5.
SCHULMAN, J. H. (1966) Ann. New York Acad. Sci. 137, 860–3.
SCOTT, E. J., TUNG, L. H. and DRICKAMER, H. G. (1951) J. Chem. Phys. 19, 1075–8.
SCRIVEN, L. E. and STERNLING, C. V. (1960) Nature 187, 186–8.
SHAKHOVA, E. M. and MEERSON, S. I. (1972) Kolloidn. Zh. 34, 589–93.
SHANBAG, V. P. (1973) Biochim. Biophys. Acta 320, 517–27.
SHIRAISHI, M. (1970) Br. Polym. J. 2, 135–40.
SHIRAISHI, M. and TOYOSHIMA, K. (1973) Br. Polym. J. 5, 417–32.
SIGWART, K. and NASSENSTEIN, H. (1956) VDI. Z. 98, 453–61.
SINFELT, J. H. and DRICKAMER, H. G. (1955) J. Chem. Phys. 23, 1095–9.
SJÖLIN, S. (1942) Acta Physiol. Scand. 4, 365–72.
SONNTAG, H. (1976) Prague Meetings on Macromolecules, fifth Discuss. Conf., lecture C 4.
STERNLING, C. V. and SCRIVEN, L. E. (1959) AIChE J. 4, 514–23.
STOCKMAYER, W. H. (1955) J. Polym. Sci. 15, 595–8.
STOCKMAYER, W. H., MOORE, L. D., FIXMAN, M. and EPSTEIN, B. (1955) J. Polym. Sci. 16,
    517–30.
STOKR, J. and SCHNEIDER, B. (1963) Collect. Czech. Chem. Commun. 28, 1946–56.
STRENGE, K. H. (1969) J. Colloid Interface Sci. 29, 732.
STROMBERG, R. R. (1967) in 'Treatise on adhesion and adhesives', ed. Patrick, R. L., Marcel
    Dekker Inc., New York, Vol. 1, 69–118.
STROMBERG, R. R., SMITH, L. E. and McCRACKIN, F. L. (1970) Discuss. Faraday Soc. 4,
    192–200.
SZEKELY, J. (1965) Chem. Eng. Sci. 20, 141–5.
TADOKORO, H., KOZAI, K., SEKI, S. and NITTA, I. (1957) J. Polym. Sci. 26, 379–82.
TANFORD, C. (1961) 'Physical chemistry of macromolecules', J. Wiley and Sons Inc., New
    York.
TINCHER, W. C. (1965) Makromol. Chem. 85, 46–57.
TING, H. P., BERTRAND, G. L. and SEARS, D. F. (1966) Biophys. J. 6, 813–23.
TOOR, H. L. and MARCHELLO, J. M. (1958) AIChE J. 4, 97–101.
TOYOSHIMA, K. (1968) in FINCH (1968) 154–87.
TOYOSHIMA, K. (1973) in FINCH (1973a) 391.
TSUNEMITSU, K. and SHOHATA, H. (1968) in FINCH (1968) 126.
TUBBS, R. K. (1965) J. Polym. Sci. Part A 3, 4181–9.

TUBBS, R. K. (1966) J. Polym. Sci. Polym. Chem. Ed. 4, 623–9.
TUBBS, R. K., INSKIP, H. K. and SUBRAMANIAN, P. M. (1968) in FINCH (1968) 88–103.
TUBBS, R. K. and WU, T. K. (1973) in FINCH (1973a) 167–81.
TUNG, L. H. and DRICKAMER, H. G. (1952) J. Chem. Phys. 20, 6–12.
UEYAMA, K., HATANAKA, J. and OGAWA, K. (1972) J. Chem. Eng. Japan 5, 248–51; 371–5.
VIGNES, A. (1960) J. Chem. Phys. 57, 980–1005.
VINCENT, B. (1974) Adv. Colloid Interface Sci. 4, 193–277.
VLIET, T. VAN (1977) Thesis, Agricultural University, Wageningen, The Netherlands; Commun. Agric. Univ. Wageningen, 77–1.
VORST, J. (1972) Focus 8, 18–21.
WACKER (1975) personal communication.
WARD, A. F. H. and BROOKS, L. H. (1952) Trans. Faraday Soc. 48, 1124–36.
WARD, W. J. and QUINN, J. A. (1964) AIChE J. 10, 155–9.
WARD, W. J. and QUINN, J. A. (1965) AIChE J. 11, 1005–12.
WHITAKER, S. (1976) J. Colloid Interface Sci. 54, 231–48.
WILKINSON, M. C. and KIDWELL, R. L. (1971) J. Colloid Interface Sci. 35, 114–9.
WOLFRAM, E. and NAGY, M. (1968) Kolloid-Z. u. Z. Polym. 227, 68–91.
WOLFRAM, E. and NAGY, M. (1969) Ann. Univ. Sci. Budap. Sect. Chim. 11, 57–71.
YAMAKAWA, H. (1971) 'Modern theory of polymer solutions', Harper and Row Publ., New York.
ZWICK, M. M. and BOCHOVE, C. VAN (1964) Text. Res. J. 34, 417–30.
ZWICK, M. M. (1965) J. Appl. Polym. Sci. 9, 2393–424.

APPENDIX A

PREPARATION OF BLOCKY PVA-AC COPOLYMERS

This procedure for the partial reacetylation of PVA is based on the method described by BERESNIEWICZ (1959a) for complete reacetylation, and on the qualitative notes of TUBBS (1966). For convenience, all amounts of chemicals are reduced to 22 g PVA-H, the starting material.

This amount was swollen in 150 ml pyridine that had been dried with potassium hydroxide and filtered over a G-3 filter. The mixture was placed in a three-necked flask equipped with a water-cooled condenser, a nitrogen inlet and a dropping funnel. Mixing was performed with a stirrer that was being operated through the condenser. The reaction was carried out in a nitrogen atmosphere that had been freed from oxygen and water by percolating the gas through a column of BTS catalyst and a solution of concentrated sulphuric acid (96%). Before the reaction was started, nitrogen was led through the mixture for a few hours.

The round-bottomed flask was heated up to 70–75 °C on a steam bath. The required amount of acetic acid anhydride (freshly distilled, b.p. 137–8 °C) was then added slowly while the mixture was being stirred vigorously. The temperature and stirring were maintained for 4 hours.

The volume of the mixture was reduced as much as possible by evaporation at 40 °C in a Rotavapor. Then it was poured into a solution of 100 ml water and 50 ml acetone of 0 °C, while stirring vigorously for 15 minutes. The mixture
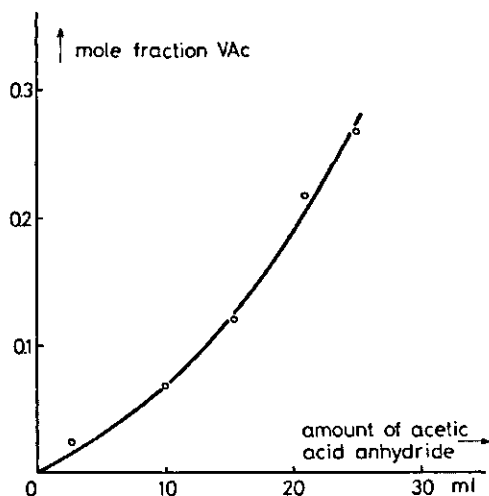

FIG. A. Dependence of the VAc content of blocky PVA-Ac on the composition of the reaction mixture (the explanation is given in appendix A).

was then poured on a paper filter and washed regularly with an identical water-acetone mixture at the same temperature until there was no longer pyridine smell from the filtrate (36–48 hours). The product was extracted with acetone in a Soxhlet extractor for 20 hours to remove the last traces of pyridine, acetic acid and ashes. Finally, the copolymer was dried in a vacuum oven (pressure 2×10^3 N.m^{-2}, temperature 60°C) over concentrated sulphuric acid and potassium hydroxyde pellets for 20 hours. The yield was almost 100%.

By varying the amount of acetic acid anhydride, five samples of different acetate content were prepared. In fig. A, the acetate content of the product is plotted as a function of the amount of acetic acid anhydride used.

APPENDIX B

PREPARATION OF RANDOM PVA-AC COPOLYMERS

This method is based on a few short notes of HAYASHI et al. (1964a) and TUBBS (1966). The experimental set-up is identical to the one described in appendix A.

In this method, 22 g of PVA-H was placed into a round-bottomed flask together with 200 ml water. Before dissolving the PVA, nitrogen (free from oxygen) was percolated through the solution for a few hours. While stirring slowly, the polymer was dissolved by increasing the temperature of the steam bath up to 95 °C. The required amount of acetic acid was added slowly to the solution together with 0.1 ml concentrated HCl that served as a catalyst (HAYASHI et al., 1964a). The solution was stirred slowly for 48 hours in a nitrogen atmosphere at 95 °C and stored in a closed flask at room temperature for 14 days. The excess reagents were removed by repeated distillation of the solution (in a Rotavapor), while replacing water until the distillate no longer smelled of acetic acid (5–7 days). Next, the solution was freeze-dried and the product extracted with acetone for 20 hours in a Soxhlet extractor. Finally, the copolymer was dried in a vacuum oven as described in appendix A. The yield was almost 100%.

Two samples were reacetylated in this way with different amounts of acetic acid: R1 (6.3 mole % acetate groups, using 50 ml acetic acid) and R2 (16.6 mole % acetate groups, using 160 ml acetic acid).

APPENDIX C

DETERMINATION OF K_b^p OF A PARTLY COVERED INTERFACE

Let us consider an axially symmetric, flat liquid-liquid interface at $z = 0$, extending between r_0 and $r = 0$, with a laminar boundary layer for $z \geqslant 0$ (fig. 6.3–1 and fig. 6.5–1). The area $r \leqslant r_1$ is covered with PVA-Ac, so that $v_{\sigma r} = 0$ in that region. If we can calculate the overall mass fluxes for both regions separately, summation and division by πr_0^2 will yield K_b^p; this will be attempted below.

We assume therefore, that the liquid velocity near the interface can be described by $v = -b/r$ at $r_1 < r \leqslant r_0$ and by $v = -az/r$ at $0 \leqslant r \leqslant r_1$ (fig. 6.3–1). The total mass flow for $r_1 < r \leqslant r_0$ is given by equation (6.3–11) multiplied by $\pi(r_0^2 - r_1^2)$. Now we assume another, hypothetical interface for $0 \leqslant r \leqslant r_2$ (with $r_1 < r_2 < r_0$), which is completely covered with PVA-Ac. We choose r_2 in such a way that at $r = r_1$ the penetration depth of the concentration for this case is identical to the one which results from the solution of the concentration profile, using $v = -b/r$ for $r_1 < r \leqslant r_0$. Then K_b^p can be expressed by (see also ch. 6.3):

$$K_b^p = \frac{5.01 \, (b_\sigma D_b)^{1/2} \, (r_0^2 - r_1^2)^{1/2} + \int_0^{r_1} \frac{(6 \, a_b \, D_b{}^2)^{1/3} \, 2\pi r}{\Gamma(^1\!/_3) \, (r_2^2 - r^2)^{1/3}} dr}{\pi r_0^2} \tag{C–1}$$

However, the determination of r_2 as a function of r_1 is tedious, since both solutions for the concentration profiles contain incomplete gamma functions. We tackled this problem with the approximate method proposed by von Kármán and Pohlhausen (e.g. SCHLICHTING, 1968 p. 187), supposing a trial solution for the concentration profile: $c_A = c_{A\sigma} \, (1 - z/\delta(r))^2$, where the concentration boundary layer $\delta(r)$ is only a function of r. With this relation equation (6.3–4) was solved with both (6.3–2) and (6.3–3) under the usual boundary conditions (ch. 6.3). From the calculated concentration profiles we obtained, finally, that insertion of r_1, in stead of r_2 in equation (C–1) results, for the system studied, in a K_b^p that is maximally 1 % too high. Because the influence of 'entrance effects' of the flow at r_1 on k_b are negligible (due to the high value of Sc_b) it seems justified to insert r_1 in stead of r_2 in equation (C–1). Integration yields:

$$K_b^p = \frac{5.01 \, (b_\sigma D_b)^{1/2} \, (r_0^2 - r_1^2)^{1/2} + 3.20 \, (a_b D_b^2)^{1/3} \, r_1{}^{2/3}}{\pi r_0^2} \tag{C–2}$$

CURRICULUM VITAE

De schrijver van dit proefschrift werd op 7 juli 1950 geboren te 's-Gravenhage. Het lager en middelbaar onderwijs volgde hij in Utrecht, waar hij in 1968 aan het Bonifatius lyceum het diploma Gymnasium-β behaalde. In datzelfde jaar begon hij de studie chemie aan de Rijksuniversiteit te Utrecht. In mei 1971 werd het kandidaatsexamen S1 afgelegd (cum laude) en in september 1973 het doctoraalexamen (specialisatie: fysische chemie; bijvak: theoretische organische chemie).

Van september 1973 tot en met december 1976 is hij als promotie-assistent werkzaam geweest op het laboratorium voor Fysische en Kolloidchemie van de Landbouwhogeschool te Wageningen. Daar werd het in dit proefschrift beschreven onderzoek uitgevoerd.

Sinds 1 maart 1977 is hij werkzaam op het Centraal Laboratorium van DSM te Geleen.